creative commons
COMMONS DEED

저작자표시-동일조건변경허락 2.0 대한민국

이용자는 아래의 조건을 따르는 경우에 한하여 자유롭게

- 이 저작물을 복제, 배포, 전송, 전시, 공연 및 방송할 수 있습니다.
- 이차적 저작물을 작성할 수 있습니다.
- 이 저작물을 영리 목적으로 이용할 수 있습니다.

다음과 같은 조건을 따라야 합니다:

저작자표시. 귀하는 원저작자를 표시하여야 합니다.

동일조건변경허락. 귀하가 이 저작물을 개작, 변형 또는 가공했을 경우에는, 이 저작물과 동일한 이용허락조건하에서만 배포할 수 있습니다.

- 귀하는, 이 저작물의 재이용이나 배포의 경우, 이 저작물에 적용된 이용허락조건을 명확하게 나타내어야 합니다.
- 저작권자로부터 별도의 허가를 받으면 이러한 조건들은 적용되지 않습니다.

저작권법에 따른 이용자의 권리는 위의 내용에 의하여 영향을 받지 않습니다.

이것은 이용허락규약(Legal Code)을 이해하기 쉽게 요약한 것입니다.

Disclaimer

dCollection

수의학 박사학위 논문

말초 신경손상으로 유도되는 물리적 이질통 형성에 대한 척수 별아교 세포 내 sigma-1 수용체의 역할

The role of sigma-1 receptor of spinal astrocyte in the development of mechanical allodynia by peripheral nerve injury

2015년 2월

서울대학교 대학원

수의학과 수의생리학 전공

문 지 영

수의학 박사학위 논문

말초 신경손상으로 유도되는 물리적 이질통 형성에 대한 척수 별아교 세포 내 sigma-1 수용체의 역할

The role of sigma-1 receptor of spinal astrocyte in the development of mechanical allodynia by peripheral nerve injury

2015년 2월

지도교수: 이 장 헌

서울대학교 대학원

수의학과 수의생리학 전공

문 지 영

Doctoral Thesis

The role of sigma-1 receptor of spinal astrocyte in the development of mechanical allodynia by peripheral nerve injury

Ji-Young Moon

Advisor: Jang-Hern Lee, D.V.M. Ph.D

Major in Veterinary Physiology
Department of Veterinary Medicine
The Graduate School
Seoul National University

February 2015

말초 신경손상으로 유도되는 물리적 이질통 형성에 대한 척수 별아교 세포 내 sigma-1 수용체의 역할

The role of sigma-1 receptor of spinal astrocyte in the development of mechanical allodynia by peripheral nerve injury

지도교수 이 장 헌

이 논문을 수의학 박사 학위논문으로 제출함

2014년 10월

서울대학교 대학원

수의학과 수의생리학 전공

문 지 영

문지영의 박사 학위논문을 인준함

2014년 12월

위 원 장 한 호 재 (인)

부위원장 이 장 헌 (인)

위 원 권 영 배 (인)

위 원 김 현 우 (인)

위 원 노 대 현 (인)

ABSTRACT

The role of sigma-1 receptor of spinal astrocyte in the development of mechanical allodynia by peripheral nerve injury

Ji-Young Moon
Major in Veterinary Physiology
Department of Veterinary Medicine
The Graduate School
Seoul National University

BACKGROUND:

Chronic pain, such as peripheral neuropathic pain, can be characterized by sensory disorders that include mechanical allodynia (MA, lowering of response threshold to light tactile stimuli) and thermal hyperalgesia (TH, an increased response to a noxious thermal stimulus). The precise mechanisms in the spinal cord underlying the development of MA and TH remain to be clearly defined. The role of sigma non-opioid intracellular receptor 1 (Sig-1R) in modulating central sensitization associated with the development of neuropathic pain has recently been investigated. Moreover, it has been recognized that spinal Sig-1Rs play an important role in the induction of MA in neuropathic pain. However, it was not clearly

demonstrated the specific mechanism related to this spinal Sig-1R under the development of MA in neuropathic pain condition.

OBJECTIVES:

The present study was designed to investigate:

1. the precise cellular location of Sig-1Rs in the spinal cord and whether Sig-1R activation mediates phosphorylation of p38, extracellular signal-regulated kinase (ERK) and c-Jun amino-terminal kinase (JNK), among mitogen-activated protein kinase (MAPK) signaling pathways. The effects of p38 and ERK inhibitor on the Sig-1R induced pain behaviors were also investigated.
2. the histological and physiological relationships among Sig-1R, p-p38 and glial activation and whether the inhibition of Sig-1R or p38 modulates astrocyte activation in chronic constriction injury (CCI) mice. I also investigated whether this Sig-1R modulation of astrocyte activation is associated with the increase of D-serine in the spinal cord dorsal horn.
3. whether the inhibition of Sig-1R or p38, which modulates astrocyte activity is associated with MA development in CCI mice. In addition, the role of D-serine in the induction of Sig-1R-mediated MA was also investigated in CCI mice.

MATERIALS AND METHODS:

Primary astrocyte-enriched cell cultures were prepared from newborn C57BL/6 mice. Other experiments were performed on male ICR mice (20-25g). A CCI of the common sciatic nerve was performed according to the method described by Bennett and Xie. For intrathecal

injection, I used the modified method of direct transcutaneous intrathecal injection on mice described by Hylden and Wilcox. Sensitization to innocuous mechanical stimulation (MA) was examined using von Frey filaments with forces of a 0.16 g. To assess nociceptive responses to heat stimuli, sensitization to noxious heat stimulation (TH) was examined with a hot-plate apparatus or Hargreaves apparatus. In the present study, the Sig-1R agonist, PRE-084 (3 nmol), its antagonist, BD-1047 (100 nmol), a ERK inhibitor, PD98059 (3, 10, 30 nmol), a p38 inhibitor, SB203580 (0.1, 0.3, 1, 3, 10 nmol), an astroglial metabolic inhibitor, fluorocitrate (0.003, 0.001, 0.03 nmol) and a serine racemase inhibitor, LSOS (1, 3, 10 nmol) were used. Immunohistochemistry and Western blot assay were performed according to each experiment procedure. The computer-assisted image analysis system (Metamorph) was utilized throughout whole experiments.

RESULTS:

1. The expression of Sig-1Rs was significantly increased in astrocytes on day 3 following CCI surgery in mice. In cultured astrocytes, Sig-1R expression was also found, and the treatment of PRE-084 increased phosphorylation of ERK and p38, but not JNK. While intrathecal pretreatment with PD98059 inhibited both PRE-084-induced MA and TH, SB203580 dose-dependently inhibited PRE-084-induced MA, but not TH induction was not affected. Intrathecal injection of PRE-084 into naïve mice time-dependently increased the expression of p38 phosphorylation (p-p38), which was blocked by pretreatment with BD-1047.

2. The activation of astrocyte and microglia were increased in the spinal cord on day 3 following CCI surgery in mice. Sustained intrathecal treatment with the BD-1047 during the

induction phase (postoperative days 0 to 3), attenuated CCI-induced increase in activation of astrocyte, but not microglia. The number of p-p38-ir astrocytes and neurons, but not microglia was also significantly increased after CCI surgery. Interestingly, intrathecal BD-1047 attenuated the expression of p-p38 selectively in astrocytes but not in neurons. Moreover, intrathecal treatment with a p38 inhibitor attenuated the GFAP expression. The level of D-serine and Serine racemase (Srr) expression were significantly increased in the spinal cord after CCI surgery. D-serine was localized in astrocyte and accumulated around neuron. Srr was also found in astrocyte. The increased level of D-serine was attenuated by sustained intrathecal treatment with BD-1047. Accordingly, Srr expression was also reduced by BD-1047 treatment and I found Srr expression was located on the same cell with Sig-1R-ir cells.

3. Sustained intrathecal treatment with the BD-1047 combined with fluorocitrate synergistically reduced the development of MA, but not TH. Moreover, intrathecal treatment with a p38 inhibitor combined with fluorocitrate synergistically blocked the induction of MA. In addition, sustained intrathecal treatment with the Srr inhibitor reduced the development of MA, and the blockade by BD-1047 treatment was reversed by exogenous D-serine.

CONCLUSIONS:

The present study demonstrates that the direct activation of spinal Sig-1R significantly increased p-p38 and the activation of spinal p38 was closely involved with the Sig-1R-mediated MA, but not TH. In CCI mice, spinal Sig-1R expression are increased in astrocytes, and that blockade of Sig-1Rs inhibits the pathologic activation of astrocytes via modulation of p-p38, which ultimately prevents the development of MA. The present study also indicates

that the Sig-1R-mediated MA is developed by an increase of Srr expression, which in turn causes an increase of D-serine level in the spinal cord of CCI mice. Collectively these findings imply that the increase of p-p38 and D-serine induced by spinal Sig-1R plays an important role in the development of MA in neuropathic pain and further suggest that MA development could be clinically controlled by the Sig-1R modulation.

Key words: Neuropathic pain, Sigma-1 receptor, Mechanical allodynia, p38, Astrocyte, D-serine

Student number: 2008-21738

Manuscripts published in

Exp Neurol. 2013 Sep;247:383-391

Br J Pharmacol. 2014 Dec;171(24):5881-5897

CONTENTS

LIST OF FIGURES

ABBREVIATIONS

ABC	Avidin-biotin-peroxidase complex
AMPA	α-amino-3-hydroxy-5-methyl-4-isoxazolepropionic acid
BDNF	Brain-derived neurotrophic factor
BD-1047	N-[2-(3,4-dichlorophenyl)ethyl]-N-methyl-2-(dimethylamino) ethylamine dihydro-bromide
$[Ca^{2+}]_i$	Intracellular Ca^{2+} concentration
CCI	Chronic constriction injury
CFA	Complete Freund's adjuvant
CNS	Central nervous system
DAAO	D-amino-acid oxidase
DAB	3,3'-diaminobenzidine
DAG	Diacylglycerol
DMEM	Dulbecco's Modified Eagle's Medium
EPSCs	Excitatory postsynaptic currents
ER	Endoplasmic reticulum
ERK	Extracellular signal-regulated kinase
GFAP	Glial fibrillary acidic protein
GluN1	NMDA receptor GluN1 subunit
GPCRs	G protein-coupled receptors
HRP	Horseradish peroxidase
IL	Interleukin

IP_3	Inositol triphosphate
ir	Immunoreactive
JNK	c-Jun amino-terminal kinase
LME	L-leucine methyl-ester
MA	Mechanical allodynia
MAPK	Mitogen-activated protein kinase
MCP-1	Monocyte chemoattractant protein-1
NECK	Neck region
NGF	Nerve growth factor
NMDA	N-methyl-D-aspartate
nNOS	Neuronal nitric oxide synthase
NO	Nitric oxide
NP	Nucleus proprius
PBS	Phosphate-buffered saline
PDBu	Phorbol 12,13-dibutyrate
pERK	Phosphorylation of ERK
pGluN1	Phosphorylated GluN1
PIP_2	Phosphatidylinositol 4,5-bisphosphate
pJNK	Phosphorylation of JNK
PLC	Phospholipase C
p-p38	Phosphorylation of p38
PRE-084	2-(4-morpholinethyl)1-phenylcyclohexanecarboxylate
pSNL	Partial sciatic nerve ligation

PWF	Percent withdrawal response frequency
RT	Room temperature
SB203580	4-(4-fluorophenyl)-2- (4-methylsulfonylphenyl)-5-(4-pyridyl)-1H-imidazole
SDH	Superficial dorsal horn
Sig-1R	Sigma non-opioid intracellular receptor 1
Srr	Serine racemase
TH	Thermal hyperalgesia
TNF-α	Tumor necrosis factor-α

BACKGROUND

Chronic pain

Pain is an unpleasant sensory and emotional experience associated with actual or potential tissue damage and is an essential early warning mechanism. This sensation is mediated in the periphery by high threshold primary sensory neurons, the nociceptors, which transmit information via nociceptive pathways in the spinal cord to the brain (von Hehn *et al.*, 2012). Alterations of the pain pathway lead to hypersensitivity, such that pain loses its usefulness as an acute warning system and instead becomes chronic and debilitating (Basbaum *et al.*, 2009). The development of chronic pain, characterized by allodynia (pain produced in response to a nonnociceptive stimulus as defined by the International Association for the Study of Pain) and hyperalgesia (increased sensitivity to a painful stimuli), is associated with a variety of pathophysiologic changes at peripheral and/or central sites (Ueda, 2006; Latremoliere *et al.*, 2009). Hyperalgesia and allodynia are classified according to the type of stimulus which elicit the sensation of pain. Mechanical and thermal (heat or cold) hyperalgesia and mechanical allodynia (MA) can be differentiated (Sandkuhler, 2009). However, the precise mechanisms underlying the development of MA versus thermal hyperalgesia (TH) remain to be accurately defined.

Peripheral and central sensitization

Peripheral sensitization occurs when the peripheral terminals of primary sensory neurons are exposed to inflammatory mediators and damaged tissue. It represents a reduction in threshold and an amplification in the responsiveness of nociceptors. Robust hypersensitivity can develop with inflammation or after injection of specific components of the inflammatory soup (Fukuoka *et al.*, 1994; Andreev *et al.*, 1995). Lack of sensitization to heat in TRPV-1

deficient mice provides genetic support for the idea that peripheral TRPV1 is a key component of the mechanism through which inflammation produces TH (Caterina *et al.*, 1997; Davis *et al.*, 2000). However, peripheral sensitization appears to play a major role in altered heat but not mechanical sensitivity, which is a major feature of central sensitization (Latremoliere *et al.*, 2009; von Hehn *et al.*, 2012).

Central sensitization is a state of hyperexcitability in the central nervous system, leading to enhanced processing of nociceptive messages. It is induced by enhanced synaptic strength in the spinal cord and brain regions, due to an increase in excitatory synaptic transmission, a glial neuronal interactions and/or a reduction in inhibitory synaptic transmission (e.g. GABA currents) (Ji *et al.*, 2007; Basbaum *et al.*, 2009).

Under acute pain conditions, postsynaptic α-amino-3-hydroxy-5-methyl-4-isoxazolepropionic acid (AMPA) receptor and kainite subtypes of ionotropic glutamate receptors are activated and generates excitatory postsynaptic currents (EPSCs) in second order dorsal horn neurons (Basbaum *et al.*, 2009). In the setting of injury, increased release of neurotransmitters, such as glutamate and neuropeptides, from nociceptors will sufficiently depolarize postsynaptic neurons to activate quiescent N-methyl-D-aspartate (NMDA) receptors or other receptors. The consequent increase in Ca^{2+} influx in the postsynaptic neurons causes downstream activation of a host of signaling pathways and second messenger systems, notably kinases (such as mitogen-activated protein kinases [MAPKs], PKA, PKC), further increases excitability of these neurons, in part by modulating NMDA receptor function (Latremoliere *et al.*, 2009; Mendell, 2011; von Hehn *et al.*, 2012) (Fig.1).

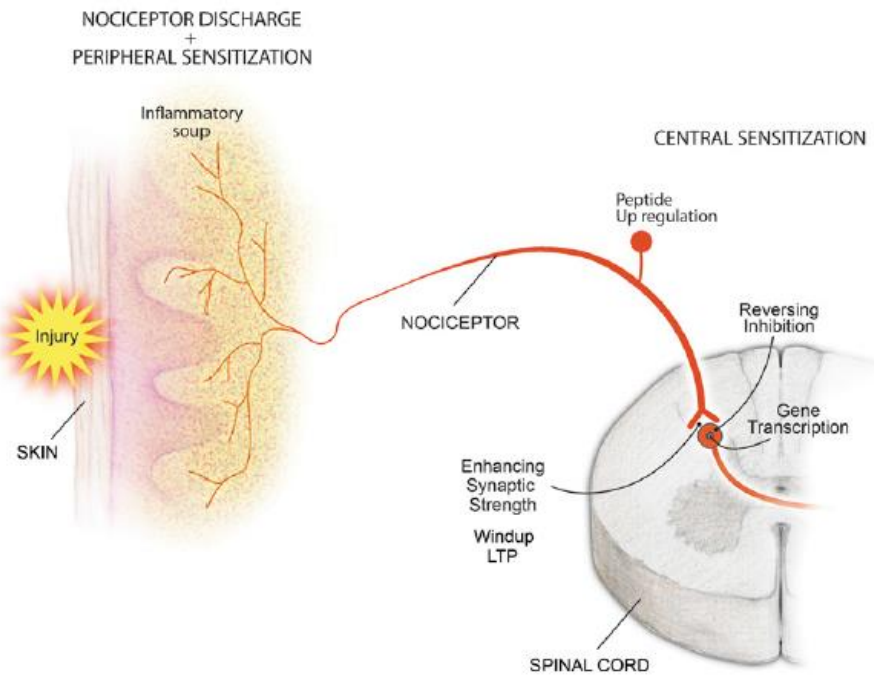

Figure 1. Schematic diagrams illustrating major mechanisms involved in peripheral and central sensitization. Inflammatory mediators released by peripheral injury enhance the magnitude of the response to a given stimulus. The increased activity in sensory neurons enhance synaptic strength in the spinal cord, due to an increase in excitatory synaptic transmission, a glial neuronal interactions and/or a reduction in inhibitory synaptic transmission. Adapted from (Mendell, 2011)

Glia activation

Although non-neuronal glial cells were originally regarded as supporting cells in the central nervous system (CNS), accumulating evidence indicate that glial cells, notably microglia and astrocytes, also participate in chronic pain. The structural and functional alterations of glia in the spinal cord have been reported in various models of chronic pain (Milligan *et al.*, 2009; Gao *et al.*, 2010a) (Fig.2). Under normal conditions, microglia functions as resident macrophages of the CNS. However, peripheral nerve injury induces a profound changes in spinal microglia including increased expression of microglial markers, CD11b and Iba-1. ATP receptor P2X4 and the chemokine receptor CX3CR1 are specifically upregulated in spinal microglia, and blocking these receptors results in decreased neuropathic pain (Tsuda *et al.*, 2003; Verge *et al*., 2004). Minocycline, a microglial inhibitor was shown to prevent or delay neuropathic pain (Ledeboer *et al.*, 2005; Ma *et al.*, 2010). Furthermore, intrathecal injection of ATP-activated microglia induces MA and TH, indicating that microglial activation is sufficient to induced pain sensitization (Tsuda *et al.*, 2003; Narita *et al.*, 2006).

Astrocytes are the most abundant glial cell type in the CNS. They modulates neuronal function, such as extracellular ion homeostasis, neurotransmitter reuptake and release, control of synaptic strength. Unlike microglia, astrocytes form networks with themselves and are closely associated with neurons and blood vessels. Astrocytes are organized in gap junction-coupled networks. They not only transmit Ca^{2+} signaling in the form of oscillations or waves through the networks but also form a tripartite synapse with pre- and postsynaptic membranes and release gliotransmitters that modulate synaptic strength (Scemes *et al.*, 2006; Agulhon *et al.*, 2008; Ben Achour *et al.*, 2010). After injury or under disease conditions, they can be converted to reactive states, which is characterized by an increase in glial fibrillary acidic

protein (GFAP) expression, an apparent enlargement of astrocytic process, a reduction in glutamate reuptake, and a release of various neuromodulatory molecules. It has been reported that spinal GFAP was shown to be upregulated in models of neuropathic pain as well as inflammatory pain (Raghavendra *et al.*, 2004; Kang *et al.*, 2011; Zhang *et al.*, 2011). Accumulating evidence indicates that activated astrocytes can enhance persistent pain states by producing pain mediators, such as proinflammatory cytokines (e.g. interleukin [IL]-1β, IL-6), chemokines (e.g. monocyte chemoattractant protein-1 [MCP-1]) and growth factors in the spinal cord (Gao *et al.*, 2009b; Gao *et al.*, 2010c; Gao *et al.*, 2010d; Weyerbacher *et al.*, 2010). In addition, astrocytes also release chemical transmitters, gliotransmitters such as D-serine, glutamate, and ATP (Parpura *et al.*, 2010; Agulhon *et al.*, 2012). Although glutamate and ATP are the most recognized chemical transmitters that mediate astrocyte-neuron signaling, it has been recently demonstrated that D-serine is an endogenous ligand for the glycine site of the NMDA receptor, which modulates NMDA receptor mediated neurotransmission (Mothet *et al.*, 2000; Henneberger *et al.*, 2010). Recently, it has also been reported that D-serine is involved in the mechanism of nociception in the spinal cord of chronic pain models (Ying *et al.*, 2006; Laurido *et al.*, 2012; Dieb *et al.*, 2013). Further study indicate that astrocytes are also required for the generation of persistent pain. Fluorocitrate and its precursor fluoroacetate are general inhibitors for glial cells, especially astrocytes (Swanson *et al.*, 1994). Low doses of fluorocitrate specially disrupt astrocytic metabolism by blocking the glial-specific enzyme aconitase at Krebs' cycle. Intrathecal injection of fluorocitrate or L-α-aminoadipate, another relative specific cytotoxin for astrocytes, has been shown to alleviate pain behaviors in several animal models of chronic pain (Qin *et al.*, 2006; Xu *et al.*, 2007b; Gao *et al.*, 2010c; Ji *et al.*, 2013). Furthermore, Zhang *et al.* reported that intrathecal injection of brain-derived

neurotrophic factor (BDNF)-activated astrocytes produce MA (Zhang *et al.*, 2011). However, another group has been reported that phorbol 12,13-dibutyrate (PDBu), a PKC activator-activated astrocytes fail to produce TH in naïve mice (Narita *et al.*, 2006). These data imply that direct activation of astrocytes in the spinal cord can play more important role in development of MA than TH.

MAPKs phosphorylation

The MAPKs regulate diverse cellular activities. Three distinct groups of MAPKs have been characterized: extracellular signal-regulated kinases (ERKs), p38 and c-Jun amino-terminal kinases (JNKs). MAPKs can be activated by phosphorylation via a variety of different stimuli and transduce extracellular stimuli into intracellular posttranslational and transcriptional responses, which represent three separate signaling pathways (Johnson *et al.*, 2002). Activation of MAPKs under various persistent pain conditions results in the induction and maintenance of pain hypersensitivity (Obata *et al.*, 2004; Ji *et al.*, 2009). Of interest, after tissue or nerve injury, ERK, p38 and JNK are differentially activated in spinal neurons and glial cells, leading to the synthesis of pronociceptive mediators, thereby enhancing and prolong pain (Obata *et al.*, 2004; Ji *et al.*, 2009).

It has been reported that phosphorylation of ERK (pERK) in dorsal horn neurons is essential for the development of central sensitization that is responsible for the generation of persistent pain (Ji *et al.*, 1999; Karim *et al.*, 2001; Gao *et al.*, 2009a). Recently accumulating evidence has demonstrated that ERK is also activated in glia in nerve injury model. Interestingly, ERK is only activated in microglia in the early phase (first 1 and 3 days) of the nerve injury (Zhuang *et al.*, 2005). On the other hand, in the late phase after nerve injury, pERK is induced in spinal astrocytes and spinal inhibition of ERK activation by intrathecal

administration of an ERK kinase inhibitor reduced MA (Ma *et al.*, 2002; Zhuang *et al.*, 2005) . In the maintenance phase of inflammatory pain induced by complete Freund's adjuvant (CFA) injection, pERK was also increased in astrocyte (Weyerbacher *et al.*, 2010). These results implicate a role of astrocytic ERK in the maintenance of chronic pain. Increase in phosphorylation of JNK (pJNK) was also found in spinal astrocytes in several models of chronic pain (Ma *et al.*, 2002; Zhuang *et al.*, 2006; Gao *et al.*, 2009b). In particular, the inhibition of JNK activation in astrocyte in spinal cord of neuropathic rats was able to prevent and reverse MA, suggesting that it plays an important role in development and maintenance of neuropathic pain (Gao *et al.*, 2009b).

p38 is regarded stress induced kinase and phosphorylation of p38 (p-p38) can be induced by elevated concentrations of intracellular Ca^{2+} and the activation of Ca^{2+} dependent enzymes (Lee *et al.*, 2000a; Hayashi *et al.*, 2007; Trang *et al.*, 2009). p38 also plays an important role in a variety of chronic pain states (Jin *et al.*, 2003; Boyle *et al.*, 2006; Xu *et al.*, 2007a; Sorkin *et al.*, 2009; Wen *et al.*, 2009). In general, mounting evidence indicates that p38 is activated in microglia under various persist pain conditions (Jin *et al.*, 2003; Boyle *et al.*, 2006; Piao *et al.*, 2006). However, the role of p38 in the spinal cord following chronic pain condition occurs in a time-specific and model–specific manner. Early treatment with p38 inhibitor prevents the development of MA by blocking cytokines such as tumor necrosis factor-α (TNF-α) synthesis (Boyle *et al.*, 2006; Xu *et al.*, 2007a; Lee *et al.*, 2010). On the other hand, post-treatment with p38 inhibitor starting on day 7 produces no effect on MA or TNF-α levels in chronic constriction injury (CCI) rats (Xu *et al.*, 2007a). In addition, increase in p-p38 was also found in spinal astrocytes or neuron in other chronic pain conditions, such as partial sciatic nerve ligation (pSNL) or first-degree burn (Xu *et al.*, 2007b; Sorkin *et al.*, 2009). Moreover, based

on experiments performed in a variety of animal pain models, spinal p38 activation appears to be involved in the pathophysiology of MA, but not TH (Sorkin *et al.*, 2009; Wen *et al.*, 2009). Accumulating evidences indicate that glia activation, relating to MAPKs phosphorylation in the dorsal horn mediates pain through different mechanisms operating at different times in various chronic pain condition.

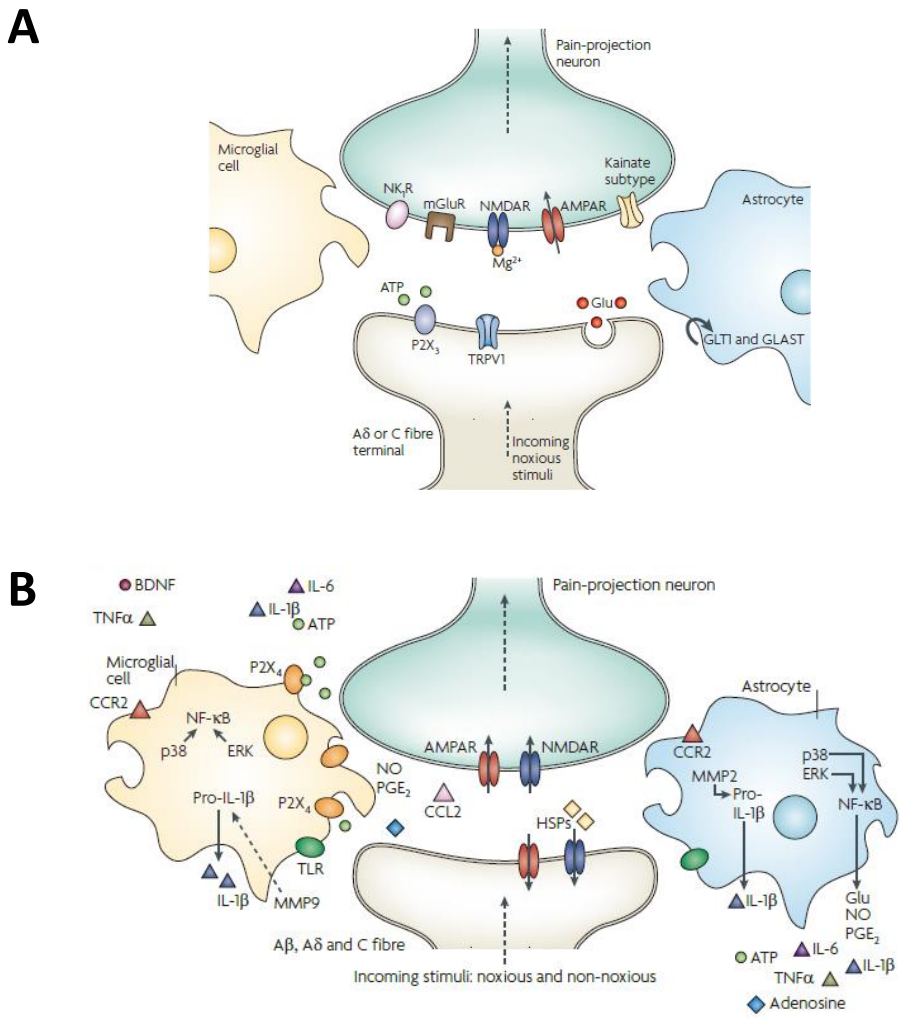

Figure 2. Schematic diagrams illustrating glia activation in pain processing. (A), Under healthy circumstances, mild noxious stimuli leads to glutamate release. AMPA receptor is activated and generates EPSCs in second order dorsal horn neurons. (B), After tissue or nerve injury, microglia and astrocyte are activated in spinal dorsal horn, leading to the synthesis of pronociceptive mediators, thereby enhancing and prolong pain. Adapted from (Milligan *et al.*, 2009).

OBJECTIVES

This study is aimed to

1. Examine: (1) the precise cellular location of Sig-1R in the spinal cord; (2) whether the treatment of the specific Sig-1R agonist, PRE-084 could modulate p38, ERK and JNK phosphorylation in cultured astrocytes; (3) whether p38 or ERK phosphorylation in the spinal cord are involved PRE-084 induced MA or TH .
2. Evaluate whether: (1) the intrathecal administration of a Sig-1R antagonist, BD-1047, given during the induction phase of neuropathic pain modulates the CCI-induced activation of microglia, astrocyte and p38 in CCI mice; (2) the intrathecal administration of a p38 inhibitor, SB203580, given during the induction phase of neuropathic pain also modulates the CCI-induced activation of astrocyte; (3) the level of D-serine and serine racemase (Srr) expression would increase in the spinal cord dorsal horn in CCI mice; (4) the inhibition of Sig-1R could modulate CCI-induced increase in D-serine or Srr expression;
3. Evaluate whether: (1) the intrathecal treatments of BD-1047 or SB203580 and/or combined with an astrocyte metabolic inhibitor, fluorocitrate during the induction phase of neuropathic pain could suppress MA or TH in CCI mice. (2) the selective inhibition of D-serine with a Srr inhibitor, LSOS in the spinal cord could suppress MA or TH development and the exogenous D-serine would reverse MA blockade by BD-1047.

INTRODUCTION

Chronic pain, such as peripheral neuropathic pain, can be characterized by sensory disorders that include MA (lowering of response threshold to light tactile stimuli) and TH (an increased response to a noxious thermal stimulus). The development of neuropathic pain is associated with a variety of pathophysiologic changes (Ueda, 2006; Latremoliere *et al.*, 2009) including peripheral sensitization and central sensitization. The precise spinal cord mechanisms underlying the development of MA and TH remain to be clearly defined, despite the fact that a number of studies have reported different signaling pathways involved with the development of MA versus TH (Ossipov *et al*., 1999; Roh *et al*., 2008a).

Sigma-1 receptors

Sig-1Rs are involved in a variety of cellular mechanisms but this involvement appears to occur via a common mechanism of regulating intracellular Ca^{2+} concentrations (Guitart *et al.*, 2004; Su *et al.*, 2010). The Sig-1Rs contains two transmembrane domains with both C- and N- terminal residing at a mitochondrion-associated ER membrane (Hayashi *et al.*, 2008; Kourrich *et al*., 2012). It is characterized by a unique mode of action via the regulation of both Ca^{2+} entry at the plasma membrane level and Ca^{2+} mobilization from endoplasmic stores (Monnet, 2005; Kourrich *et al.*, 2012) (Fig.3). The role of Sig-1R in modulating chronic pain has recently been investigated. Recently using Sig-1R knockout mice, it has been shown that Sig-1Rs have a pronociceptive effect in formalin-induced nociception and in nerve injury-induced pain (Cendan *et al.*, 2005; de la Puente *et al.*, 2009). Further support for a pronociceptive role for this receptor comes from a previous study from my laboratories demonstrating that intrathecal administration of the Sig-1R antagonists BD-1047 or BMY-

14802 reduces nociceptive behaviors and spinal Fos expression associated with the formalin test (Kim *et al.*, 2006). In addition, the previous study from my laboratories have shown that the direct activation of spinal cord Sig-1Rs enhances the response to peripheral mechanical and thermal stimuli via Ca^{2+}-dependent second messenger cascades (Roh *et al.*, 2008b). In addition, intrathecal injection of the Sig-1R antagonist, BD-1047 attenuates MA when administered during the induction phase (days 0-5 after CCI surgery), but not the maintenance phase (days 15-20 after CCI surgery) in CCI rats. On the other hand, BD-1047 treatment during either the induction or maintenance phases had no effect on TH (Roh *et al.*, 2008c). These findings demonstrated that the activation of spinal Sig-1Rs is associated with the induction of MA, but not TH in a rat model of neuropathic pain. Although it is well recognized that Sig-1Rs are widely distributed in mammalian peripheral organs and throughout the CNS (Hellewell *et al.*, 1994; Alonso *et al.*, 2000; Palacios *et al.*, 2003), the identity of specific cell types expressing Sig-1Rs in the spinal cord dorsal horn is unknown. Identification of the cell type expressing the Sig-1Rs would provide an important clue to understanding the role of Sig-1Rs in relation to development of chronic MA.

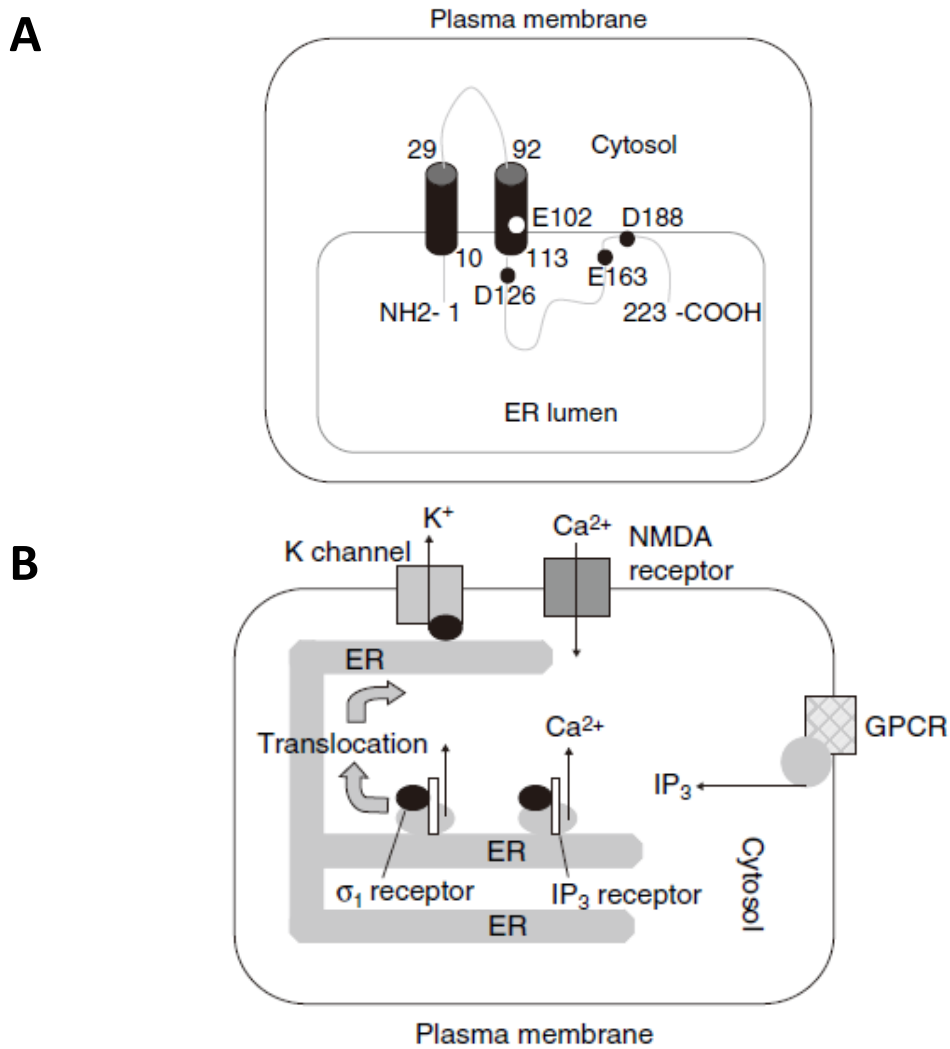

Figure 3. Schematic diagrams illustrating biological function of the Sig-1R. (A), Cellular distribution of Sig-1Rs. The Sig-1Rs contains two transmembrane domains with a short N-terminus and a long C terminus facing the ER lumen. (B), Sig-1Rs can modulate intracellular Ca^{2+} concentration. Sig-1Rs at the ER regulate Ca^{2+} efflux from the ER by associating with IP_3 receptors. After stimulation by ligands, activated Sig-1Rs translocate to plasma membrane, thus regulating functional proteins, including ion channels (K^+ or NMDA channels). Adapted from (Hayashi *et al.*, 2008).

Astrocyte activation

It is increasingly recognized that glial cells (astrocytes and microglia) play an important role in chronic pain processing (Gosselin *et al.*, 2010). In particular astrocytes represent the most abundant cells in the central nervous system and dynamically modulate neuronal function under both physiological and pathological conditions (Halassa *et al.*, 2007; Gao *et al.*, 2010c; Wang *et al.*, 2012). Accumulating evidence suggests that astrocyte activation contributes to the development and maintenance of chronic pain induced by nerve injury, inflammation, paclitaxel and paw incision.(Xu *et al.*, 2007b; Gao *et al.*, 2009b; Ikeda *et al.*, 2012; Zhang *et al.*, 2012). Furthermore, Ji *et al*. recently reported that MA was dose-dependently attenuated by intrathecal administration of L-α-aminoadipate in a rat chemotherapy-induced neuropathic pain model (Ji *et al.*, 2013). Moreover, intrathecal administration of L-α-aminoadipate reversed CFA-induced MA, while it produced no effect on the CFA-induced heat hyperalgesia (Gao *et al.*, 2010b). These data imply that spinal astrocytes can play an important role in regulating MA but not TH under chronic pain conditions.

p38 MAPK

p38 is a stress-activated protein kinase which is activated by phosphorylation (Ji *et al.*, 2007). It has been reported that p38 plays an important role in a variety of chronic pain states (Jin *et al.*, 2003; Boyle *et al.*, 2006; Xu *et al.*, 2007a; Sorkin *et al.*, 2009; Wen *et al.*, 2009). Moreover, based on experiments performed in a variety of animal pain models, spinal p38 activation appears to be involved in the pathophysiology of MA, but not TH (Sorkin *et al.*, 2009; Wen *et al.*, 2009). p38 activation is regulated by elevated concentrations of intracellular Ca^{2+} and the activation of Ca^{2+} dependent enzymes (Lee *et al.*, 2000a; Hayashi *et al.*, 2007; Trang *et al.*, 2009). Since Sig-1R sense endoplasmic reticulum (ER) Ca^{2+} concentration and

the activation of Sig-1R modulate intracellular Ca^{2+} signaling via the efflux of Ca^{2+} into the cytoplasm, I hypothesized that changes in p-p38 might be regulated by Sig-1R activation, which may ultimately contribute to the development of MA following peripheral nerve injury.

D-serine

D-serine is an endogenous ligand for the glycine site of the NMDA receptor, which modulates NMDA receptor mediated neurotransmission (Mothet *et al.*, 2000). Activation of NMDA receptors requires binding of glutamate at the glutamate binding site, but also of a co-agonist glycine or D-serine at their glycine site for the efficient opening of the receptor. D-serine is synthesized by Srr which converts L- to D-serine. In the brain, D-serine is predominantly synthesized in astrocytes (Panatier *et al.*, 2006), and Ca^{2+}-dependent release of D-serine controls NMDA receptor-dependent long-term potentization (Henneberger *et al.*, 2010). Evidence to date supports the hypothesis that astroglial D-serine is involved in pain mechanisms. Intrathecal administered fluorocitrate or D-amino-acid oxidase (DAAO), which catalyzes the oxidative deamination of D-amino acids, inhibited tetanic sciatic stimulation-induced MA in rats (Ying *et al.*, 2006). In addition, intrathecal injection of the Srr inhibitors, LSOS and LEHA, decreased wind-up potentiation in an arthritic pain model (Laurido *et al.*, 2012). Despite findings reported in these studies, the involvement of D-serine in the spinal cord on the development of MA and TH in CCI mice remains unknown. The previous study from my laboratories provided evidence that PKC-dependent phosphorylation of the NMDA receptor GluN1 subunit (GluN1, pGluN1) in spinal cord dorsal horn are critical to the induction of MA related with Sig-1R in CCI rats (Roh *et al.*, 2008c). In addition, spinal Sig-1R-mediated nociceptive action is mediated by an increase in neuronal nitric oxide synthase (nNOS), which is associated with an nitric oxide (NO)-induced increase in PKC-dependent

pGluN1 expression (Roh *et al.*, 2011). Based on these findings I also hypothesize that Sig-1R modulation of astrocytes plays an important role in the induction of MA through a D-serine mechanism in an animal model of neuropathic pain.

MATERIALS AND METHODS

Animal preparation

All experiments were performed on male ICR mice (20-25g) except primary astrocyte culture. Experimental animals were purchased from the Laboratory Animal Center of Seoul National University (Seoul, Republic of Korea). They had free access to food and water and were maintained in temperature and light controlled rooms (23±2℃, 12/12h light/dark cycle with lights on at 08:00) for at least 1 week prior to beginning an experiment. The experimental protocols for animal usage were reviewed and approved by the SNU Animal Care and Use Committee and conform to NIH guidelines (NIH publication No. 86-23, revised 1985). A CCI of the common sciatic nerve was performed according to the method described by Bennett and Xie (Bennett *et al.*, 1988). Briefly, the left sciatic nerve was exposed at the mid-thigh level, and three loose ligatures of 6-0 silk were placed around the dissected nerve with a 1.0- to 1.5-mm interval between each ligature. Sham surgery consisted of exposing the sciatic nerve in the same manner, but without ligating the nerve. Animals were anesthetized by intraperitoneal injection with 50μl of a combination of Zoletil 50® (Virbac, Carros, France), Rompun® (Bayer AG, Leverkusen, Germany) and saline (a ratio of 2:1:2 respectively). Total numbers of mice used in the study were 491.

Primary astrocyte cultures

Primary astrocyte-enriched cell cultures were prepared from newborn C57BL/6 mice (postnatal day 1) according to a previously published method (Hamby *et al.*, 2006). Briefly, I isolated the hemispheres, transferred them to an ice-cold Hank's buffer, and carefully removed the meninges. Tissues were then minced into ~1mm pieces and filtered through a 40 μm nylon

screen, and collected by centrifugation at 1250g for 10 min. The pellets were broken with a pipette and resuspended in a medium containing 10% fetal bovine serum in glucose Dulbecco's Modified Eagle's Medium (DMEM). Cellular suspension was separated into 5ml and directly plated on 75 cm^2 flasks. I cultured the plated cells for 15 days, replacing the medium twice a week. Once the cells had grown to 95% confluence, L-leucine methyl-ester (LME) at 20mM (Sigma-Aldrich) was added in culture flasks for 1 hour at 37℃ incubator to remove microglial cells and macrophages. For Western blot, the cells were plated in 6 well plate and cultured in a medium containing 10% fetal bovine serum in low glucose DMEM. The cells were plated on round coverslips (22 mm diameter) placed in culture dishes (50 mm diameter) for immunocytochemistry analysis and incubated in 2-3 days. I added 0.15mM dibutyryl cAMP (Sigma–Aldrich, St. Louis, MO, USA) to induce differentiation. Three days later, I used the cells for experiments. I performed GFAP (1:2000, MAB360, Chemicon International Inc., CA, USA) immunostaining to confirm the astrocyte's purity. Confluent monolayers of astrocytes showed >95% positive staining for GFAP.

Intrathecal drug injection

For intrathecal injection, I used the modified method of direct transcutaneous intrathecal injection on mice (Hylden *et al.*, 1980). Intrathecal injections were made into the L5-L6 intervertebral space of animals using a 50 μl Hamilton syringe. The flick of the tail was considered indicative of a successful intrathecal administration. Mice were briefly anesthetized with 3% isoflurane in a mixed nitrous oxide–oxygen gas before intrathecal drug injection to prevent any handling-induced stress. Then, while the animals were under anesthesia, drugs were slowly infused. Animals awoke immediately after the intrathecal injection procedure and were freely moving within 45 s after injection. All drugs treated in

mice were dissolved in 5 μl of vehicle. Intrathecal treatments were performed twice a day on postoperative days 0-3 for the induction period. Animals were randomly assigned to experimental groups and subsequent drug treatment and analysis were performed blindly.

The following drugs were used: 2-(4-morpholinethyl)1-phenylcyclohexanecarboxylate (PRE-084, 3 nmol, Tocris Cookson Ltd, Bristol, UK), a sigma-1 receptor agonist; N-([2-(3,4-dichlorophenyl)ethyl]-N-methyl-2-(dimethylamino) ethylamine dihydro-bromide (BD-1047, 100 nmol, Tocris Cookson Ltd), a sigma-1 receptor antagonist; 4-(4-fluorophenyl)-2- (4-methylsulfonylphenyl)-5-(4-pyridyl)-1H-imidazole (SB203580, 0.1, 0.3, 1, 3, 10 nmol, Sigma–Aldrich, St. Louis, MO, USA), a p38 inhibitor; Fluorocitrate (Fc, 0.03, 0.001, 0.003 nmol, Sigma-Aldrich), an astroglial metabolic inhibitor; L-serine O-sulfate potassium salt (LSOS, 1, 3, 10 nmol, Santa Cruz Biotechnology Inc., CA, USA), serine racemase inhibitor; D-serine (50, 500 nmol; Sigma–Aldrich). The doses of PRE-084, BD-1047 and fluorocitrate used were based on those used in previous studies from my laboratories showing that these doses produce maximal effects with no detectable side-effects (Roh *et al.,* 2008b; Roh *et al.*, 2008c; Kang *et al.,* 2011). The doses of SB203580 and LSOS used in the present study were selected based on doses previously used in the literature (Wu *et al.*, 2006; Lee *et al.*, 2009; Laurido *et al.*, 2012). SB203580 was dissolved in 1% DMSO in saline, while other drugs were dissolved in physiological saline.

Mechanical allodynia assay

Sensitization to innocuous mechanical stimulation (MA) was examined using von Frey filaments (North Coast Medical, Morgan Hill, CA) as described in previous studies from my laboratories (Roh *et al.,* 2008b; Roh *et al.,* 2008c). A 0.16 g von Frey filament was selected for testing. In experimental PRE-084 injected mice group, mechanical responses to von Frey

filaments were measured before treatment for the baseline values and at the 30, 60, and 120 min time points after treatment with PRE-084 (or saline). In CCI animals, mechanical responses to von Frey filaments were assessed 1 day before CCI or sham surgery in all animals to obtain normal baseline values and then animals were tested again following CCI or sham surgery for a period of 21 days as described above. These von Frey filaments were applied from underneath the metal mesh flooring to each hind paw. The filament was applied 10 times to each paw with each application separated by 10 second intervals. The number of paw withdrawal responses to the 10 von Frey applications was then recorded. The results of the mechanical response testing in each experimental animal were expressed as a percent withdrawal response frequency (PWF, %), which represented the percentage of paw withdrawals out of a maximum of 10 as previously described (Roh *et al.*, 2008c; Roh *et al.*, 2011).

Thermal hyperalgesia assay

To assess nociceptive responses to heat stimuli in PRE-084 injected mice group, sensitization to noxious heat stimulation (TH) was examined with a hot-plate apparatus (Model-35100, Ugo Basile, Comerio, Italy) (Duman *et al.*, 2006) . The temperature of plate was maintained at 55 ± 0.5 ℃. Animals were placed into an acrylic cylinder (20 cm in diameter, 25 cm high) on the heated surface, and the time (in seconds) between placement and shaking or licking or lifting of their hind paws or jumping (whichever occurred first), was recorded as the responses latency (second). Baseline latency responses (8-12 seconds) were determined before experimental treatment. The latency responses were then measured before treatment and at 30, 60, and 120 min after treatment with PRE-084 (or saline) in each experimental mice. To assess nociceptive responses to heat stimuli in CCI mice, I measured

paw withdrawal response latency by using the plantar paw-flick latency test as previously described by Hargreaves *et al*.(Hargreaves *et al*., 1988). Briefly, animals were placed in a plastic chamber with a glass floor and were allowed to acclimatize for 1 hour before testing. A radiant heat source was positioned under the glass floor beneath the hind paw to be tested, and withdrawal latency was measured using a plantar analgesia meter (IITC Life Science Inc., Woodland Hills, CA). The test was repeated in the ipsilateral hind paw of each animal, and the mean withdrawal latency was calculated. Cutoff time in the absence of a response was set at 20 s. TH assay was performed 1 day before CCI surgery on all animals to obtain normal baseline values of thermal stimuli.

Western blotting analysis

In cultured astrocytes, MAPKs phosphorylation were measured at the 0, 5, 15, 30, 60 and 120 min time points after treatment with PRE-084. After treatment, monolayers were washed with ice-cold phosphate-buffered saline (PBS) and lysed in ice-cold modified RIPA buffer (Thermo scientific. Waltham, MA, USA) after collected. In PRE-084 injected mice group, mice were sacrificed at several time points (60 and 120 min) after intrathecal injection of PRE-084 (3 nmol). In CCI mice group, the spinal cords were collected from CCI mice on day 1, 3, 7 and 14 days after surgery or sham surgery mice to measure changes in the expression of target proteins. Mice were first deeply anesthetized and the location of the L4–L6 spinal cord segments were then verified by identifying the attachment site of each lumbar spinal nerve in the anesthetized animals. The spinal cord was extracted by pressure expulsion with air into an ice-cooled, saline-filled glass dish. Subsequently the spinal cord was separated into left and right halves under a neuro-surgical microscope. The spinal cord was further subdivided into dorsal and ventral halves by cutting straight across from the central canal laterally to a

midpoint in the white matter. The ipsilateral and contralateral dorsal quadrants of each spinal cord were separated and half containing the ipsilateral spinal cord dorsal horn was subsequently processed for Western blot analysis.

The collected astrocytes and L_{4-6} spinal cord dorsal segments were homogenized in RIPA buffer. The total amount of protein in each sample was determined using the Bradford dye assay prior to loading on polyacrylamide gels. The homogenates (20 μg protein) were separated using 10% SDS-polyacrylamide gel electrophoresis and transferred to nitrocellulose. After the blots had been washed with TBST (10 mM Tris-HCl (pH 7.6), 150 mM NaCl, 0.05% Tween-20), the membranes were blocked with 5% skim milk for 1 hr and incubated at 4℃ overnight with a primary antibody specific for β-actin (1:1000, loading control, sc-47778, Santa Cruz Biotechnology Inc.), GFAP (1:2000, MAB360, Chemicon International Inc.), ERK (1:1000, sc-94, Santa Cruz Biotechnology Inc.), pERK (1:1000, #4377, Cell signaling technology, Beverly, MA, USA), JNK (1:1000, sc-7345, Santa Cruz Biotechnology Inc.), pJNK (1:1000, sc-6254, Santa Cruz Biotechnology Inc.), p38 (1:500, #9212, Cell signaling technology), p-p38 (1:1000, #9211, Cell signaling technology), Srr (1:1000, sc-48741, Santa Cruz Biotechnology Inc.) and Sig-1R (1:1000, anti-opioid receptor sigma 1 [OPRS1] antibody, ab53852, Abcam Inc., Cambridge, MA, USA). After washing with TBST, membranes were incubated for 4 hours at room temperature (RT) with horseradish peroxidase (HRP)-conjugated anti-rabbit IgG or anti-mouse IgG secondary antibody (1:2000, Santa Cruz Biotechnology Inc.). The bands were visualized with enhanced chemiluminescence (Amersham Biosciences, Buckinghamshire, UK).

Immunohistochemistry

For double immunofluorescence staining in cultured astrocytes, monolayer were fixed

for 10min with 4% paraformaldehyde. After washing, blocking non-specific binding sites with PBS containing 5% fetal bovine serum and 5% normal goat serum were performed for 1 hour at room temperature. The mixture of rabbit anti-Sig-1R antibody (1:1000), and mouse anti-GFAP (1:1000) in blocking solution were added and monolayers incubated overnight at room temperature. After washing, cyanine 3 anti-rabbit IgG (1:400, Jackson ImmunoResearch, West Grove, PA, USA) and Alexa fluor 488 anti-mouse IgG (1:400, Invitrogen, Carlsbad, CA, USA) antibodies were used as the secondary antibodies and incubated for 1 hour at RT.

In PRE-084 treated mice groups, mice were deeply anesthetized and perfused with fixative at several time points (60 and 120 min) after intrathecal injection of PRE-084. In CCI mice, the perfusion was performed on 1, 3 and 7 after CCI or sham surgery. Mice were perfused transcardially with Ca^{2+}-free Tyrode's solution followed by a fixative containing 4% paraformaldehyde and 0.2% picric acid in 0.1M phosphate buffer (pH 6.9). The spinal cords were removed immediately after perfusion, post-fixed in the identical fixative for 12h and then placed in 30% sucrose in PBS (pH 7.4) for 2-3 days at 4° C. Serial transverse sections (40 μm) of the spinal cord were cut using a cryostat (Microm, Walldorf, Germany).

For p-p38 immunohistochemistry analysis in PRE-084 treated mice, spinal L4-L6 tissue sections were processed for p-p38 (1:500) immunohistochemistry using the avidin-biotin-peroxidase complex (ABC) procedure as previously described (Osuka *et al.*, 2007). Visualization of the ABC complex was performed using 3,3'-diaminobenzidine (DAB; Sigma-Aldrich) and the DAB reaction was intensified with 0.2% nickel chloride. For immunofluorescence analysis in CCI mice, transverse spinal cord sections were incubated in blocking solution for 1h at RT and then incubated for 48h at 4℃ with one of the following several primary antibodies: rabbit anti-Sig-1R antibody (1:1000), rabbit anti-D-serine

antibody (1:500, ab6472, Abcam Inc.) or mouse anti-GFAP (1:1000). Following incubation, tissue sections were washed and incubated for 1h at RT in secondary antibodies. Cyanine 3 anti-rabbit IgG (1:400, Jackson ImmunoResearch, West Grove, PA, USA) and Alexa fluor 488 anti-mouse IgG (1:400, 1hr at RT, Invitrogen, Carlsbad, CA, USA) antibodies were used as the secondary antibodies, respectively. To confirm the specificity of the Sig-1R antibody immunoreactivity, I performed a preabsorption test in which the antibody was mixed with the OPRS1 recombinant protein (25μg of peptide/ml of diluted primary antibody, Novus Biologicals, US) overnight at 4℃ prior to staining. Double-immunofluorescence labeling was used to study the distribution of Sig-1R, p-p38, D-serine and Srr in spinal cord dorsal horn cells. For double immunofluorescence staining, floating sections were first incubated for 48 hours at 4℃ with a rabbit anti-Sig-1R, anti-p-p38, anti D-serine or anti-Srr antibody (1:500). After washing with TPBS, the sections were then incubated for 2hr at RT with a cyanine 3 or Alexa 488 conjugated anti-rabbit IgG antibody (1:200). After washing, slices were incubated for 48 hours at 4℃ with GFAP, neuronal-specific nuclear protein (NeuN) (mouse, 1:1000; Millipore, Billerica, MA, USA) or Iba-1 (goat, 1:500, Abcam Inc.) followed by Alexa fluor 488 or 555 anti-mouse IgG secondary antibody (1:200) for 2hr at RT. For double immunofluorescence staining of Srr and Sig-1R, a rabbit anti- Sig-1R and a mouse anti-Srr antibody (1:500, sc-365217, Santa Cruz Biotechnology Inc.) were used. The slides were viewed under a confocal microscope (Fluoview4.3, Olympus).

Image analysis

The positive pixel area of specific bands from Western blot gels was measured with a computer-assisted image analysis system and normalized against the corresponding β-actin loading control bands. The mean value of the ratio in animals prior to PRE-084 treatment or

sham surgery were set at 100% for control group. Thus, the % change relative to the control group was then calculated for each time-point in each group.

To quantify p-p38-immunoreactive (ir) cells in the spinal cord of naïve mice after intrathecal injection of PRE-084, tissue sections were examined under a brightfield microscope (Zeiss Axioscope, Hallbergmoos, Germany) and five spinal cord sections from the L4-6 lumbar spinal cord segments were randomly selected from each animal, and subsequently scanned. Individual sections were digitized with 4096 grey levels using a cooled CCD camera (Micromax Kodak 1317, Princeton Instruments, AZ, UK) connected to a computer-assisted image analysis system (Metamorph version 6.3r2, Molecular Devices Corporation, PA). To maintain a constant threshold for each image and to compensate for subtle variability of the immunostaining, I only counted cells that were at least 70% darker than the average gray level of each image after background subtraction and shading correction. The average number of p-p38-ir cells per section from each animal was obtained and these values were averaged across each group and presented as group data. To analyze immunofluorescence images, three to five spinal cord sections from the L4-5 lumbar spinal cord segments were randomly selected from each animal, and were analyzed using a computer-assisted image analysis system (Metamorph version 7.7.2; Molecular Devices Corporation). The average number of GFAP-ir cells from each animal was obtained and these values were averaged across each group and presented as group data. To maintain a constant threshold for each image and to compensate for subtle variability of the immunostaining, I only counted cells that were at least 45% brighter than the average level of each image after background subtraction and shading correction. To analyze colocalization images, pairs of fluorescent images were acquired on the confocal microscope as green and red channels. A

qualitative analysis of Sig-1R and p-p38 antibody colocalization were performed using metamorph. The background for each image was subtracted by an automatic algorithm without user intervention before analysis. Overlap of the red/green images were visualized in merged images as yellow pixels, and areas of overlap were considered colocalized. The extent of colocalization of Sig-1R with GFAP, NeuN or Iba-1 was analyzed using Pearson's correlation coefficient for metamorph. The range of values of the correlation coefficient is -1.0 to +1.0. A value of 1.0 shows that the data are perfectly matched with one another and a value of -1.0 is observed when there is an inverse relationship between intensities in the two images (Dunn *et al.*, 2011). As negative control, the same images were used, but one of the images was rotated by 90 degrees and then the same analysis was repeated. The extent of colocalization of p-p38 with NeuN was measured as the number of areas of overlap between the two fluorescent probes in each spinal cord region using metamorph. To analyze the extent of colocalization of p-p38 in GFAP labeled cells, I have directly quantified the number of cells showing astrocytic nuclei that contained p-p38 immunolabeling.

I quantified immunostaining in the following three dorsal horn regions: 1) the superficial dorsal horn (SDH, laminae I and II); 2) the nucleus proprius (NP, laminae III and IV); and 3) the neck region (NECK, laminae V and VI). All analytical procedures described above were performed blindly without knowledge of the experimental conditions.

Statistical analysis

All values are expressed as the mean ± SEM. Statistical analysis was performed using Prism 5.0 (Graph Pad Software, San Diego, USA). Repeated measures two-way ANOVA was performed to determine overall differences in the time-course of all nociceptive behavioral tests. One-way ANOVA was used to determine differences across all experimental groups

(immunohistochemistry and Western blot assay). Post-hoc analysis was performed using the Bonferroni's multiple comparison test in order to determine the *P* value among experimental groups. In all cases, $P<0.05$ was considered statistically significant.

RESULTS

1. Cellular distribution of spinal Sig-1Rs and related MAPKs phosphorylation

1-1. Cellular distribution of Sig-1Rs in the ipsilateral dorsal horn in CCI mice

In this study, I utilized a Sig-1R antibody to stain mouse lumbar spinal cord sections at 3 days after CCI surgery. The specificity of the antibody was first tested using a pre-absorption test with a Sig-1R recombinant protein. Sig-1R-immunoreactivity was not detected in any of the spinal sections processed with pre-absorbed Sig-1R antibody (Fig.4A). The lack of immunostaining in the specificity controls validates the specificity of the antibody. To determine which specific cell types express Sig-1R on the ipsilateral dorsal horn in CCI mice, double staining was performed at day 3 post-CCI using an anti-Sig-1R antibody in combination with antibodies specific for astrocytes (GFAP), neurons (NeuN), or microglial cells (Iba-1). Double immunostaining with GFAP showed that the increased expression of Sig-1R was located to astrocytes (Fig.4B and E). No coexpression of Sig-1R was observed with the NeuN, the neuronal marker (Fig.4C), or Iba-1, a microglial marker (Fig.4D). Pearson's coefficient (r) was used to quantify the degree of colocalization of Sig-1R with GFAP, NeuN or Iba-1 (Fig.4F). There was a high correlation between Sig-1R and GFAP-ir cells in the spinal cord of CCI mice (r =0.801). The average correlation coefficient dropped when the same region was analyzed again after one of the two images of the image pair had been rotated 90 degrees (r =0.011). In contrast, the average correlation coefficient between Sig-1R and NeuN was -0.0893. While the correlation between the Sig-1R and Iba-1 was a little higher (r = 0.129),

there was no significant difference in the average when it was compared to the average of the same images, when one member of the pair was rotated 90 degrees (Fig.4F). These results indicate that the co-expression values that I obtained provided a meaningful measure of the relative colocalization Sig-1R and GFAP expression in spinal cord sections (Dunn *et al.*, 2011) and suggest that Sig-1R expression occurs primarily in astrocytes.

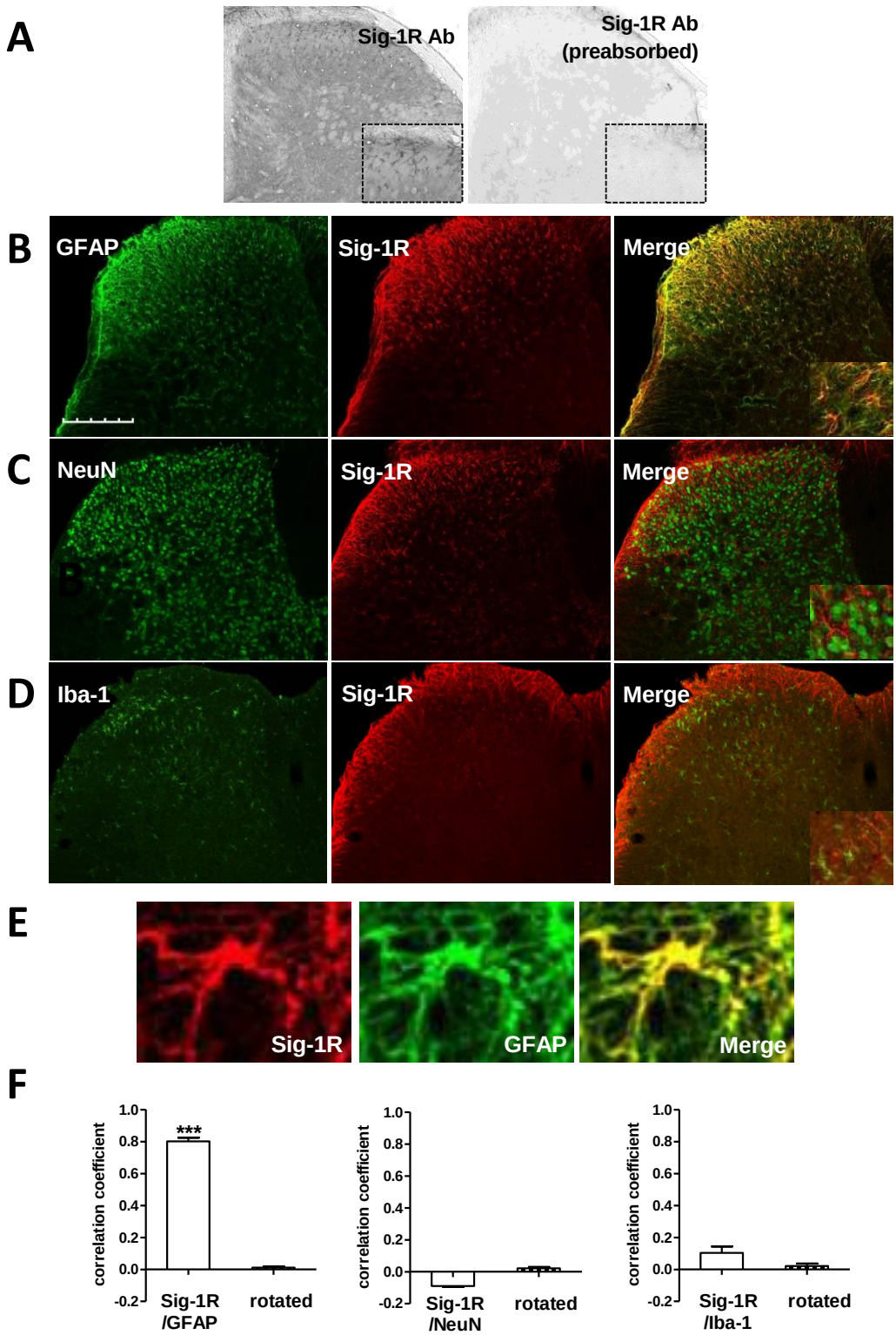
A
Sig-1R Ab
Sig-1R Ab
(preabsorbed)
B
GFAP
Sig-1R
Merge
C
NeuN
Sig-1R
Merge
D
Iba-1
Sig-1R
Merge
E
Sig-1R
GFAP
Merge
F
correlation coefficient
1.0
0.8
0.6
0.4
0.2
0.0
-0.2
***
Sig-1R /GFAP
rotated
Sig-1R /NeuN
Sig-1R /Iba-1

Figure 4. Sig-1R expression was selectively increased in astrocytes after CCI. Transverse sections through the lumbar spinal cord obtained from mice at day 3 post-CCI were processed for double immunofluorescence staining. (A), Sig-1R-immunoreactivity was not detected in any of the spinal sections processed with Sig-1R-antisera pre-absorbed with a Sig-1R peptide overnight. (B-E), immunofluorescence labeling was performed with an antibody against Sig-1R (Sig-1R, red) and double labeled with GFAP, a marker for astrocytes, NeuN, a marker for neurons or Iba-1, a marker for microglia, antibodies (green staining). Sig-1R-ir cells were colocalized with GFAP-ir cells, but not with NeuN or Iba-1 immunostained cells at postoperative day 3 in the ipsilateral dorsal horn spinal cord of CCI mice. (E), Representative fluorescent photomicrographs depicting immunolabelling for Sig-1R (red) and the astrocyte marker, GFAP (green). Double immunolabelling for Sig-1R and GFAP (yellow). (F)**,** The average correlation coefficient between Sig-1R and GFAP was 0.801, but this correlation coefficient was significantly reduced when a region within the spinal cord dorsal horn in one of the images was rotated 90 degrees with respect to the other image. In contrast, the average correlation coefficient of Sig-1R with either NeuN or Iba-1 was very low. (n=6 for each of the CCI groups). ***$p<0.001$ as compared with those of the rotated group. Scale bar, 200 μm.

1-2. Sig-1R expression in cultured astrocytes and effect of PRE-084 treatment on MAPKs phosphorylation

Primary cultures astrocytes isolated form neonatal mouse were used to determine whether Sig-1R activation directly induced MAPK phosphorylation. First, I found that primary astrocytes expressed Sig-1R receptors using immunofluorescence analysis (Fig.5A). To determine cultured astrocytes express Sig-1R, double staining was performed using an anti-Sig-1R antibody in combination with anti-GFAP antibody. Double staining with GFAP showed that the Sig-1R expression was located to astrocytes. Immunofluorescence staining without primary antibodies were processed for negative control (N.C). To test whether Sig-1R mediates MAPK activation in astrocytes, the phosphorylation of p38, ERK and JNK were probed as a function of PRE-084 exposure time using Western blot analysis. As shown in Fig.5B, the relative pixel area (%) of p-p38 expression in Western blots was significantly increased by 2 μM PRE-084 treatment, but there was no change in p38 levels, in astrocyte homogenates as early as 5 min after PRE-084 treatment and remained phosphorylated for 2 hour. Similarly, ERK was also phosphorylated by PRE-084 treatment after 5 min, whereas ERK levels was not changed (Fig.5C). On the other hand, treatment with PRE-084 did not affect the phosphorylation of JNK (Fig.5D). These data demonstrated that Sig-1R activated p38 and ERK, but not JNK in astrocytes.

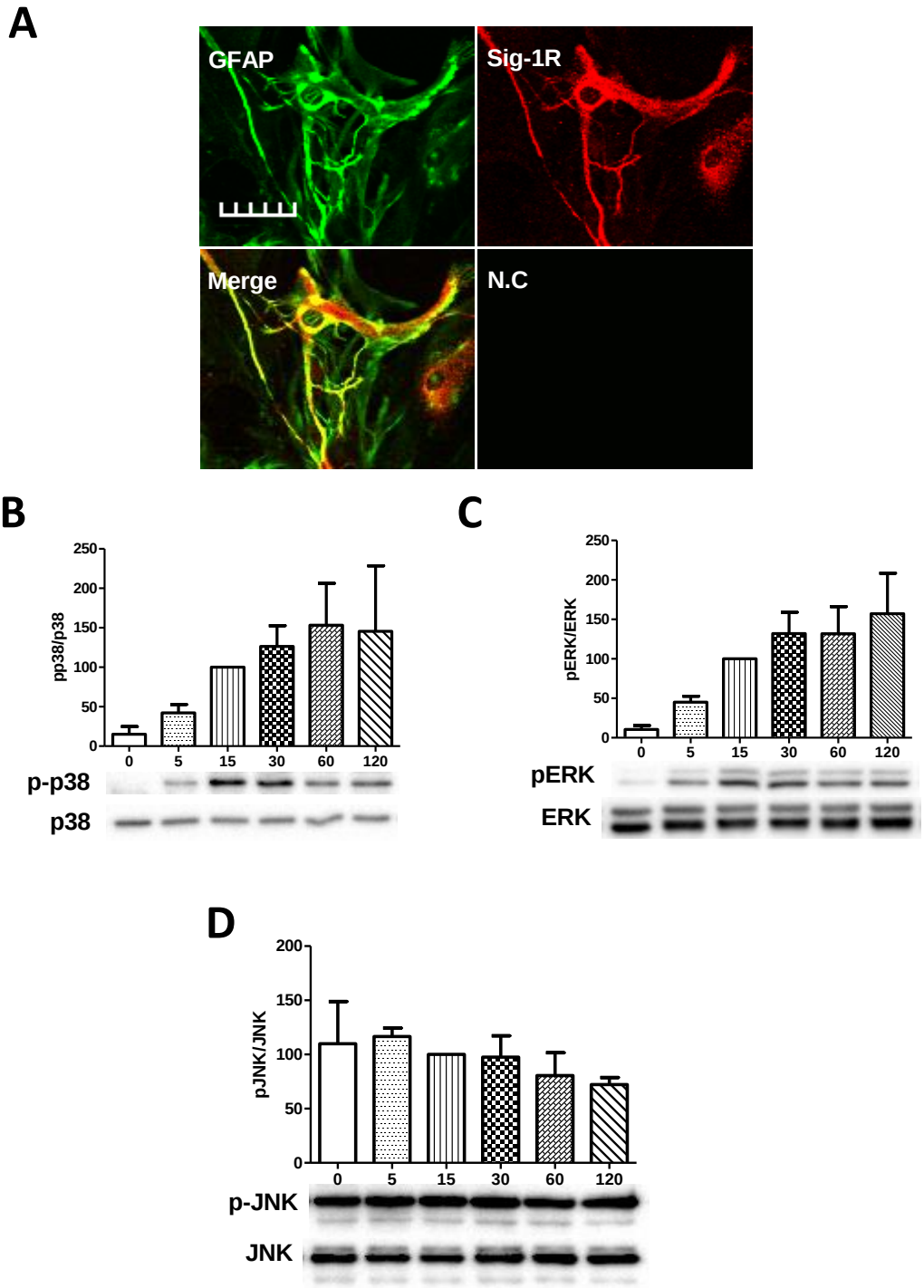
A
GFAP
Sig-1R
Merge
N.C
B
pp38/p38
250
200
150
100
50
0
0
5
15
30
60
120
p-p38
p38
C
pERK/ERK
250
200
150
100
50
0
0
5
15
30
60
120
pERK
ERK
D
pJNK/JNK
200
150
100
50
0
0
5
15
30
60
120
p-JNK
JNK

Figure 5. Sig-1R expression in cultured astrocyte and Sig-1R activation induced phosphorylation of p38 and ERK but not JNK. (A), Immunofluorescence labeling was performed with an antibody against Sig-1R (Sig-1R, red) and double labeled with GFAP (green). Sig-1R-ir cells were colocalized with GFAP-ir cells. Immunofluorescence labeling without primary antibodies was performed for negative control (N.C). (B), Western blot analysis indicated that p-p38 expression was significantly increased at 5min after 2 μM PRE-084 treatment and remained phosphorylated for 2 hour. A graph depicting the change in the p-p38 is shown in upper portion, and the representative bands of p-p38 and p38 expression are presented in the lower portion of 2B. (C), pERK expression was also significantly increased by PRE-084 treatment. (D), However, pJNK was not altered by PRE-084 treatment. Scale bar = 50 μm.

1-3. Effects of intrathecal pretreatment with ERK and p38 inhibitor on PRE-084 induced pain hypersensitivity in naïve mice

To determine whether the PRE-084-induced pain behaviors involve the activation of ERK and p38, I examined the effects of intrathecal pretreatment with the ERK inhibitor, PD98059 and p38 inhibitor, SB203580 on PRE-084-induced pain hypersensitivity in mice. The intrathecal administration of the Sig-1R agonist, PRE-084 (3 nmol, VEH + PRE), significantly increased time-dependent PWF (%) to innocuous mechanical stimuli (MA, Fig.6A and C) and decreased response latency (sec) to noxious heat stimuli (TH, Fig.6B and D) as compared with those of the vehicle (VEH + VEH) treated group. Intrathecal pretreatment with PD98059 (3, 10, 30 nmol), dose dependently suppressed these both of PRE-084-induced MA and TH (Fig.6A and B). Intrathecal pretreatment with SB203580 (0.3, 1, 3 nmol), also dose-dependently suppressed this PRE-084-induced increase in PWF (Fig.6C). On the other hand, intrathecal pretreatment with SB203580 (3, 10 nmol, Fig.6B) did not affect the PRE-084-induced decrease in thermal response latency. The intrathecal injection of this inhibitor alone (SB + VEH), in the absence of PRE, did not affect PWF or thermal response latency in comparison with the VEH + VEH group.

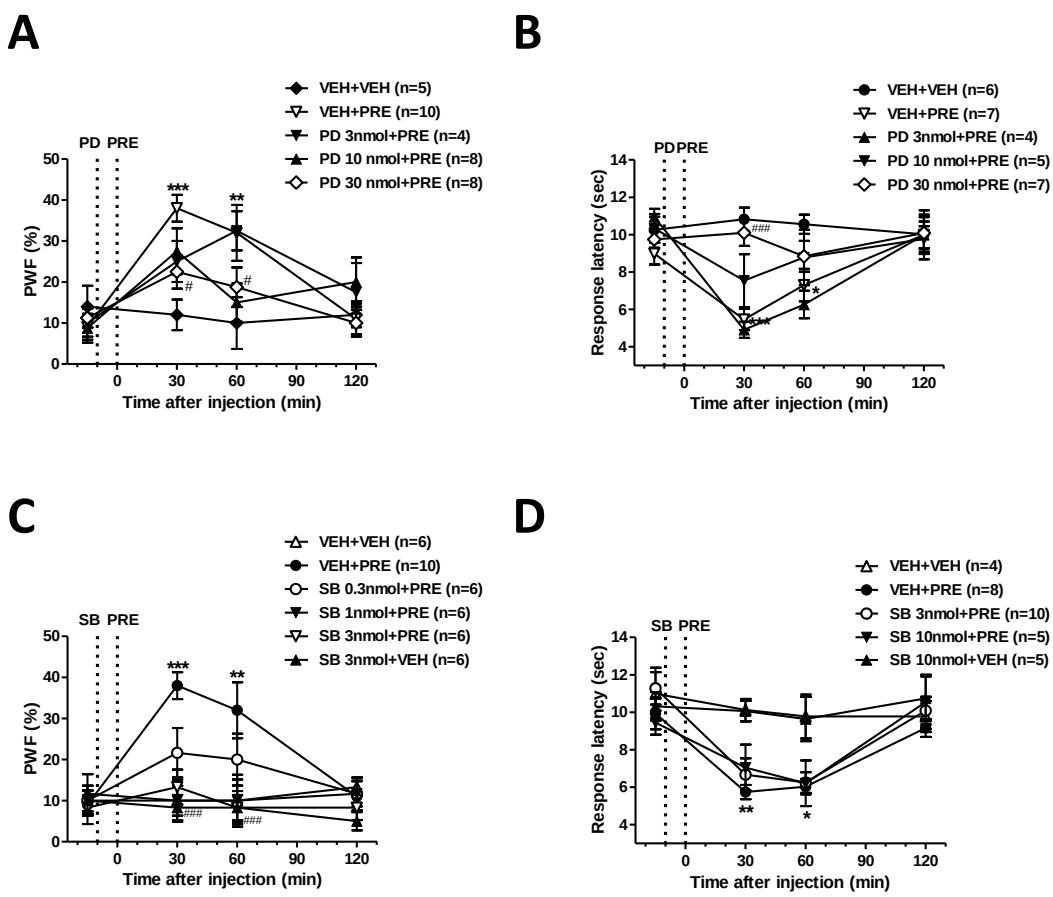
A
VEH+VEH (n=5)
VEH+PRE (n=10)
PD 3nmol+PRE (n=4)
PD 10 nmol+PRE (n=8)
PD 30 nmol+PRE (n=8)
PD PRE
PWF (%)
Time after injection (min)
B
VEH+VEH (n=6)
VEH+PRE (n=7)
PD 3nmol+PRE (n=4)
PD 10 nmol+PRE (n=5)
PD 30 nmol+PRE (n=7)
PD PRE
Response latency (sec)
Time after injection (min)
C
VEH+VEH (n=6)
VEH+PRE (n=10)
SB 0.3nmol+PRE (n=6)
SB 1nmol+PRE (n=6)
SB 3nmol+PRE (n=6)
SB 3nmol+VEH (n=6)
SB PRE
PWF (%)
Time after injection (min)
D
VEH+VEH (n=4)
VEH+PRE (n=8)
SB 3nmol+PRE (n=10)
SB 10nmol+PRE (n=5)
SB 10nmol+VEH (n=5)
SB PRE
Response latency (sec)
Time after injection (min)

Figure 6. Spinal pERK mediates PRE-084 induced MA and TH, whereas p38 mediated only in PRE-084 induced MA, but not TH. Graphs illustrating the effects of intrathecal administration of the pERK inhibitor, PD98059 (PD+PRE) and p38 inhibitor, SB203580 (SB+PRE) on the PRE-084-induced changes in the paw withdrawal frequency over time (PWF, MA), and in the thermal latency responses (TH) of mice. The inhibitors were applied 10 min before PRE-084 injection. (A), Intrathecal pretreatment with PD98059 blocked the increase in PWF that occurred in PRE-084 treated group in dose dependent manner. (B), Intrathecal pretreatment with PD98059 also blocked response latency. (C), Intrathecal pretreatment with SB203580 reduced PRE-084-induced MA in dose dependent manner. (D), However, the decrease in latency responses to heat stimuli was unaffected by intrathecal pretreatment with even the highest dose of SB203580 tested. $*P < 0.05$, $**P < 0.01$ and $***P<0.001$ as compared with those of the VEH+VEH group and $\#P < 0.05$ and $\#\#\#P <0.001$ as compared with those of the VEH + PRE group.

1-4. Effect of intrathecal PRE-084 injection on p-p38 expression in the mouse spinal cord dorsal horn

An anti-p-p38 antibody was used to examine changes in p38 activation. To determine whether p38 was activated by Sig-1 R, I performed immunohistochemistry and Western blot analysis. The expression of p-p38 was examined initially in the spinal cord of naïve mice that received administration of the PRE-084. The intrathecal administration of PRE-084 (3 nmol, VEH + PRE), significantly increased the number of p-p38-ir cells in the spinal dorsal horn at the 60 min post-injection time point as compared with that of a vehicle-treated group (Fig.7A and B). To further determine whether this increase in the number of p-p38-ir cells was a direct and specific result of activation of spinal Sig-1R, I next pretreated a separate group of mice with a Sig-1R antagonist prior to intrathecal treatment with PRE-084. As illustrated in Fig.7A, intrathecal pretreatment with the Sig-1 R antagonist, BD-1047 (100 nmol, BD + PRE), completely blocked the PRE-084-induced increase in the number of p-p38-ir cells at the 60 min post-injection time point. The intrathecal injection of this inhibitor alone (BD + VEH), in the absence of PRE, did not affect the number of p-p38-ir cells in comparison to the vehicle injected group. Western blot analysis also confirmed the effects of intrathecal administration of PRE-084 on p-p38 levels in the spinal cord of naïve mice (Fig.7C). Thus, the relative pixel area (%) of p-p38 expression in Western blots was significantly increased by PRE-084 treatment (Fig.7C), but there was no change in p38 levels, in spinal cord homogenates 60 min after intrathecal injection of PRE-084 as compared with the vehicle pretreatment group. In addition, intrathecal pretreatment with the Sig-1 R antagonist, BD-1047 (100 nmol, BD + PRE), completely blocked the PRE-084-induced increase in p-p38 expression at the 60 min post-injection time point which confirms the immunocytochemical data.

A

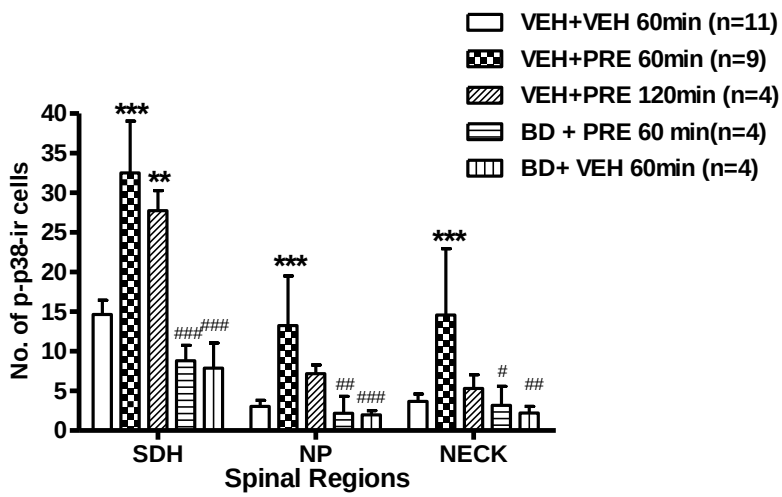
VEH+VEH 60min (n=11)
VEH+PRE 60min (n=9)
VEH+PRE 120min (n=4)
BD + PRE 60 min(n=4)
BD+ VEH 60min (n=4)
No. of p-p38-ir cells
40
35
30
25
20
15
10
5
0
***
**
***
***
###
###
##
###
#
##
SDH
NP
NECK
Spinal Regions

B

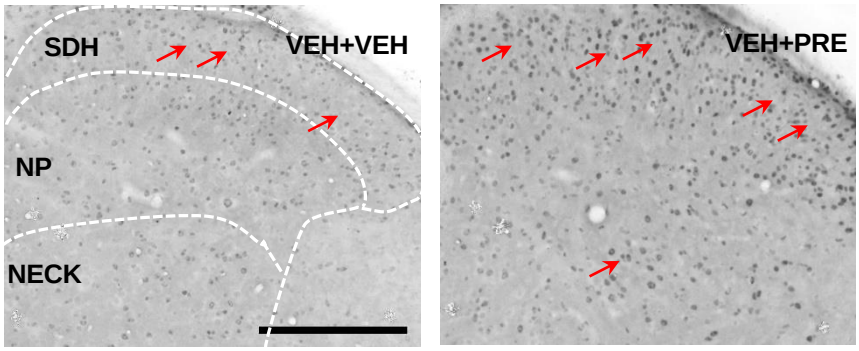
SDH
VEH+VEH
NP
NECK
VEH+PRE

C

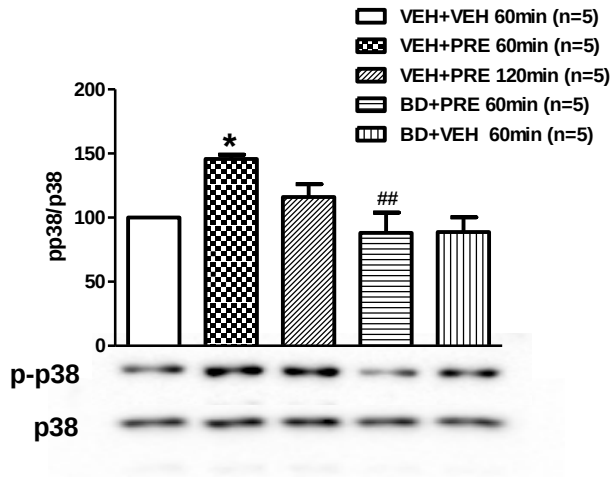
VEH+VEH 60min (n=5)
VEH+PRE 60min (n=5)
VEH+PRE 120min (n=5)
BD+PRE 60min (n=5)
BD+VEH 60min (n=5)
pp38/p38
200
150
100
50
0
*
##
p-p38
p38

Figure 7. The effect of intrathecal administration of PRE-084 on p-p38 in the mouse spinal cord dorsal horn. Quantitative graphs and representative photomicrographs illustrating the effect of intrathecal injection of PRE-084 (PRE, 3 nmol) on the number of p-p38-ir cells in the spinal cord dorsal horn. (A), The number of p-p38-ir cells in the superficial dorsal horn (SDH, lamina I–II), in the nucleus proprius (NP, lamina III–IV) and in the neck region (NECK, lamina V–VI) of the spinal dorsal horn are depicted graphically. Intrathecal administration of PRE-084 (VEH+PRE), significantly increased the number of p-p38-ir cells in the dorsal horn as compared with that of the vehicle-treated group (VEH+VEH) at the 60 min post-injection time point. Moreover, pretreatment with the sigma-1 receptor antagonist BD-1047 (BD+PRE, 100 nmol) before sigma-1 receptor agonist injection completely blocked the effect of PRE-084 on p-p38 expression (B), Representative photomicrographs depicting p-p38-ir cells in the SDH, NP, and NECK of the spinal dorsal horn from vehicle and PRE-084 treated mice. Arrows indicate representative p-p38-ir cells. (C) Western blot analysis illustrating the effect of intrathecal administration of the PRE-084 on p-p38. A graph depicting the change in the p-p38 is shown in the upper portion, and the representative bands of p-p38 and p38 are presented in the lower portion. Representative Western blots showing an increase in p-p38 (top), but no change in p38 (bottom). $*P < 0.05$, $**P < 0.01$ and $***P<0.001$ as compared with those of the VEH+VEH group and $\#P < 0.05$, $\#\#P < 0.01$ and $\#\#\#P <0.001$ as compared with those of the VEH + PRE group. Scale bar = 200 μm.

2. The histological and physiological relationships among Sig-1R, p-p38 and astrocyte activation in the spinal cord of CCI mice

2-1. Changes of Sig-1R, microglia and astrocyte expressions in the spinal cord of CCI mice

I performed Western blot analysis to confirm the changes of Sig-1R, microglia and astrocyte expressions in the spinal cord of mice at 1, 3, 7 and 14 day after CCI surgery. Increased expression of microglial markers Iba-1 and astrocyte markers GFAP were used for microglia and astrocyte activation, respectively. There was a significant CCI-induced increase in Sig-1R expression on Western blots that peaked at 3 days post-surgery and this increased expression was restored to sham surgery values by 7 days post-surgery (Fig.8A). The expression of Iba-1 on immunoblots was significantly increased from day 1 to 3 after CCI (Fig.8B). The expression of GFAP was significantly increased from day 3 to 7 after CCI (Fig.8C).

A

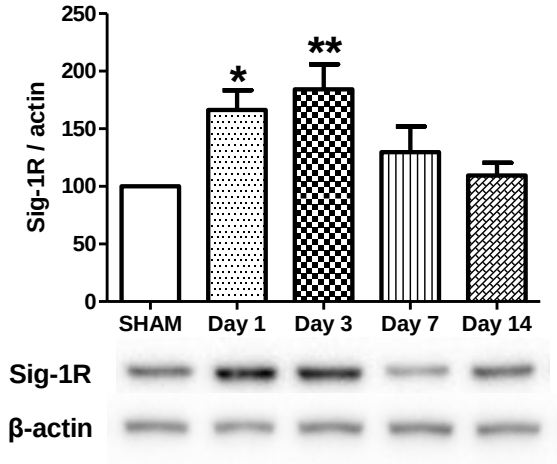
Sig-1R / actin
250
200
150
100
50
0
*
**
SHAM
Day 1
Day 3
Day 7
Day 14
Sig-1R
β-actin

B

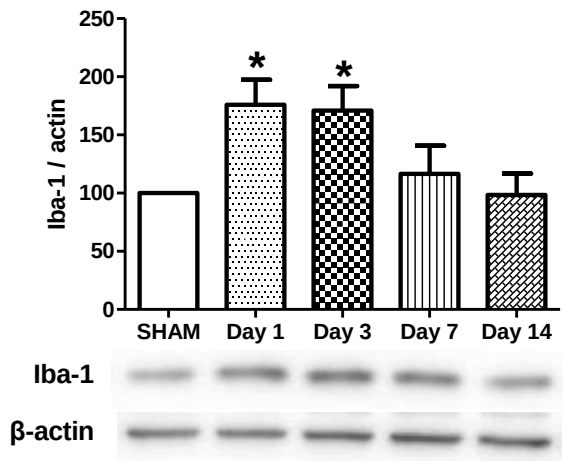
Iba-1 / actin
250
200
150
100
50
0
*
*
SHAM
Day 1
Day 3
Day 7
Day 14
Iba-1
β-actin

C

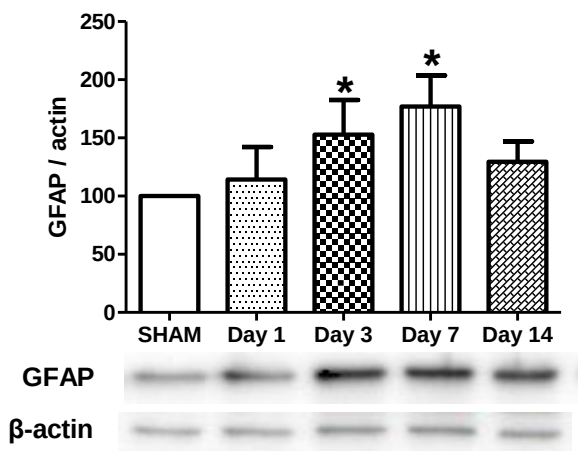
GFAP / actin
250
200
150
100
50
0
*
*
SHAM
Day 1
Day 3
Day 7
Day 14
GFAP
β-actin

Figure 8. CCI-induced changes in the expression of Sig-1R, Iba-1 and GFAP in the spinal cord of mice. Western blot analysis indicated that Sig-1R expression was significantly increased by postoperative day 1 and reached a peak level by postoperative day 3 when compared with Sig-1R expression in sham surgery animals (n=9 at each time point in the CCI or sham surgery groups). (B), Iba-1 expression also was significantly increased by postoperative days 1 and 3 (n=5 at each time point). (C), GFAP expression was significantly increased by postoperative day 3 and reached a peak level by postoperative day 7 when compared with that of sham surgery animals (n= 5 at each time point). *$p<0.05$ and **$p<0.01$ as compared with those of SHAM group.

2-2. Effects of intrathecal BD-1047 administration on the Iba-1 and GFAP expression in CCI mice

I performed a Western blot analysis to examine whether the CCI-induced increase in Iba-1 and GFAP expression was regulated by Sig-1R activation during the induction phase. Intrathecal administration of the Sig-1R antagonist, BD-1047 (100 nmol, CCI+BD) on postoperative days 0-3 significantly attenuated the CCI-induced increase in GFAP expression on day 3 post-CCI surgery as compared with the vehicle treated group (Fig.9A). However, CCI-induced increase in Iba-1 expression was not altered by intrathecal treatment with BD-1047 (Fig.9B). Immunohistochemistry analysis also confirmed that intrathecal administration of BD-1047 effectively attenuated the CCI-induced increase in the number of GFAP-ir cells in the SDH and NP region (Fig.9C).

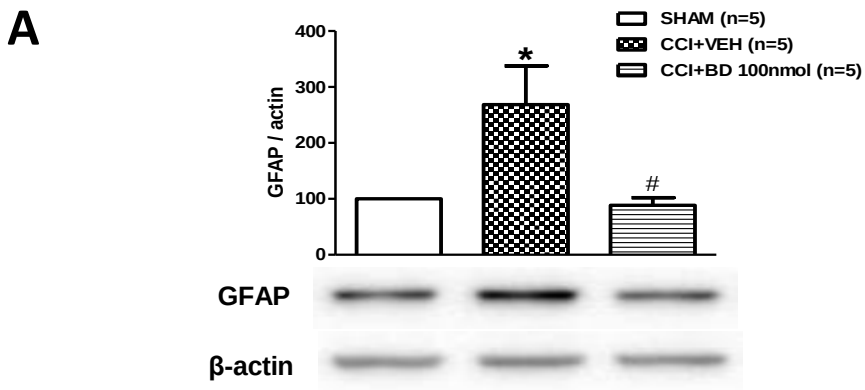
A
SHAM (n=5)
CCI+VEH (n=5)
CCI+BD 100nmol (n=5)
GFAP / actin
400
300
200
100
0
*
#
GFAP
β-actin

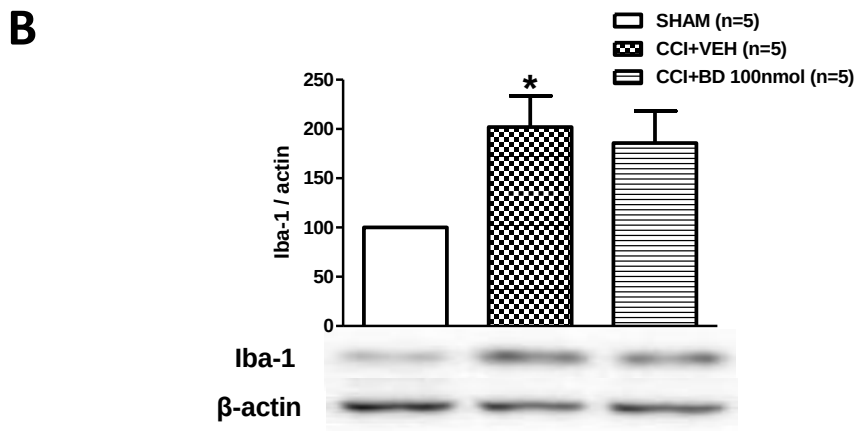
B
SHAM (n=5)
CCI+VEH (n=5)
CCI+BD 100nmol (n=5)
Iba-1 / actin
250
200
150
100
50
0
*
Iba-1
β-actin

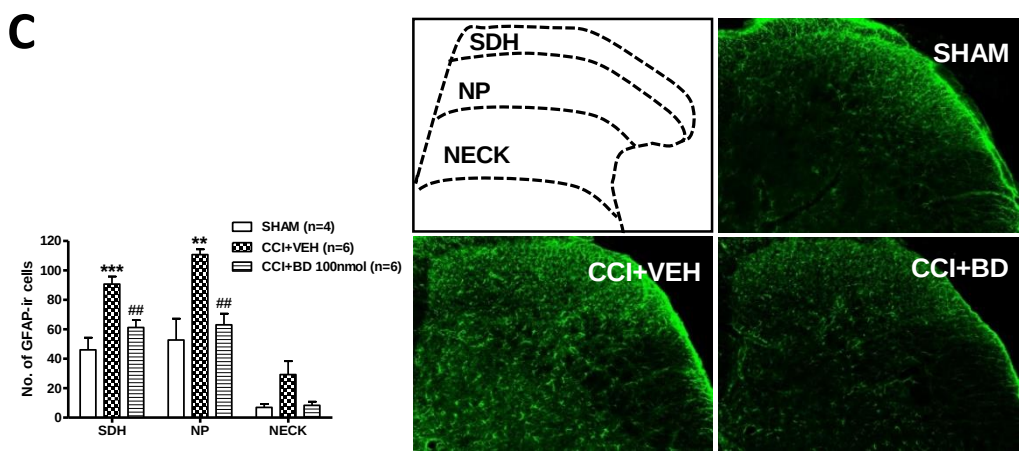
C
SHAM (n=4)
CCI+VEH (n=6)
CCI+BD 100nmol (n=6)
No. of GFAP-ir cells
120
100
80
60
40
20
0
***
**
##
##
SDH
NP
NECK
SDH
NP
NECK
SHAM
CCI+VEH
CCI+BD

Figure 9. The CCI-induced increase in GFAP expression is blocked by spinal injection of the Sig-1R antagonist, BD-1047. (A), Western blot analysis showed that intrathecal injection of BD-1047 (CCI+BD, 100 nmol, administered from days 0 to 3 after surgery) significantly decreased the level of CCI-induced GFAP expression as compared with the vehicle treated group. A graph depicting the change in the GFAP is shown in the upper portion, and the representative bands of GFAP and β-actin expression are presented in the lower portion of 6A. (B), However, CCI-induced increase in Iba-1 expression was unaffected by intrathecal BD-1047 treatment. (C), Immunohistochemistry also demonstrated that intrathecal treatment of BD-1047 robustly suppressed the number of GFAP-ir cells in ipsilateral spinal cord dorsal horn as compared with the vehicle treated group. Photomicrographs of representative L4-5 spinal cord sections illustrating GFAP-ir cells in the sham group (SHAM), in the saline treated CCI group (CCI+VEH) and in the BD-1047 treated CCI group (CCI+BD). An illustration depicting the location of the different spinal cord regions analyzed in this study is shown in the upper left panel of this Figure. *$p<0.05$, **$p<0.01$ and ***$p<0.001$ as compared with those of SHAM group, and #$p<0.05$ and ##$p<0.01$ as compared with those of the CCI+VEH group.

2-3. Cellular distribution of p-p38 in spinal cord dorsal horn after CCI

Because the activation of p38 in the spinal cord contributes to the PRE-084-induced MA and that p-p38 is regulated by Sig-1R activation in naïve mice, I also confirm the contribution of p-p38 relation with Sig-1R in CCI mice. First, I performed immunofluorescence analysis to confirm the cellular distribution of p-p38 in mice lumbar spinal cord sections on day3 after surgery (Fig.10). To determine which cell types express p-p38 in the spinal cord dorsal horn in CCI mice, double staining was performed using NeuN, GFAP or an Iba-1 antibody. I found that the majority of the p-p38 staining was in the nucleus of astrocytes (Fig.10A) or neurons (Fig.10B). There was no evidence of p-p38 staining in Iba-1-positive microglia (Fig.10C).

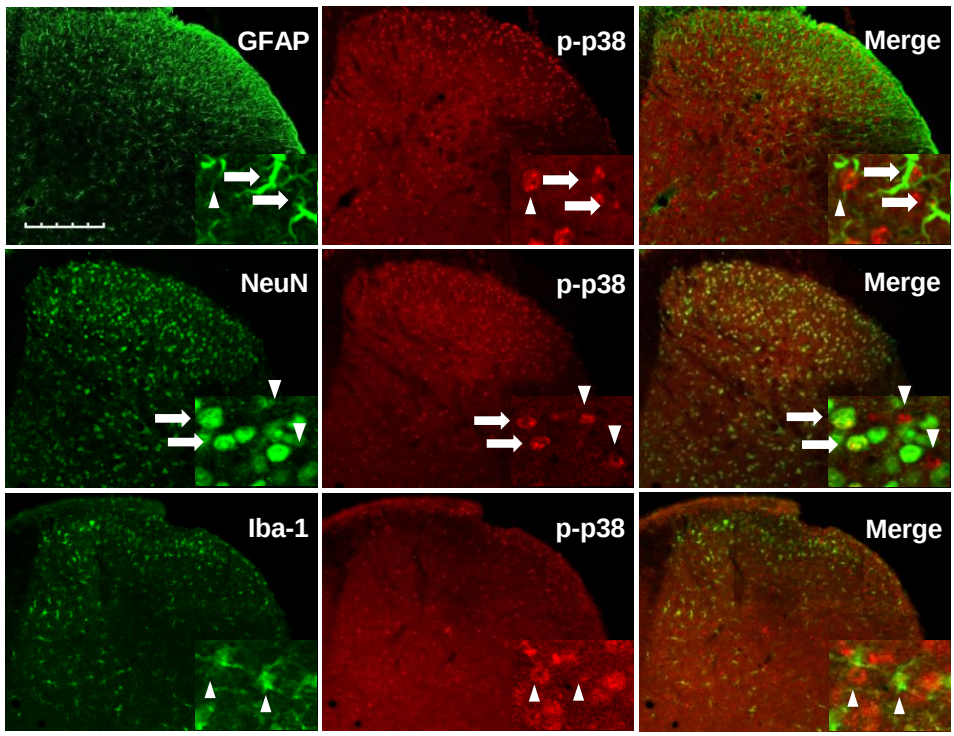

Figure 10. p-p38 was located in spinal astrocytes and neurons following CCI in mouse ipsilateral spinal cord dorsal horn. Transverse sections through the lumbar spinal cord segment 3 d after CCI were labeled with an antibody against phospho-p38 (p-p38, red) and double labeled with GFAP, Iba-1 or NeuN antibodies (green). (A and B), The increased p-p38-ir staining was preferentially located in the nuclei of GFAP-positive and NeuN-positive cells. (A), Some of the p-p38-labeled cells were GFAP-positive astrocytes (arrows), while others were not GFAP positive (arrowheads). (B), p-p38-labeled cells were clearly double labeled with NeuN antisera, a neuronal marker (arrows), although some phospho-p38-labeled cells were not NeuN-positive neurons (arrowheads). (C), No colocalization was detected for phospho-p38 and Iba-1, a microglia marker (arrowheads). Scale bar, 200 μm

2-4. Effects of intrathecal BD-1047 administration on p-p38 expression in astrocytes or neurons in CCI mice

The CCI-induced increased in p-p38 expression was decreased by BD-1047 treatment during the induction phase on day 3 after CCI surgery (Fig.11A). I next performed double staining to examine whether the p-p38 located in astrocytes or neurons or both is regulated by Sig-1Ractivation. There was a CCI-induced increase in p-p38 immunostaining in both GFAP and NeuN positive cells in the SDH and NP regions of the dorsal horn as compared with that of the sham group (Fig.11B and C). Repeated daily, i.t administration of BD-1047 significantly decreased the level of CCI-induced p-p38 expression in GFAP labeled cells (Fig.11B), but not in NeuN labeled cells (Fig.11C), as compared to the vehicle treated group.

A

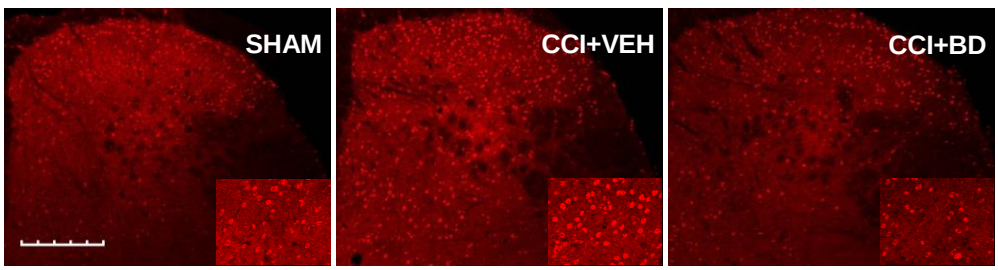
SHAM
CCI+VEH
CCI+BD

B

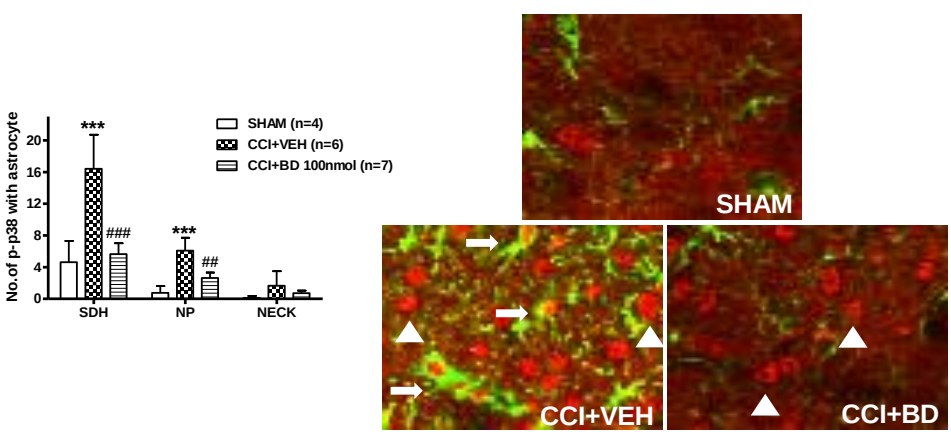
No.of p-p38 with astrocyte
SHAM (n=4)
CCI+VEH (n=6)
CCI+BD 100nmol (n=7)
***
###
***
##
SDH
NP
NECK
SHAM
CCI+VEH
CCI+BD

C

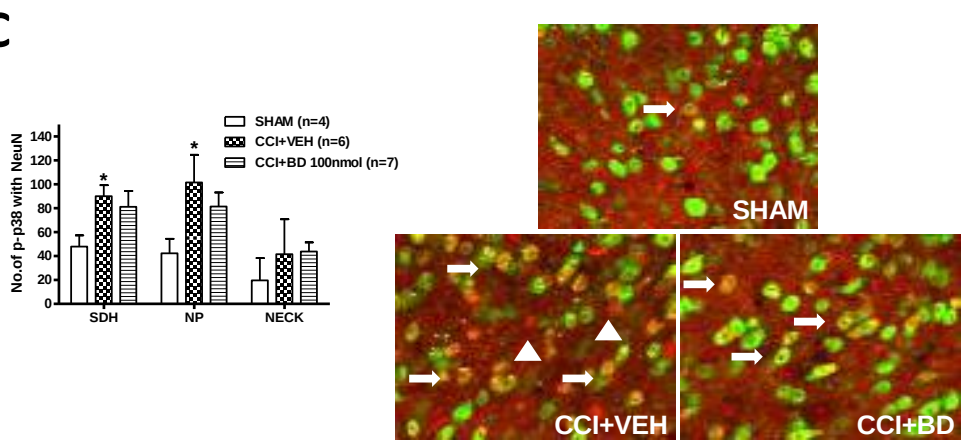
No.of p-p38 with NeuN
SHAM (n=4)
CCI+VEH (n=6)
CCI+BD 100nmol (n=7)
*
*
SDH
NP
NECK
SHAM
CCI+VEH
CCI+BD

Figure 11. Intrathecal treatment with the Sig-1R antagonist, BD-1047 decreased the level of CCI-induced p-p38 expression located in astrocytes, but not in neurons. (A), p-p38 expression was significantly increased on day 3 after CCI surgery, and this CCI-induced increase in p-p38 expression was suppressed by BD-1047 treatment during the induction phase. (B), Intrathecal administration of BD-1047 decreased the level of CCI-induced p-p38 expression colocalized with GFAP as compared with the vehicle treated group. (C) However, increased p-p38 expression colocalized with NeuN was not altered by intrathecal treatment with BD-1047. *$p<0.05$ and ***$p<0.001$ as compared with those of SHAM group, and ##$p<0.01$ and ###$p<0.001$ as compared with those of the CCI+VEH group. Scale bar, 200 μm

2-5. Effects of intrathecal SB203580 administration on the GFAP expression in CCI mice

I performed a Western blot analysis and immunohistochemistry to examine whether the CCI-induced increase in GFAP expression was regulated by p38 activation. Sustained i.t administration of the p38 inhibitor, SB203580, (3 nmol, CCI+SB) on postoperative days 0-3 significantly reduced the CCI-induced increase in GFAP expression, as compared with vehicle-treated CCI mice (Fig.12A). Immunohistochemistry analysis also confirmed that the i.t administration of SB203580 during the induction phase effectively attenuated the CCI-induced increase in the number of GFAP-ir cells in all dorsal horn laminae (Fig.12B).

A

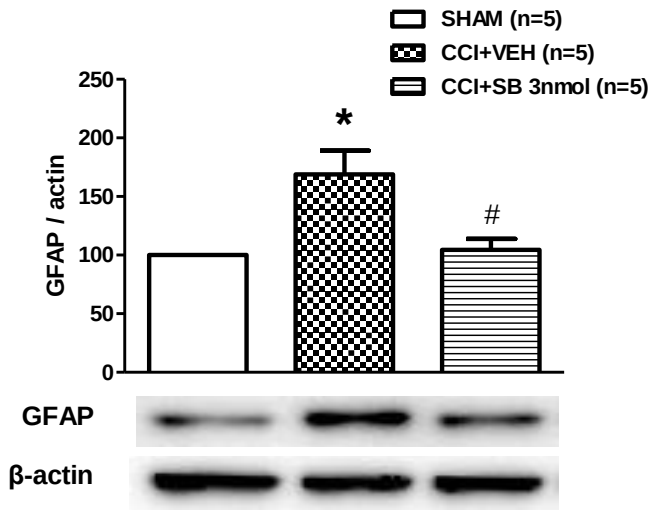
SHAM (n=5)
CCI+VEH (n=5)
CCI+SB 3nmol (n=5)
GFAP / actin
250
200
150
100
50
0
*
#
GFAP
β-actin

B

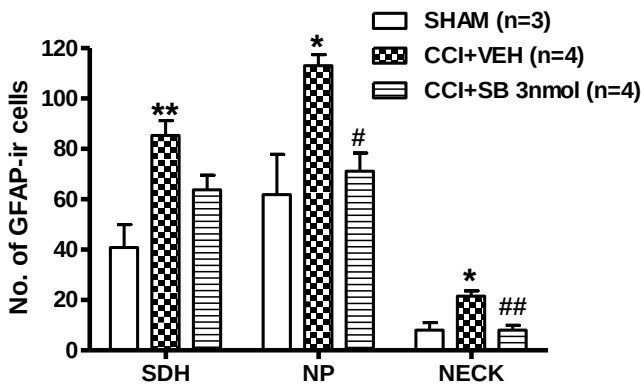
SHAM (n=3)
CCI+VEH (n=4)
CCI+SB 3nmol (n=4)
No. of GFAP-ir cells
120
100
80
60
40
20
0
**
*
#
*
##
SDH
NP
NECK

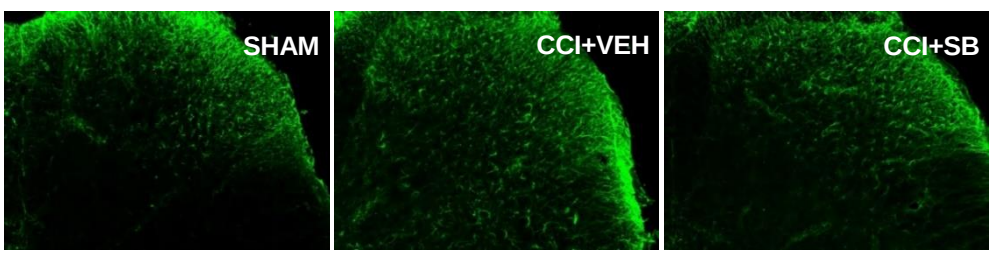
SHAM
CCI+VEH
CCI+SB

Figure 12. The CCI-induced GFAP increase is blocked by spinal injection of the p38 inhibitor, SB203580. (A), Western blot analysis showed that intrathecal injection of SB203580 (CCI+SB, 3 nmol, administered from days 0 to 3 after surgery) significantly decreased the level of CCI-induced GFAP expression as compared with the vehicle treated group. A graph depicting the change in GFAP is shown in the upper portion of 9A, and the representative bands of GFAP and β-actin expression are presented in the lower portion. (B), Immunohistochemistry also demonstrated that intrathecal treatment of SB203580 robustly suppressed the number of GFAP-ir cells in the ipsilateral dorsal horn as compared with the vehicle treated group. Photomicrographs of representative L4-5 spinal cord sections illustrating GFAP-ir cells in the sham group (SHAM), in the saline treated CCI group (CCI+VEH) and in the SB203580 treated CCI group (CCI+SB). *$p<0.05$ and **$p<0.01$ as compared with those of SHAM group, #$p<0.05$ and ##$p<0.01$ as compared with those of the CCI+VEH group.

3. Releasing factor induced by spinal Sig-1R in CCI mice

3-1. CCI-induced changes in the levels of D-serine and its cellular distribution in the dorsal horn of neuropathic mice

To investigate the potential roles of D-serine in CCI mice, I performed immunohistochemistry analysis using an anti-D-serine antibody on mouse lumbar spinal cord sections at 1, 3 and 7 day after CCI surgery. The level of D-serine in the ipsilateral spinal cord dorsal horn was significantly increased from day 1 to day 3 after CCI as compared with that of sham surgery group (Fig.13A). The distribution of increased D-serine was primarily in the SDH and NP regions. The upper right hand panel in Figure 13 shows representative photomicrographs of L4-5 spinal cord sections demonstrating D-serine-ir cells after sham surgery or at 1, 3 and 7 day after CCI surgery. Double staining was performed at day 3 post-CCI surgery to determine which cell types express D-serine on the dorsal horn in CCI mice (Fig.13B-D). Anti-D-serine antibody was used in combination with GFAP, NeuN and Iba-1 antibodies. Double-labeling with D-serine and GFAP revealed a colocalization of D-serine and astrocytes in the SDH regions (Fig.13B). By comparison, in the deep dorsal horn, D-serine was found primarily associated with neurons rather than astrocytes (Fig.13C). D-serine labeling in the somata of such neurons was punctate and absent from the nucleus. There was no evidence of D-serine staining in Iba-1 positive microglia (Fig.13D).

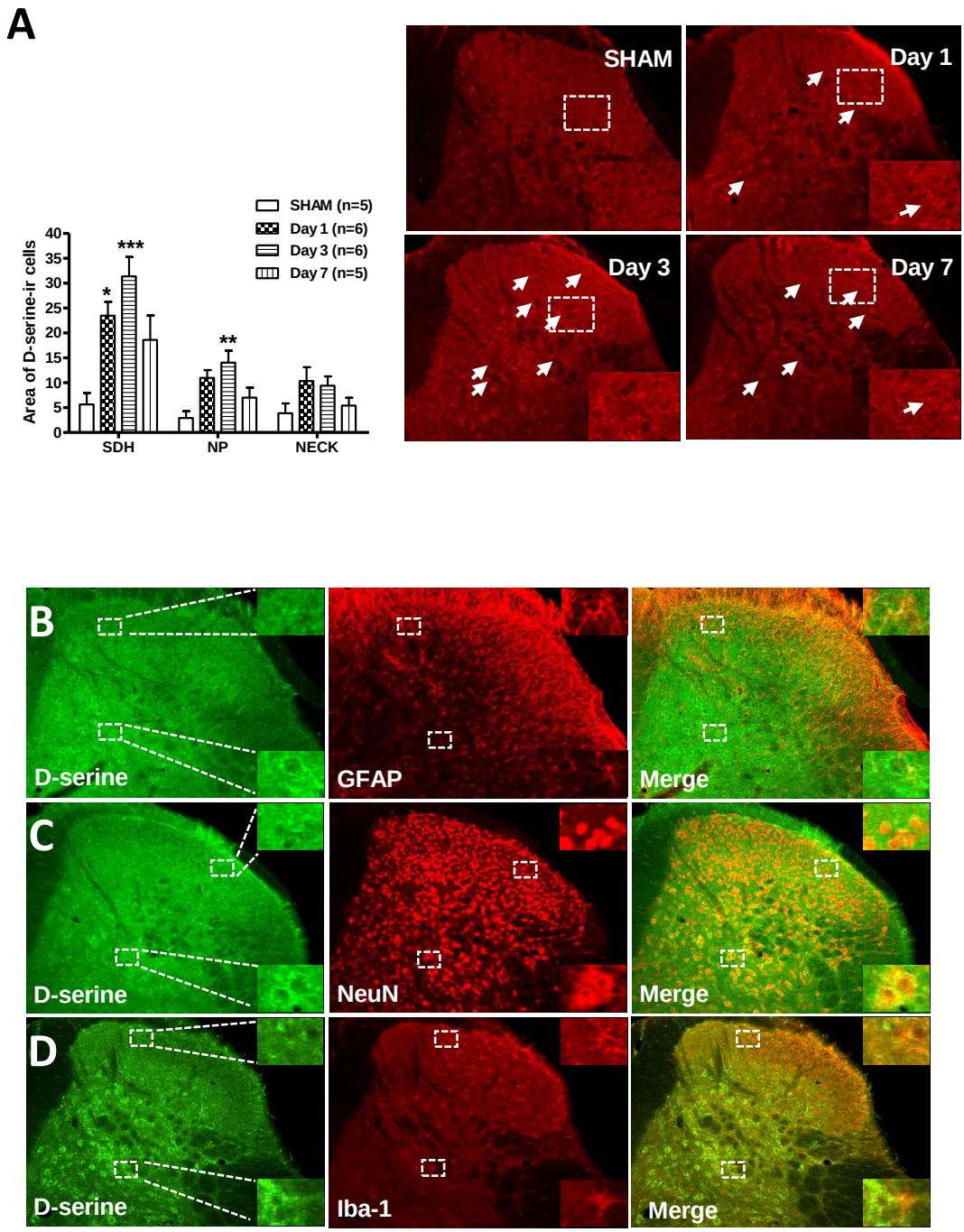
A
SHAM
Day 1
Day 3
Day 7
SHAM (n=5)
Day 1 (n=6)
Day 3 (n=6)
Day 7 (n=5)
Area of D-serine-ir cells
40
35
30
25
20
15
10
5
0
*
***
**
SDH
NP
NECK
B
D-serine
GFAP
Merge
C
D-serine
NeuN
Merge
D
D-serine
Iba-1
Merge

Figure 13. Elevation of D-serine levels in the spinal cord following CCI surgery and its distribution in astrocytes and neurons. (A), Immunofluorescence analysis with an anti-D-serine antibody was performed on lumbar spinal cord sections from CCI mice. D-serine-ir cells were significantly increased from days 1 to 3 post-CCI as compared with that of sham surgery group. Representative photomicrographs of D-serine-ir cells indicates that D-serine is significantly increased in the ipsilateral superficial layers of the dorsal horn, but also increased in the deeper laminae of CCI mice compared to the that of sham surgery groups. (B-D), Double Immunofluorescence labeling was performed with an antibody against D-serine (D-serine, green) and an antibody against GFAP, a marker for astrocytes, NeuN, a marker for neurons or Iba-1, a marker for microglia (red). (B), D-serine was colocalized with GFAP-positive astrocytes in the superficial lamina of dorsal horn. (C), Double immunofluorescence analysis also showed that D-serine accumulated along the surface of the NeuN-positive neurons in the deep dorsal horn in lumbar spinal cord sections from CCI mice. D-serine labeling in the somata of such neurons was punctate and absent from the nucleus. (D), There was no evidence of D-serine staining in Iba-1 positive microglia. Arrows indicated D-serine-ir cells. *$p<0.05$, **$p<0.01$ and ***$p<0.001$ as compared with those of sham surgery group. Scale bar, 200 μm.

3-2. CCI-induced changes in serine racemase expression and cellular distribution in the dorsal horn of neuropathic mice

Because D-serine is primarily generated by the conversion of L-serine induced by Srr, I performed Western blot analysis to determine the levels of Srr expression at 1, 3 and 7 day after CCI surgery. The expression of Srr in the ipsilateral dorsal horn was significantly increased on day 1 following CCI as compared that of sham surgery group (Fig.14A). By 7 days post-CCI, Srr expression was restored to normal pre-CCI values, and no statistical significance was evident when compared with that of the sham surgery group. Double staining was performed at day 1 post-CCI surgery to determine which cell types express Srr in the ipsilateral dorsal horn in CCI mice. The anti-Srr antibody was used in combination with GFAP, NeuN and Iba-1. Double-labeling with Srr and GFAP revealed a distinct colocalization of Srr and astrocytes (Fig.14B). There was no evidence of Srr staining in neurons or Iba-1 positive microglia (Fig.14C and D). Accordingly, the elevation of the D-serine levels in CCI mice appears to be caused by increased Srr expression in dorsal horn astrocytes.

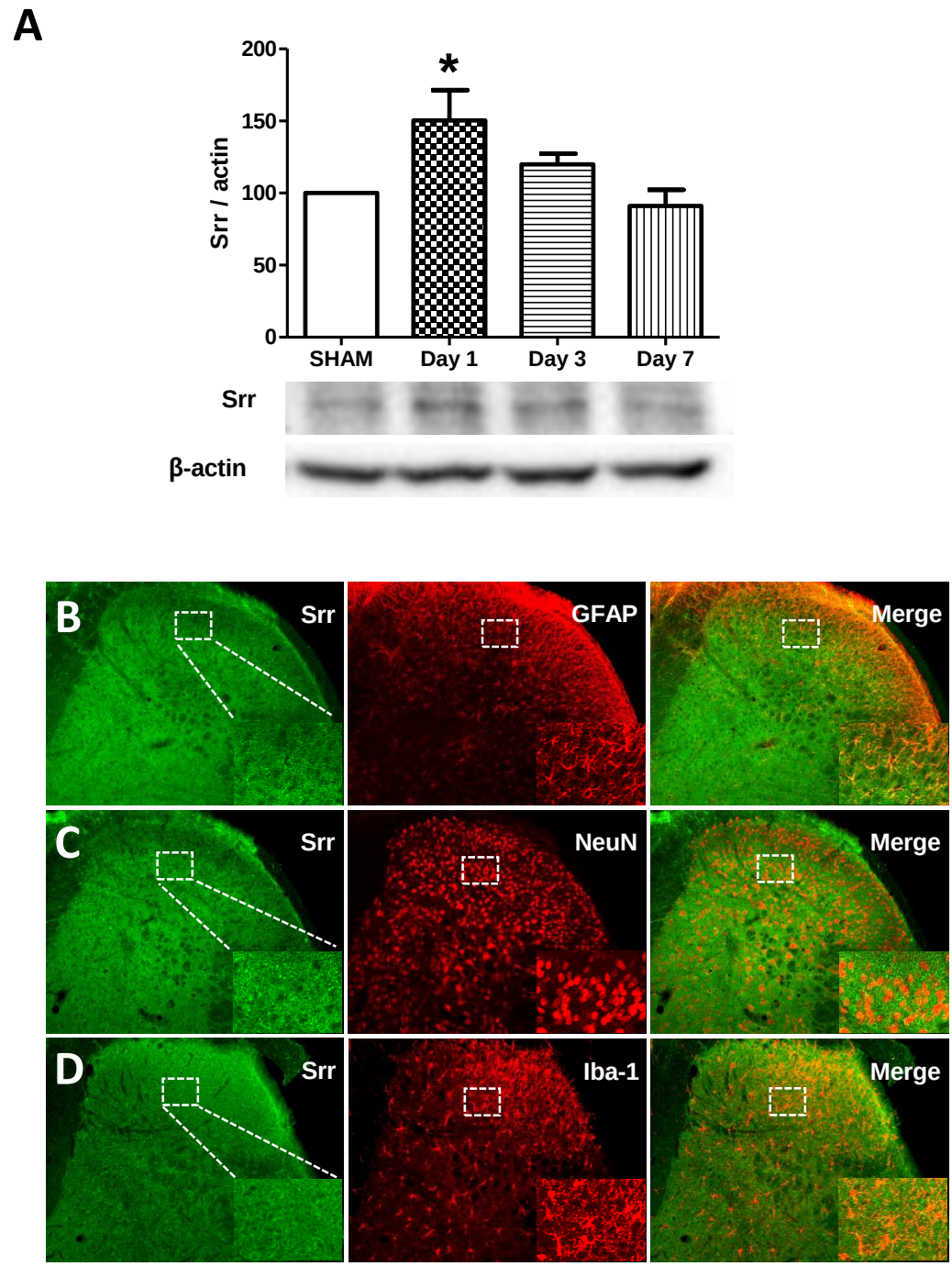
A
200
150
100
50
0
Srr / actin
*
SHAM
Day 1
Day 3
Day 7
Srr
β-actin
B
Srr
GFAP
Merge
C
Srr
NeuN
Merge
D
Srr
Iba-1
Merge

Figure 14. Elevation of Srr expression in the spinal cord after CCI surgery and specific localization to dorsal horn astrocytes. (A), Western blot analysis indicated that Srr expression was significantly increased by postoperative day 1 to 3 when compared with Srr expression in sham surgery animals (n=5 at each time point in the CCI or sham surgery groups). (B-D), Double staining was performed at day 1 post-CCI surgery to determine which cell types express Srr in the ipsilateral dorsal horn in CCI mice. (B), Double-labeling with Srr and GFAP revealed a distinct colocalization of Srr in astrocytes. (C and D), There was no evidence of Srr staining in neurons or Iba-1 positive microglia. *$p<0.05$ as compared with those of SHAM surgery group. Scale bar, 200 μm.

3-3. Effects of intrathecal BD-1047 administration on the increased level of D-serine in CCI mice

To determine whether the CCI-induced increase in the level of D-serine was induced by Sig-1R activation during the induction phase, I performed immunohistochemistry analysis on day 3 post-CCI surgery. Sustained intrathecal administration of the Sig-1R antagonist, BD-1047 (100 nmol, CCI+BD) on postoperative 0-3 significantly attenuated the CCI-induced increase in the levels of D-serine in the SDH and NP regions of the dorsal horn compared with the vehicle treated group (Fig.15A). Representative photomicrographs of L4-5 spinal cord sections illustrating D-serine-ir cells in the sham group (SHAM), in the saline treated CCI group (CCI+VEH) and in the BD-1047-treated CCI group (CCI+BD) is shown in Figure 15B. An illustration depicting the location of the different spinal cord regions analyzed in this study is shown in the upper left panel of this Figure (Fig.15B).

A

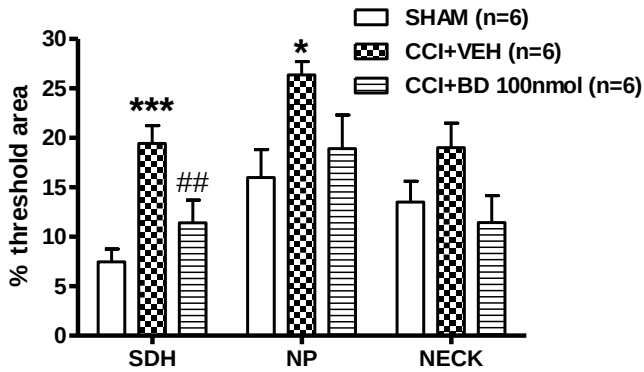
SHAM (n=6)
CCI+VEH (n=6)
CCI+BD 100nmol (n=6)
% threshold area
30
25
20
15
10
5
0
***
*
##
SDH
NP
NECK

B

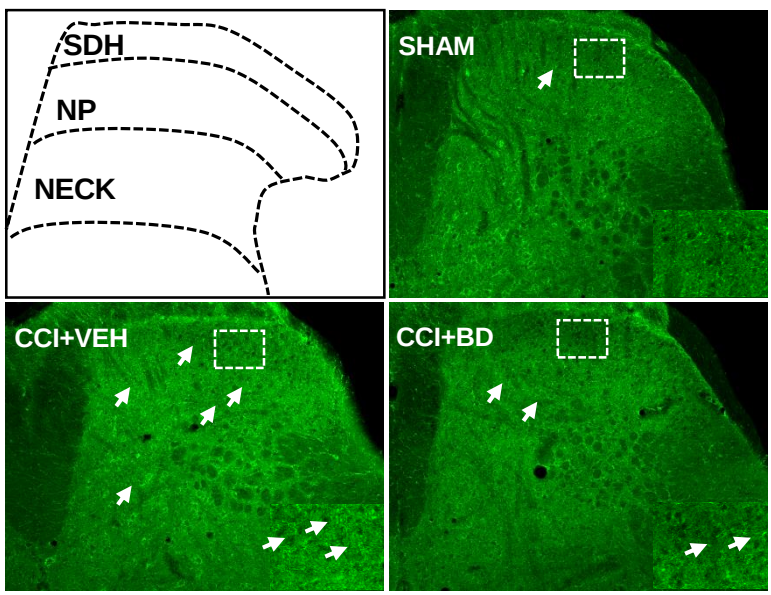
SDH
NP
NECK
SHAM
CCI+VEH
CCI+BD

Figure 15. The CCI-induced increase of D-serine level is blocked by spinal injection of the Sig-1R antagonist, BD-1047. (A), Immunofluorescence analysis indicated that sustained intrathecal administration of the Sig-1R antagonist, BD-1047 (100 nmol, CCI+BD) on postoperative 0-3 significantly attenuated the CCI-induced increase in the number of D-serine-ir cells in the SDH and NP regions compared with the vehicle treated group. (B), Photomicrographs of representative L4-5 spinal cord sections illustrating D-serine-ir cells in the sham group (SHAM), in the saline treated CCI group (CCI+VEH) and in the BD-1047 treated CCI group (CCI+BD). *$p<0.05$, and ***$p<0.001$ as compared with those of SHAM group, ##$p<0.01$ as compared with those of the CCI+VEH group.

3-4. Effects of intrathecal BD-1047 administration on serine racemase expression and colocalization of serine racemase in Sig-1R-immunoreactive cells in CCI mice

To determine whether the CCI-induced increase in Srr expression was regulated by Sig-1R activation during the induction phase, I performed Western blot analysis on day 1 after CCI surgery. Intrathecal treatment with BD-1047 during the induction phase significantly reduced the CCI-induced increase in Srr expression (Fig.16A). The relative pixel area (%) of Srr and β-actin expression was significantly reduced by BD-1047 treatment during the induction period as compared with mice in the vehicle-treated CCI group. Because I found that Sig-1Rs are located in astrocytes in the spinal cord in CCI mice, I performed double staining on day 1 with an anti-Srr antibody in combination with antibodies for Sig-1R. Double staining with the Sig-1R and Srr antibodies showed that the increased expression of Srr was localized to Sig-1R-ir cells (Fig.16B). These results indicate that Srr and Sig-1R expression occur in the same cells in the spinal cord dorsal horn in CCI mice.

A

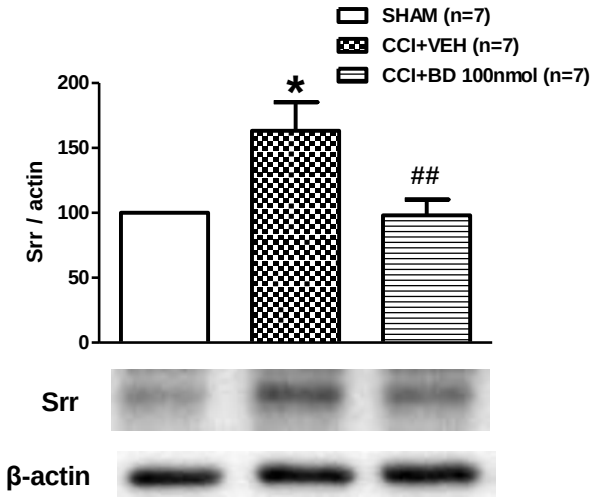
SHAM (n=7)
CCI+VEH (n=7)
CCI+BD 100nmol (n=7)
Srr / actin
200
150
100
50
0
*
##
Srr
β-actin

B

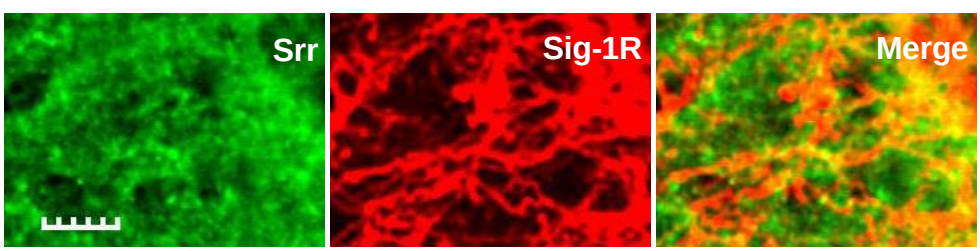
Srr
Sig-1R
Merge

Figure 16. The CCI-induced increase in Srr expression is blocked by spinal injection of the Sig-1R antagonist, BD-1047 and Srr coexists in Sig-1R-ir cells in the dorsal horn. (A), Western blot analysis was performed on day 1 after CCI surgery to determine whether CCI-induced increase in Srr expression was regulated by Sig-1R activation during the induction phase. Intrathecal treatment with BD-1047 during the induction phase significantly reduced the CCI-induced increase in Srr expression as compared with mice in the vehicle-treated CCI group. (B), Double staining was performed at day 1 post-CCI surgery using an anti-Srr antibody in combination with antibodies for Sig-1R. Double staining with Sig-1R antibody showed that the increased expression of Srr was localized to Sig-1R-ir cells. These results indicate that Srr and Sig-1R expression occur in the same cells in the spinal cord in CCI mice. *$p<0.05$ as compared with those of SHAM group, and ##$p<0.01$ as compared with those of the CCI+VEH group. Scale bar, 10 μm.

4. Effects on CCI-induced MA and TH

4-1. Effects of BD-1047, fluorocitrate or concomitant fluorocitrate and BD-1047 treatment on the development of CCI-induced MA and TH

I first confirmed the antinociceptive effect of the Sig-1R antagonist, BD-1047 (BD) during the induction phase (Fig.17A and B). Sustained intrathecal treatment with BD-1047 (10, 30, 100 nmol, BD) reduced the CCI-induced increase in PWF (%) to innocuous mechanical stimuli in a dose dependent manner (Fig.17A). Following the termination of these repeated BD-1047 injections on day 3, this suppressive anti-allodynia effect of BD-1047 was sustained throughout the 21-day experimental period following CCI surgery. On the other hand, repeated intrathecal administration of BD-1047 did not affect the CCI-induced TH (Fig.17B). To confirm the contribution of astrocyte activation to the CCI-induced pain behavior, the astroglial metabolic inhibitor, fluorocitrate was injected intrathecally on postoperative days 0-3. Similar to the antinociceptive effect of BD-1047, intrathecal treatment with fluorocitrate (0.003, 0.01, 0.03 nmol, Fc) significantly attenuated the CCI-induced MA in a dose dependent manner (Fig.17C). On the other hand CCI-induced TH was not influenced by repeated intrathecal treatment of fluorocitrate (Fig.17D). While intrathecal treatment of either a low dose of BD-1047 (10 nmol) alone or a low dose of fluorocitrate (0.003 nmol) alone did not alter the MA, the combination of the two treatments (Fc+BD) significantly suppressed MA development (Fig.17E). These results suggest a significant interaction between Sig-1Rs and astrocyte activation. However, CCI-induced TH was not affected by concomitant BD-1047 and fluorocitrate treatment (Fig.17F).

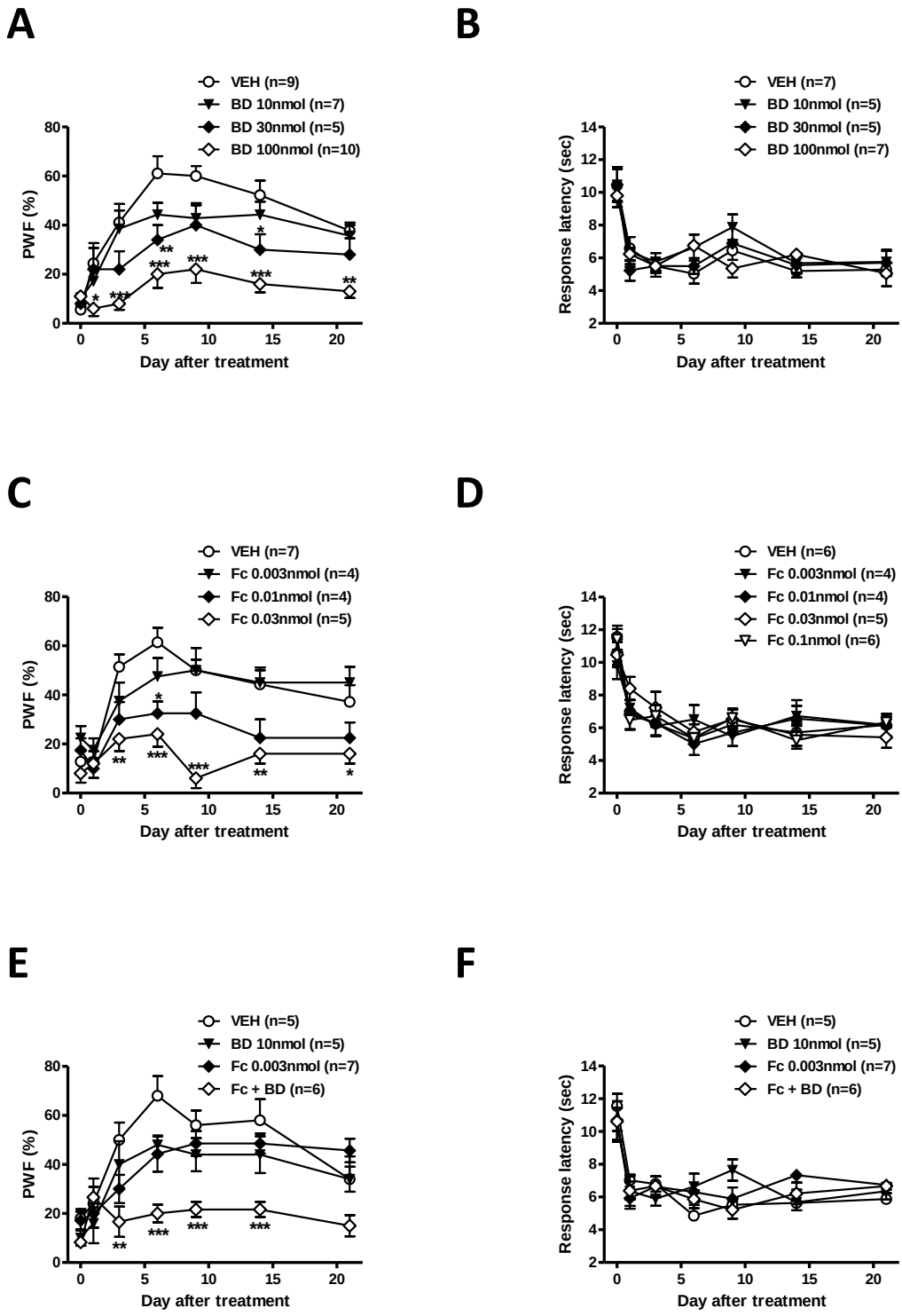
A
VEH (n=9)
BD 10nmol (n=7)
BD 30nmol (n=5)
BD 100nmol (n=10)
PWF (%)
Day after treatment
B
VEH (n=7)
BD 10nmol (n=5)
BD 30nmol (n=5)
BD 100nmol (n=7)
Response latency (sec)
Day after treatment
C
VEH (n=7)
Fc 0.003nmol (n=4)
Fc 0.01nmol (n=4)
Fc 0.03nmol (n=5)
PWF (%)
Day after treatment
D
VEH (n=6)
Fc 0.003nmol (n=4)
Fc 0.01nmol (n=4)
Fc 0.03nmol (n=5)
Fc 0.1nmol (n=6)
Response latency (sec)
Day after treatment
E
VEH (n=5)
BD 10nmol (n=5)
Fc 0.003nmol (n=7)
Fc + BD (n=6)
PWF (%)
Day after treatment
F
VEH (n=5)
BD 10nmol (n=5)
Fc 0.003nmol (n=7)
Fc + BD (n=6)
Response latency (sec)
Day after treatment

Figure 17. The concomitant treatment with low doses of BD-1047 and fluorocitrate also reduced the development of MA, but had no effect on CCI-induced TH. (A), Intrathecal injection of BD-1047 in CCI mice blocked the increase in PWF (%) that occurred in vehicle-treated CCI mice in a dose dependent manner. (B), However, the decrease in response latency (seconds) to heat stimuli was unaffected by repeated intrathecal treatment with even at the highest dose of BD-1047 tested (100 nmol). (C and D), Repeated daily treatment with fluorocitrate significantly attenuated MA, but not TH as compared with the vehicle treated group. (E), When a combination of BD-1047 and fluorocitrate was given, MA was reduced, compared with the effects shown in either the BD-1047 or fluorocitrate alone treatment groups. (F), TH was not affected by concomitant BD-1047 and fluorocitrate treatment. *$p < 0.05$, **$p<0.01$ and ***$p<0.001$ as compared with those of CCI+VEH group.

4-2. Effects of SB203580 or concomitant fluorocitrate and SB203580 treatment on the development of CCI-induced MA and TH

To confirm the relation between p-p38 expression and astrocyte activation to CCI-induced pain behaviors, I intrathecally administered SB203580 or fluorocitrate on postoperative days 0-3. Sustained i.t treatment with SB203580 (0.3, 1, 3 nmol, SB) significantly attenuated the CCI-induced increase in PWF(%) to innocuous mechanical stimuli in a dose dependent manner (Fig.18A). However, SB203580 administration did not affect the CCI-induced TH (Fig.18B). While i.t. treatment of either a low dose of SB203580 (0.3 nmol) or a low dose of fluorocitrate (0.003 nmol) alone did not alter CCI-induced MA, the combination of the two treatments (Fc+SB) significantly suppressed MA development (Fig.18C). These results suggest that there is a significant interaction between p-p38 and astrocyte activation. Conversely, CCI-induced TH was not affected by concomitant SB203580 and fluorocitrate treatment (Fig.18D).

A

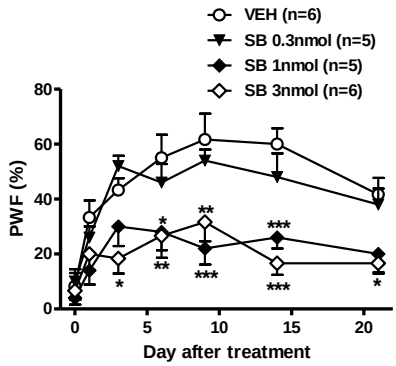
VEH (n=6)
SB 0.3nmol (n=5)
SB 1nmol (n=5)
SB 3nmol (n=6)
PWF (%)
Day after treatment

B

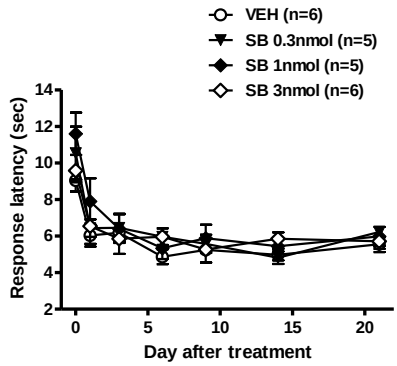
VEH (n=6)
SB 0.3nmol (n=5)
SB 1nmol (n=5)
SB 3nmol (n=6)
Response latency (sec)
Day after treatment

C

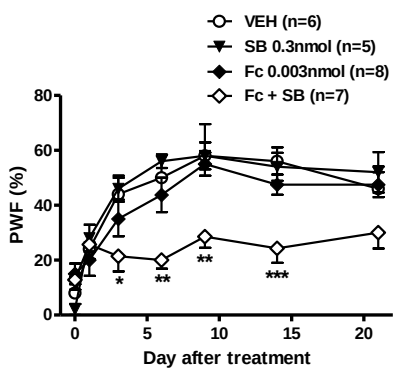
VEH (n=6)
SB 0.3nmol (n=5)
Fc 0.003nmol (n=8)
Fc + SB (n=7)
PWF (%)
Day after treatment

D

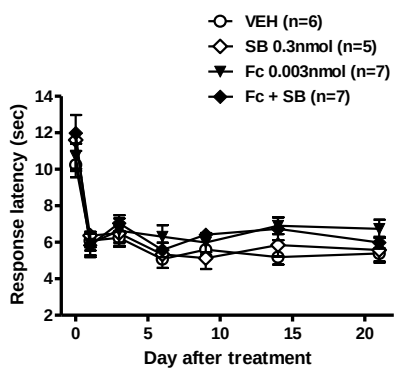
VEH (n=6)
SB 0.3nmol (n=5)
Fc 0.003nmol (n=7)
Fc + SB (n=7)
Response latency (sec)
Day after treatment

Figure 18. The concomitant treatment with low doses of SB203580 and fluorocitrate also reduced the development of MA, but had no effect on TH. (A), Intrathecal injection of SB203580 blocked the increase in PWF (%) that was observed in vehicle-treated CCI mice in dose dependent manner. (B), However, the decrease in response latency (seconds) to heat stimuli was unaffected by repeated intrathecal treatment with SB203580. (C and D), The lowest dose of SB203580 had no effect on CCI-induce MA and TH. When a combination of SB203580 and fluorocitrate was given, MA was reduced, compared with the effects showed in either the SB203580 or fluorocitrate alone treated group. TH was not effected by concomitant SB203580 and fluorocitrate treatment. *$p<0.05$, **$p<0.01$ and ***$p<0.001$ as compared with those of CCI+VEH group.

4-3. Effects of LSOS treatment and concomitant D-serine and BD-1047 treatment on the development of CCI-induced MA and TH

To investigate the contribution of increased D-serine to pain behaviors during the induction phase, I intrathecally administered the Srr inhibitor, LSOS on postoperative days 0-3. Repeated daily, intrathecal treatment with LSOS (1, 3, or 10 nmol) reduced the CCI-induced increase in PWF (%) to innocuous mechanical stimuli, as compared with vehicle treated CCI mice (Fig.19A). Following the termination of these repeated LSOS injections on day 3, this suppressive anti-allodynia effect of LSOS was sustained throughout the 21-day experimental period following CCI surgery. On the other hand, the CCI-induced decrease in response latency (seconds) to heat stimuli (TH) was not influenced by repeated intrathecal treatment with LSOS throughout the 21-day testing period (Fig.19B). Next, I intrathecally injected exogenous D-serine in combination of BD-1047 on postoperative days 0-3 to confirm the potential role of D-serine in the development of MA induced by Sig-1R activation in CCI mice. Treatment with BD-1047 reduced the CCI-induced increase in the PWF (%) to innocuous mechanical stimuli, while this same treatment did not affect CCI-induced TH. Treatment with exogenous D-serine (50 or 500 nmol in association with BD-1047) restored the CCI-induced mechanical allodynia that was blocked by BD-1047 (Fig.19C). However, CCI-induced TH was not affected by concomitant D-serine and BD-1047 treatment (Fig.19D).

A

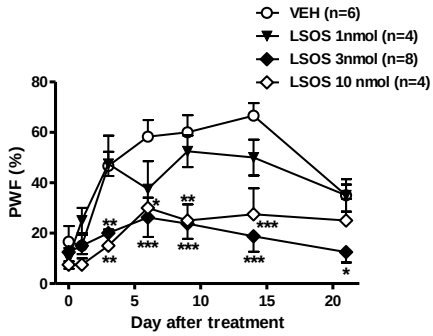
VEH (n=6)
LSOS 1nmol (n=4)
LSOS 3nmol (n=8)
LSOS 10 nmol (n=4)
PWF (%)
Day after treatment

B

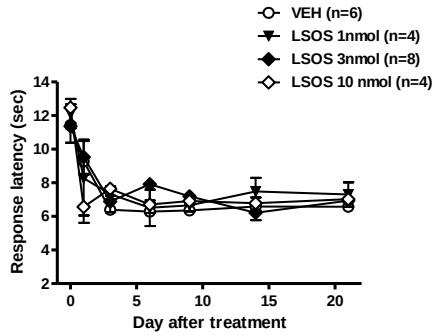
VEH (n=6)
LSOS 1nmol (n=4)
LSOS 3nmol (n=8)
LSOS 10 nmol (n=4)
Response latency (sec)
Day after treatment

C

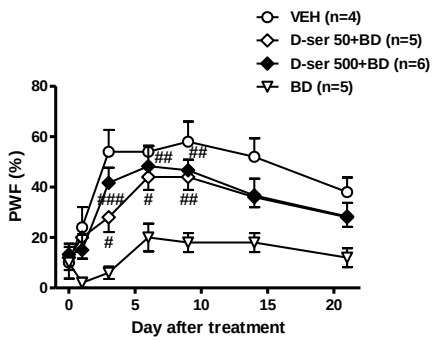
VEH (n=4)
D-ser 50+BD (n=5)
D-ser 500+BD (n=6)
BD (n=5)
PWF (%)
Day after treatment

D

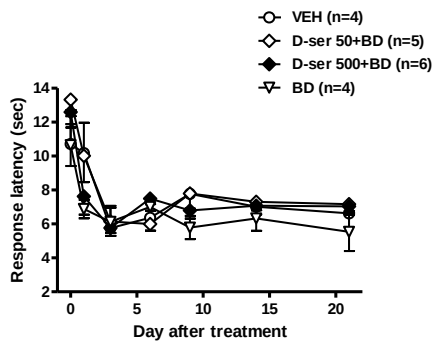
VEH (n=4)
D-ser 50+BD (n=5)
D-ser 500+BD (n=6)
BD (n=4)
Response latency (sec)
Day after treatment

Figure 19. Effects of endogenous and exogenous D-serine on development of MA and TH in CCI mice. (A and B), Intrathecal treatment with LSOS reduced the development of MA, but had no effect on TH in CCI mice. (A), Intrathecal treatment with LSOS (1, 3, or 10 nmol) reduced the CCI-induced increase in PWF (%) to innocuous mechanical stimuli, as compared with vehicle-treated CCI mice in a dose dependent manner. After the termination of repeated LSOS injection on day 3, this suppressive anti-allodynia effect of LSOS was sustained throughout the 21-day experimental period following CCI surgery. (B), On the other hand, the CCI-induced decrease in response latency (seconds) to heat stimuli (TH) was not influenced by repeated intrathecal treatment with LSOS throughout the 21-day testing period. (C and D), Intrathecal treatment with exogenous D-serine restores MA that is blocked by BD-1047 administration in CCI mice. (C), Treatment with BD-1047 reduced the CCI-induced increase in PWF (%) to innocuous mechanical stimuli. Treatment with exogenous D-serine (50 or 500 nmol in association with BD-1047) restored the CCI-induced allodynia that was blocked by BD-1047. (D), Conversely, the decrease in response latency (seconds) to heat stimuli was unaffected by repeated intrathecal treatment with BD-1047 or concomitant D-serine and BD-1047 treatment. *p <0.05, **p<0.01 and ***p<0.001 as compared with those of CCI+VEH group, #p <0.05, ##p<0.01 and ###p<0.001 as compared with those of the CCI+BD group.

DISCUSSION

The spinal Sig-1R expression is increased in astrocyte after CCI

Although the role of Sig-1Rs in central sensitization and pain hypersensitivity has been demonstrated in several pain models (de la Puente *et al.*, 2009; Carlsson *et al.*, 2010; Nieto *et al.*, 2012), the cellular distribution of Sig-1Rs in the spinal cord dorsal horn has not been reported previously, particularly as it relates to a chronic pain condition. There are two possibilities with respect to the mechanism underlying the action of spinal Sig-1Rs in the induction of chronic pain. The first hypothesis is that Sig-1Rs are upregulated in spinal neurons and can directly modulate these neurons (central terminals of primary afferent neurons or 2^{nd} order neuron in dorsal horn) under conditions of chronic pain; and the second hypothesis is that spinal cord Sig-1Rs can indirectly modulate neuronal activity via a signaling mechanism associated with glial cells (astrocytes and/or microglia). Interestingly, the first finding of the present study demonstrated that Sig-1R expression is significantly and selectively increased only in astrocytes and not in spinal cord neurons on day 3 post-CCI surgery. This is consistent with the work of Ruscher *et al.*, which demonstrated a significant increase in Sig-1R expression in reactive astrocytes and not neurons or microglia after experimental stroke (Ruscher *et al.*, 2011).

A growing number of studies have used Ca^{2+} as an indicator of astrocytic activity and demonstrated that an increase in cytoplasmic Ca^{2+} concentration ($[Ca^{2+}]_i$) in astrocytes is correlated with gliotransmitter release and modulation of neuronal activity (Agulhon *et al.*, 2008; Ben Achour *et al.*, 2010). Astrocytes exhibit a large number of G protein-coupled metabotropic receptors (GPCRs) linked to Ca^{2+} mobilization from internal stores or ionotropic glutamate channels or receptors linked to extracellular Ca^{2+} entry (Agulhon *et al.*, 2008;

Miyano *et al.*, 2010). The stimulation of the GPCRs coupled to PLC hydrolyzes the membrane lipid phosphatidylinositol 4,5-bisphosphate (PIP_2) to generate diacylglycerol (DAG) and inositol triphosphate (IP_3), leading to IP_3 receptor (IP_3 R) activation and Ca^{2+} release from the ER. It has been reported that Sig-1Rs normally reside at a mitochondrion-associated ER membrane where Sig-1Rs regulate ER-mitochondrion Ca^{2+} signaling and ER-nucleus crosstalk (Su *et al.*, 2010). When cells are stimulated by Sig-1R ligands or undergo prolonged stress, Sig-1Rs have been shown to activate IP_3-induced Ca^{2+} efflux from the ER (Hayashi *et al.*, 2001). In addition, activated Sig-1Rs translocate to plasma membrane, thus regulating functional proteins, including ion channels, receptors and kinases (Su *et al.*, 2009; Su *et al.*, 2010). Recent studies from my laboratories have also demonstrated that spinal Sig-1R-mediated nociceptive action is associated with Ca^{2+} dependent second messenger cascades including PLC and PKC (Roh *et al.*, 2008b; Roh *et al.*, 2010), which are also known to be closely linked to an increase in $[Ca^{2+}]_i$ in astrocytes. These findings suggest that the increased expression or upregulation of Sig-1Rs in CCI animals occurs primarily in spinal cord astrocytes and thus they can regulate a variety of cellular functions via $[Ca^{2+}]_i$ modulation in these glial cells. Conversely, there are several reports that Sig-1Rs are also located in motor neurons of spinal cord ventral horn (Mavlyutov *et al.*, 2010; Mancuso *et al.*, 2012) and that Sig-1R mRNA is found in cultured microglial cells (Gekker *et al.*, 2006) and that Sig-1Rs are present in retinal microglia (Zhao *et al.*, 2014) as well as brain astrocytes (Francardo *et al.*, 2014). Clearly there are some discrepancies among the various studies with regard to which cell types express Sig-1R receptors and this could be due to the use of different animal species (mouse versus rat versus human) and to the use of different Sig-1R antibodies. It is also likely that the pattern of cellular distribution of Sig-1Rs may different under different physiological or pathologic conditions and among different animal models of disease or pain. However, in

the mouse CCI model used here, the only significant change in Sig-1R expression occurred in astrocytes in the spinal cord dorsal horn.

Sig-1R-mediated increase in spinal p-p38 leads to the induction of MA in CCI mice

The present study indicate that phosphorylation of p38 and ERK is increased by direct activation of spinal Sig-1Rs in cultured astrocytes. Sig-1Rs have been shown to modulate intracellular Ca^{2+} signaling and activate Ca^{2+}-dependent enzymes, which lead to p38 and pERK phosphorylation in dorsal horn neurons (Lee *et al.*, 2000a; Hayashi *et al.*, 2007; Roh *et al.*, 2008b; Trang *et al.*, 2009). A potential relationship between Sig-1R activation and p-p38 or pERK has been previously reported. Nishimura *et al*. demonstrated that stimulation of Sig-1Rs potentiate the nerve-growth factor (NGF)-induced neurite outgrowth in PC 12 cells through the interaction with IP3 receptors and several subsequent signaling molecules including p38 (Nishimura *et al.*, 2008). In addition, De la Puente *et al*. reported that in contrast to wild-type mice, Sig-1R knockout mice did not show pERK in the spinal cord 14 days after partial sciatic nerve injury surgery (de la Puente *et al.*, 2009). However, the cellular location of pERK in the spinal cord of this model is unknown. Previous study from my laboratories have demonstrated that direct activation of spinal Sig-1Rs induces both mechanical allodynic and thermal hyperalgesic behaviors in mice (Roh *et al.*, 2008b). Remarkably, the present study shows that intrathecal pretreatment with a p38 inhibitor only attenuated the MA, but not the TH produced by intrathecal administration of a Sig-1R agonist, while the pretreatment of ERK inhibitor reduced both of PRE-084 induced MA and TH. In addition, the inhibition of spinal p38 activation during the induction phase of neuropathic pain reduces the development of MA, but not TH in CCI mice. These results corroborate those of the effect of intrathecal treatment

with a Sig-1R antagonist. The present results indicate that the activation of spinal p38 is closely involved with the induction of Sig-1R-mediated MA, but not TH, in a model of neuropathic pain. Recently several studies have also reported that spinal p38 activation plays an important role in the pathophysiological mechanism of MA in a variety of experimental pain models. p38 phosphorylation is immediately increased by plantar incision, which is coincident with the development of incisional pain (Wen *et al.*, 2009). Single intrathecal of another p38 inhibitor, FR167653 potently attenuated incision-induced MA for 2 days after pretreatment incision, whereas a higher dose of FR167653 only resulted in a very brief inhibition on TH. In addition, intrathecal pretreatment of SB203580 dose-dependently blocked the development of tactile allodynia induced by a first-degree burn in the rat (Sorkin *et al.*, 2009). These results imply that the activation of spinal Sig-1Rs and the subsequent signaling of p38 are more closely associated with the development of MA, but not TH in chronic pain conditions.

In addition, Xu *et al*. reported that pretreatment or early treatment with the SB203580 significantly reduced in TNF-α synthesis and subsequent development of MA, while post-treatment with SB203580 starting on Day 7 produces no effect on MA or TNF-α levels in CCI rats (Xu *et al.*, 2007a). In this regard it is reported that spinal Sig-1R expression was upregulated only the induction phase, and the early blockade of spinal Sig-1Rs inhibits both the development of CCI-induced MA and the CCI-induced increase in spinal GluN1 expression and phosphorylation. In contrast, BD-1047 treatment during the maintenance phase of neuropathic pain had no effect on MA or pGluN1 expression (Roh *et al.*, 2008c). These results suggest that the activation of spinal Sig-1R plays a critical role in the induction of MA rather than the maintenance of MA in CCI-induced neuropathic pain. Collectively it appears that p38 activation is regulated by Sig-1R stimulation, which ultimately leads to the induction of MA, rather than the maintenance of MA in CCI animals.

Moreover, Romero *et al*. recently reported that mice receiving systemic administration of S1RA, a new Sig-1R antagonist exhibit antinociceptive effects on MA as well as TH (Romero *et al.*, 2012). In contrast, I demonstrate in the present study that inhibition of spinal Sig-1Rs only inhibits the development of MA, but not TH. This discrepancy may be due to the difference in administration of the Sig-1R antagonist between the two studies such that the reduction in CCI-induced TH produced by systemic Sig-1R antagonism is mediated by the inhibition of Sig-1Rs located either in supra-spinal brain regions or in the periphery, where Sig-1Rs have been shown to modulate some ion channels like Kv 1.4 potassium channels in dorsal root ganglion cells (Aydar *et al.*, 2002; Matsuyoshi *et al.*, 2012). Thus, spinal Sig-1R activation may be more important for the development of CCI-induced MA rather than TH.

Sig-1Rs activate astrocytes via p-p38 leading to the development of MA in CCI mice

I found that the activation of p38 occurs predominantly in both spinal dorsal horn neurons and astrocytes and that intrathecal treatment with a Sig-1R antagonist during the induction phase significantly reduced p-p38 expression in astrocytes, but not in neurons. Although many studies using chronic pain models in rats have reported that p38 is activated exclusively in microglia (Tsuda *et al.*, 2004; Terayama *et al.*, 2008; Wen *et al.*, 2009), I found that p-p38-ir staining was preferentially localized to the nucleus of GFAP-positive astrocytes and NeuN-positive neurons. These results are in line with several studies using chronic pain models in mice. Xu *et al*. reported p38 was activated in the nucleus of astrocytes or neurons, but that there was no evidence of p-p38 staining in microglia, after pSNL in lumbar spinal sections in mice (Xu *et al.*, 2007b). They reported that multiple intrathecal injections of a p38 inhibitor reduced spinal astrocyte proliferation after pSNL. Zhang *et al*. also reported recently that the

inhibitory effect of TNF-α on GABAergic neurons is mediated by p-p38, which is expressed in neurons and astrocytes (Zhang *et al.*, 2010). The expression of TNF receptor 1 and p-38 in spinal astrocytes suggests that astrocytes are involved in the TNF-α-induced spinal disinhibition. Collectively these results together with my data suggest that the p38 pathway may play an important role in astrocyte modulation and the subsequent induction of MA under chronic pain conditions. Moreover, the fact that intrathecal BD-1047 injection specifically inhibited p-p38 expression in astrocytes, but not neurons, provides evidence that furthers my understanding of the possible relationship between p-p38 modulation and the cellular distribution of Sig-1Rs in the spinal cord.

In addition, it was previously reported that p38 has at least four different isoforms, α, β, γ and δ, which differ in their substrate preference, activation modes and response to inhibitors. (Kumar *et al.*, 2003). The conventional p38 inhibitor, SB203580 inhibits only p38α and p38β2 (Barone *et al.*, 2001). In addition, among the four isoforms, p38α and p38β are constitutively expressed in the spinal cord (Svensson *et al.*, 2005). Svensson *et al*. also demonstrated that intraplantar formalin and intrathecal substance P in rats produced nocifensive flinching and p-p38 expression, and this was prevented when spinal p38β, but not p38α, was down-regulated. Meanwhile, in mouse brain, both p38α and p38β are present in neurons, while p38β is also expressed in glial cells (Lee *et al.*, 2000b). Thus, this diversity in the pattern of p-p38 subtype expression might reflect the fact that p38 subtypes can be differentially activated under a variety of pain conditions. Thus, it is possible that the different p-p38 subtypes, especially p38α and p38β, are differentially distributed in the spinal cord dorsal horn in CCI mice and affected differentially by Sig-1R activation.

The present study shows that intrathecal treatment with the astroglial inhibitor, fluorocitrate as well as the Sig-1R antagonist, BD-1047 given during the induction phase of

neuropathic pain, significantly reduced the development of MA, but not TH, in CCI mice. Interestingly, low doses of fluorocitrate produced synergic suppressive effects on MA development when combined with low doses of BD-1047 or the p38 inhibitor, SB203580. In addition, the CCI-induced increase in GFAP expression was significantly reduced when BD-1047 or SB203580 were injected intrathecally during the induction phase. Recently several studies have also reported that spinal astrocytes can directly contribute to the development of MA, but not TH in various pain conditions. GAO *et al*. reported that intrathecal administration of the L-α-aminoadipate on post-CFA day 2 reversed CFA-induced bilateral MA, but not TH (Gao *et al.*, 2010b). They also reported that spinal intrathecal injection of TNF-α-activated astrocytes produce MA by releasing MCP-1 in naïve mice (Gao *et al.*, 2010d). In addition, Zhang *et al*. reported that MA can be induced by the intrathecal administration of exogenous BDNF-stimulated astrocytes to naïve rats (Zhang *et al.*, 2011). Furthermore, a single intrathecal injection of spinal astrocytes activated by a PKC activator failed to produce TH in naïve mice, while intrathecal injection of a microglia cell line activated by ATP significantly decreased paw withdrawal latency to a thermal stimulus (Narita *et al.*, 2006). These results imply that the spinal Sig-1Rs can modulate astrocyte activation via phosphorylation of p38 and contribute to the development of MA, but not TH in neuropathic mice.

Spinal Sig-1R activation increases the expression of D-serine from astrocytes leading to the development of MA in CCI mice

It has been reported that activated astrocytes released proinflammatory cytokines or chemokines or growth factors under chronic pain conditions (Cao *et al.*, 2008; Gao *et al.*, 2010c). However, I hypothesized that D-serine may be involved in this process, because Sig-1R-induced MA development is NMDA receptor dependent. D-serine is an endogenous ligand

that acts at the strychnine-insensitive glycine site of the NMDA receptor, and controls NMDA receptor activity (Mothet *et al.*, 2000; Henneberger *et al.*, 2010). D-serine is synthesized by Srr in astrocytes, but it has also been reported to be synthesized by microglia or neurons in the brain (Wu *et al.*, 2004b; Miya *et al.*, 2008). In the present study I demonstrate that D-serine is localized to astrocytes and neurons, while Srr is only expressed in astrocytes. In the deep dorsal horn, D-serine is localized around neurons, suggesting a correlation between the D-serine accumulation and NMDA receptor activity in neuron. Collectively, these data suggest that D-serine is produced in astrocytes in the superficial dorsal horn and potentially mediates NMDA receptor activation during the induction phase of CCI-induced neuropathic pain.

It has been reported that D-serine has diverse effects on chronic pain in variety of pain models. Wake *et al*. reported that the second phase of the formalin-induced licking response was significantly increased in mutant mice lacking DAAO (Wake *et al.*, 2001). In addition, intrathecally injected LSOS or another Srr inhibitor, LEHA, decreased wind-up potentiation in an arthritic pain model and this antinociceptive effects were abolished when D-serine was injected intrathecally (Laurido *et al.*, 2012). Furthermore, Dieb *et al*. reported that spinal astrocytes are involved in the modulation of orofacial post-traumatic neuropathic pain through the secretion of D-serine (Dieb *et al.*, 2013). However, Hopkins *et al*. showed that systemic administration of the DAAO inhibitor attenuated pain behavior in a neuropathic pain model and also reduced spontaneous activity in recordings obtained both centrally and peripherally (Hopkins *et al.*, 2013). In addition, intracerebroventricular administration of D-serine has been shown to significantly and dose-dependently decrease formalin-induced pain behaviors (Ito *et al.*, 2014). These discrepancies among the various studies could be due to differential localization of D-serine in different animal models of pain. Collectively, these results indicate that D-serine may play a differential role in chronic pain based on its location and specifically

spinal D-serine may be involved in the processing of the nociceptive transmission under chronic pain conditions.

In addition, I show that endogenous D-serine reduction in the spinal cord induced by intrathecal treatment with a Srr inhibitor, contribute to MA, but not TH. These results are consist with the reports indicating that spinal astrocytes contribute to the development of MA, but not TH, under various chronic pain conditions. (Narita *et al.*, 2006; Gao *et al.*, 2010b; Gao *et al.*, 2010d; Zhang *et al.*, 2011). In the present study I demonstrated that D-serine and Srr are both localized to astrocytes in the spinal cord in CCI mice and that sustained administration of a Srr inhibitor reduced MA, but not TH development. These results imply that the spinal endogenous D-serine can be increased in astrocyte and contribute to the development of MA, but not TH in CCI mice.

I also found that the CCI-induced increase in Srr expression is reduced by BD-1047 treatment during the induction phase, and that Srr is colocalized in the same cells as Sig-1Rs. The precise mechanism by which activation of Sig-1Rs induces an increase in Srr expression is certainly complex and requires further extensive investigation. The possible mechanisms by which Srr induces an increase in D-serine production and release either by elevating transcription or by increasing its enzymatic remains to be determined. It has been reported that increased Srr expression can elevated D-serine release in cultured microglia. Wu *et al*. reported that amyloid β-peptide stimulation elevated D-serine release by increasing expression of Srr mediated by a JNK MAP kinase-dependent activation of a transcription factor activator protein-1 in cultured microglia (Wu *et al.*, 2004a; Wu *et al.*, 2004b). SaSabe *et al.* also showed that elevation of Srr expression, initially induced by glial activators, subsequently increased D-serine levels in activated glia in amyotrophic lateral sclerosis (Sasabe *et al.*, 2007). I founded that Sig-1R can increase p38 phosphorylation, another MAP kinase activation, in astrocyte

during the induction phase. So there is a possibility that the increased expression of Srr in CCI mice is mediated by a p38-dependent activation of a transcription factors induced by Sig-1Rs in astrocytes. Another possibility is that there is an increase in the activity of Srr. An increase in intracellular Ca^{2+} concentration in astrocytes and direct Ca^{2+} binding to the Srr causes activation of this enzyme, which in turn leads to an increase in D-serine levels (Cook *et al.*, 2002). This suggests that Ca^{2+} could also be an important Srr cofactor. It has been reported that Sig-1Rs normally reside at a mitochondrion-associated ER membrane and cause IP_3-induced Ca^{2+} efflux from the ER when cells are stimulated by Sig-1R ligands or undergo prolonged stress (Hayashi *et al.*, 2001; Su *et al.*, 2010). These findings suggest a potential model by which the upregulation of Sig-1Rs in astrocytes regulates Srr expression and/or activation leading to an increase in D-serine in these glial cells.

Finally, I demonstrate that MA induced by Sig-1R activation in CCI mice is dependent on D-serine. I found that removal of endogenous D-serine by a Srr inhibitor prevented MA, but not TH. In addition, in conditions in which Sig-1Rs were inactivated by BD-1047, exogenous D-serine treatment restored MA. I can thus conclude that the Sig-1R-induced D-serine release from dorsal horn astrocytes contributes to MA development in CCI mice. In support of this theory, Miraucourt *et al*. reported that intracisternal treatment with the astrocyte inhibitor, fluorocitrate prevented MA induced by removal of glycine inhibition and this effect was restored with intracisternal administration of exogenous D-serine (Miraucourt *et al.*, 2011). Because both neurons and astrocytes have been reported to express NMDA receptors (Schipke *et al.*, 2001; Petrenko *et al.*, 2003), there is a possibility that D-serine could also be acting on astrocytes to induced the release of other factors. However, astrocytes cannot be the only target of D-serine, because exogenous D-serine is able to recovered MA when astrocytes are inactivated by a Sig-1R antagonist, as discussed by Miraucourt *et al*. in their study (Miraucourt

et al., 2011).

In conclusion, the current study has demonstrated that intrathecal treatment with a Sig-1R antagonist during the induction phase of CCI induced neuropathic pain significantly reduces the CCI-induced pathologic activation of astrocytes in the spinal cord dorsal horn. Moreover, this effect of a Sig-1R antagonist on spinal astrocyte activation is mediated in part by the inhibition of p-p38, which can dramatically suppress the induction of MA, but not TH, in neuropathic mice. This spinal Sig-1R-induced MA is also mediated by an increase in Srr expression, which in turn causes an increase in the production and possible release of D-serine. Collectively these findings suggest that the pharmacological inhibition of spinal Sig-1Rs may be a useful approach for the management of astrocyte-mediated MA development in neuropathic pain patients.

SUMMARY

Recently, it has been recognized that the role of Sig-1R in modulating central sensitization associated with the development of neuropathic pain. Moreover, it has been reported that spinal Sig-1Rs play an important role in the induction of MA in neuropathic pain. However, it was not clearly demonstrated that the specific mechanism related to this spinal Sig-1R under the development of MA in neuropathic pain condition.

The results demonstrated that direct activation of Sig-1R time-dependently increased the expression of p38 phosphorylation, and the p-p38 was correlated with Sig-1R induced MA, but not TH in PRE-084 injected mice. The expression of Sig-1Rs was significantly increased in astrocytes on day 3 following CCI surgery and sustained intrathecal treatment with the BD-1047, attenuated CCI-induced increase in GFAP-ir astrocytes. Interestingly, intrathecal BD-1047 attenuated the expression of p-p38 selectively in astrocytes but not in neurons, and intrathecal treatment with a p38 inhibitor attenuated the GFAP expression. These data suggest that spinal Sig-1Rs are localized in astrocytes, and that blockade of Sig-1Rs inhibits the pathologic activation of astrocytes via modulation of p-p38 in neuropathic mice. The level of D-serine and Srr expression were significantly increased in the spinal cord after CCI surgery. D-serine was localized in astrocyte and accumulated around neuron. The increased level of D-serine was attenuated by sustained intrathecal treatment with BD-1047. Accordingly, Srr expression was also reduced by BD-1047 treatment and I found Srr expression located on the same cell with Sig-1R-ir cells. These data suggest indicates that spinal Sig-1R activation increases Srr expression, which in turn causes an increase of D-serine.

In the pain behavior, sustained intrathecal treatment with the BD-1047, combined with

fluorocitrate synergistically reduced the development of MA, but not TH. Moreover, intrathecal treatment with a p38 inhibitor combined with fluorocitrate also synergistically blocked the induction of MA. In addition, sustained intrathecal treatment with the Srr inhibitor reduced the development of MA, and the MA blockade induced by BD-1047 treatment was reversed by exogenous D-serine.

Collectively these findings suggest that spinal Sig-1Rs are localized in astrocytes, and that blockade of Sig-1Rs inhibits the pathologic activation of astrocytes via modulation of p-p38, which ultimately prevents the development of MA in neuropathic mice. I also demonstrate that the spinal Sig-1R-mediated MA is developed by an increase of Srr expression, which in turn causes an increase of D-serine. Accordingly these results imply that chronic neuropathic pain - especially MA development could be clinically controlled by the spinal Sig-1R modulation.

REFERENCES

Agulhon C, Sun MY, Murphy T, Myers T, Lauderdale K, Fiacco TA (2012). Calcium Signaling and Gliotransmission in Normal vs. Reactive Astrocytes. Front Pharmacol 3**:** 139.

Agulhon C, Petravicz J, McMullen AB, Sweger EJ, Minton SK, Taves SR, *et al.* (2008). What is the role of astrocyte calcium in neurophysiology? Neuron 59**:** 932-946.

Alonso G, Phan V, Guillemain I, Saunier M, Legrand A, Anoal M, *et al.* (2000). Immunocytochemical localization of the sigma-1 receptor in the adult rat central nervous system. Neuroscience 97**:** 155-170.

Andreev N, Dimitrieva N, Koltzenburg M, McMahon SB (1995). Peripheral administration of nerve growth factor in the adult rat produces a thermal hyperalgesia that requires the presence of sympathetic post-ganglionic neurones. Pain 63**:** 109-115.

Aydar E, Palmer CP, Klyachko VA, Jackson MB (2002). The sigma receptor as a ligand-regulated auxiliary potassium channel subunit. Neuron 34**:** 399-410.

Barone FC, Irving EA, Ray AM, Lee JC, Kassis S, Kumar S, *et al.* (2001). Inhibition of p38 mitogen-activated protein kinase provides neuroprotection in cerebral focal ischemia. Med Res Rev 21**:** 129-145.

Basbaum AI, Bautista DM, Scherrer G, Julius D (2009). Cellular and molecular mechanisms of pain. Cell 139**:** 267-284.

Ben Achour S, Pont-Lezica L, Bechade C, Pascual O (2010). Is astrocyte calcium signaling relevant for synaptic plasticity? Neuron Glia Biol 6**:** 147-155.

Bennett GJ, Xie YK (1988). A peripheral mononeuropathy in rat that produces disorders of pain sensation like those seen in man. Pain 33**:** 87-107.

Boyle DL, Jones TL, Hammaker D, Svensson CI, Rosengren S, Albani S, *et al.* (2006). Regulation of

peripheral inflammation by spinal p38 MAP kinase in rats. PLoS Med 3**:** e338.

Cao H, Zhang YQ (2008). Spinal glial activation contributes to pathological pain states. Neurosci Biobehav Rev 32**:** 972-983.

Carlsson A, Ohsawa M, Hallberg M, Nyberg F, Kamei J (2010). Substance P(1-7) induces antihyperalgesia in diabetic mice through a mechanism involving the naloxone-sensitive sigma receptors. Eur J Pharmacol 626**:** 250-255.

Caterina MJ, Schumacher MA, Tominaga M, Rosen TA, Levine JD, Julius D (1997). The capsaicin receptor: a heat-activated ion channel in the pain pathway. Nature 389**:** 816-824.

Cendan CM, Pujalte JM, Portillo-Salido E, Montoliu L, Baeyens JM (2005). Formalin-induced pain is reduced in sigma-1 receptor knockout mice. Eur J Pharmacol 511**:** 73-74.

Cook SP, Galve-Roperh I, Martinez del Pozo A, Rodriguez-Crespo I (2002). Direct calcium binding results in activation of brain serine racemase. J Biol Chem 277**:** 27782-27792.

Davis JB, Gray J, Gunthorpe MJ, Hatcher JP, Davey PT, Overend P, *et al.* (2000). Vanilloid receptor-1 is essential for inflammatory thermal hyperalgesia. Nature 405**:** 183-187.

de la Puente B, Nadal X, Portillo-Salido E, Sanchez-Arroyos R, Ovalle S, Palacios G, *et al.* (2009). Sigma-1 receptors regulate activity-induced spinal sensitization and neuropathic pain after peripheral nerve injury. Pain 145**:** 294-303.

Dieb W, Hafidi A (2013). Astrocytes are involved in trigeminal dynamic mechanical allodynia: potential role of D-serine. J Dent Res 92**:** 808-813.

Duman EN, Kesim M, Kadioglu M, Ulku C, Kalyoncu NI, Yaris E (2006). Effect of gender on antinociceptive effect of paroxetine in hot plate test in mice. Prog Neuropsychopharmacol Biol Psychiatry 30**:** 292-296.

Dunn KW, Kamocka MM, McDonald JH (2011). A practical guide to evaluating colocalization in

biological microscopy. Am J Physiol Cell Physiol 300**:** C723-742.

Francardo V, Bez F, Wieloch T, Nissbrandt H, Ruscher K, Cenci MA (2014). Pharmacological stimulation of sigma-1 receptors has neurorestorative effects in experimental parkinsonism. Brain 137**:** 1998-2014.

Fukuoka H, Kawatani M, Hisamitsu T, Takeshige C (1994). Cutaneous hyperalgesia induced by peripheral injection of interleukin-1β in the rat. Brain Res 657**:** 133-140.

Gao YJ, Ji RR (2009a). c-Fos and pERK, which is a better marker for neuronal activation and central sensitization after noxious stimulation and tissue injury? Open Pain J 2**:** 11-17.

Gao YJ, Ji RR (2010a). Chemokines, neuronal-glial interactions, and central processing of neuropathic pain. Pharmacol Ther 126**:** 56-68.

Gao YJ, Ji RR (2010b). Light touch induces ERK activation in superficial dorsal horn neurons after inflammation: involvement of spinal astrocytes and JNK signaling in touch-evoked central sensitization and mechanical allodynia. J Neurochem 115**:** 505-514.

Gao YJ, Ji RR (2010c). Targeting astrocyte signaling for chronic pain. Neurotherapeutics 7**:** 482-493.

Gao YJ, Zhang L, Ji RR (2010d). Spinal injection of TNF-α-activated astrocytes produces persistent pain symptom mechanical allodynia by releasing monocyte chemoattractant protein-1. Glia 58**:** 1871-1880.

Gao YJ, Zhang L, Samad OA, Suter MR, Yasuhiko K, Xu ZZ, *et al.* (2009b). JNK-induced MCP-1 production in spinal cord astrocytes contributes to central sensitization and neuropathic pain. J Neurosci 29**:** 4096-4108.

Gekker G, Hu S, Sheng WS, Rock RB, Lokensgard JR, Peterson PK (2006). Cocaine-induced HIV-1 expression in microglia involves sigma-1 receptors and transforming growth factor-β 1. Int Immunopharmacol 6**:** 1029-1033.

Gosselin RD, Suter MR, Ji RR, Decosterd I (2010). Glial cells and chronic pain. Neuroscientist 16**:** 519-531.

Guitart X, Codony X, Monroy X (2004). Sigma receptors: biology and therapeutic potential. Psychopharmacology 174**:** 301-319.

Halassa MM, Fellin T, Haydon PG (2007). The tripartite synapse: roles for gliotransmission in health and disease. Trends Mol Med 13**:** 54-63.

Hamby ME, Uliasz TF, Hewett SJ, Hewett JA (2006). Characterization of an improved procedure for the removal of microglia from confluent monolayers of primary astrocytes. J Neurosci Methods 150**:** 128-137.

Hargreaves K, Dubner R, Brown F, Flores C, Joris J (1988). A new and sensitive method for measuring thermal nociception in cutaneous hyperalgesia. Pain 32**:** 77-88.

Hayashi T, Su TP (2001). Regulating ankyrin dynamics: Roles of sigma-1 receptors. Proc Natl Acad Sci U S A 98**:** 491-496.

Hayashi T, Su TP (2007). Sigma-1 receptor chaperones at the ER-mitochondrion interface regulate Ca^{2+} signaling and cell survival. Cell 131**:** 596-610.

Hayashi T, Su TP (2008). An update on the development of drugs for neuropsychiatric disorders: focusing on the sigma-1 receptor ligand. Expert Opin Ther Targets 12**:** 45-58.

Hellewell SB, Bruce A, Feinstein G, Orringer J, Williams W, Bowen WD (1994). Rat liver and kidney contain high densities of sigma-1 and sigma-2 receptors: characterization by ligand binding and photoaffinity labeling. Eur J Pharmacol 268**:** 9-18.

Henneberger C, Papouin T, Oliet SH, Rusakov DA (2010). Long-term potentiation depends on release of D-serine from astrocytes. Nature 463**:** 232-236.

Hopkins SC, Zhao FY, Bowen CA, Fang X, Wei H, Heffernan ML, *et al.* (2013). Pharmacodynamic

effects of a D-amino acid oxidase inhibitor indicate a spinal site of action in rat models of neuropathic pain. J Pharmacol Exp Ther 345**:** 502-511.

Hylden JL, Wilcox GL (1980). Intrathecal morphine in mice: a new technique. Eur J Pharmacol 67**:** 313-316.

Ikeda H, Kiritoshi T, Murase K (2012). Contribution of microglia and astrocytes to the central sensitization, inflammatory and neuropathic pain in the juvenile rat. Mol Pain 8**:** 43.

Ito M, Yoshikawa M, Ito K, Matsuda M, Jin XL, Takahashi S, *et al.* (2014). Antinociceptive effect of intracerebroventricular administration of D-serine on formalin-induced pain. J Anesth 28**:** 228-234.

Ji RR, Suter MR (2007). p38 MAPK, microglial signaling, and neuropathic pain. Mol Pain 3**:** 33.

Ji RR, Baba H, Brenner GJ, Woolf CJ (1999). Nociceptive-specific activation of ERK in spinal neurons contributes to pain hypersensitivity. Nat Neurosci 2**:** 1114-1119.

Ji RR, Gereau RWt, Malcangio M, Strichartz GR (2009). MAP kinase and pain. Brain Res Rev 60**:** 135-148.

Ji XT, Qian NS, Zhang T, Li JM, Li XK, Wang P, *et al.* (2013). Spinal astrocytic activation contributes to mechanical allodynia in a rat chemotherapy-induced neuropathic pain model. PLoS One 8**:** e60733.

Jin SX, Zhuang ZY, Woolf CJ, Ji RR (2003). p38 mitogen-activated protein kinase is activated after a spinal nerve ligation in spinal cord microglia and dorsal root ganglion neurons and contributes to the generation of neuropathic pain. J Neurosci 23**:** 4017-4022.

Johnson GL, Lapadat R (2002). Mitogen-activated protein kinase pathways mediated by ERK, JNK, and p38 protein kinases. Science 298**:** 1911-1912.

Kang SY, Kim CY, Roh DH, Yoon SY, Park JH, Lee HJ, *et al.* (2011). Chemical stimulation of the ST36

acupoint reduces both formalin-induced nociceptive behaviors and spinal astrocyte activation via spinal α-2 adrenoceptors. Brain Res Bull 86**:** 412-421.

Karim F, Wang CC, Gereau RWt (2001). Metabotropic glutamate receptor subtypes 1 and 5 are activators of extracellular signal-regulated kinase signaling required for inflammatory pain in mice. J Neurosci 21**:** 3771-3779.

Kim HW, Kwon YB, Roh DH, Yoon SY, Han HJ, Kim KW, *et al.* (2006). Intrathecal treatment with sigma-1 receptor antagonists reduces formalin-induced phosphorylation of NMDA receptor subunit 1 and the second phase of formalin test in mice. Br J Pharmacol 148**:** 490-498.

Kourrich S, Su TP, Fujimoto M, Bonci A (2012). The sigma-1 receptor: roles in neuronal plasticity and disease. Trends Neurosci 35**:** 762-771.

Kumar S, Boehm J, Lee JC (2003). p38 MAP kinases: key signalling molecules as therapeutic targets for inflammatory diseases. Nat Rev Drug Discov 2**:** 717-726.

Latremoliere A, Woolf CJ (2009). Central sensitization: a generator of pain hypersensitivity by central neural plasticity. J Pain 10**:** 895-926.

Laurido C, Hernandez A, Pelissier T, Constandil L (2012). Antinociceptive effect of rat D-serine racemase inhibitors, L-serine-O-sulfate, and L-erythro-3-hydroxyaspartate in an arthritic pain model. ScientificWorldJournal 2012**:** 279147.

Ledeboer A, Sloane EM, Milligan ED, Frank MG, Mahony JH, Maier SF, *et al.* (2005). Minocycline attenuates mechanical allodynia and proinflammatory cytokine expression in rat models of pain facilitation. Pain 115**:** 71-83.

Lee KM, Jeon SM, Cho HJ (2009). Tumor necrosis factor receptor 1 induces interleukin-6 upregulation through NF-κB in a rat neuropathic pain model. Eur J Pain 13**:** 794-806.

Lee KM, Jeon SM, Cho HJ (2010). Interleukin-6 induces microglial CX3CR1 expression in the spinal

cord after peripheral nerve injury through the activation of p38 MAPK. Eur J Pain 14**:** 682. e681-682. e612.

Lee SA, Park JK, Kang EK, Bae HR, Bae KW, Park HT (2000a). Calmodulin-dependent activation of p38 and p42/44 mitogen-activated protein kinases contributes to c-fos expression by calcium in PC12 cells: modulation by nitric oxide. Brain Res Mol Brain Res 75**:** 16-24.

Lee SH, Park J, Che Y, Han PL, Lee JK (2000b). Constitutive activity and differential localization of p38α and p38β MAPKs in adult mouse brain. J Neurosci Res 60**:** 623-631.

Ma L, Nagai J, Ueda H (2010). Microglial activation mediates de novo lysophosphatidic acid production in a model of neuropathic pain. J Neurochem 115**:** 643-653.

Ma W, Quirion R (2002). Partial sciatic nerve ligation induces increase in the phosphorylation of extracellular signal-regulated kinase (ERK) and c-Jun N-terminal kinase (JNK) in astrocytes in the lumbar spinal dorsal horn and the gracile nucleus. Pain 99**:** 175-184.

Mancuso R, Olivan S, Rando A, Casas C, Osta R, Navarro X (2012). Sigma-1R agonist improves motor function and motoneuron survival in ALS mice. Neurotherapeutics 9**:** 814-826.

Matsuyoshi H, Takimoto K, Yunoki T, Erickson VL, Tyagi P, Hirao Y, *et al.* (2012). Distinct cellular distributions of Kv4 pore-forming and auxiliary subunits in rat dorsal root ganglion neurons. Life Sci 91**:** 258-263.

Mavlyutov TA, Epstein ML, Andersen KA, Ziskind-Conhaim L, Ruoho AE (2010). The sigma-1 receptor is enriched in postsynaptic sites of C-terminals in mouse motoneurons. An anatomical and behavioral study. Neuroscience 167**:** 247-255.

Mendell LM (2011). Computational functions of neurons and circuits signaling injury: relationship to pain behavior. Proc Natl Acad Sci U S A 108 Suppl 3**:** 15596-15601.

Milligan ED, Watkins LR (2009). Pathological and protective roles of glia in chronic pain. Nat Rev

Neurosci 10**:** 23-36.

Miraucourt LS, Peirs C, Dallel R, Voisin DL (2011). Glycine inhibitory dysfunction turns touch into pain through astrocyte-derived D-serine. Pain 152**:** 1340-1348.

Miya K, Inoue R, Takata Y, Abe M, Natsume R, Sakimura K, *et al.* (2008). Serine racemase is predominantly localized in neurons in mouse brain. J Comp Neurol 510**:** 641-654.

Miyano K, Morioka N, Sugimoto T, Shiraishi S, Uezono Y, Nakata Y (2010). Activation of the neurokinin-1 receptor in rat spinal astrocytes induces Ca^{2+} release from IP_3-sensitive Ca^{2+} stores and extracellular Ca^{2+} influx through $TRPC_3$. Neurochem Int 57**:** 923-934.

Monnet FP (2005). Sigma-1 receptor as regulator of neuronal intracellular Ca^{2+}: clinical and therapeutic relevance. Biol Cell 97**:** 873-883.

Mothet JP, Parent AT, Wolosker H, Brady RO, Jr., Linden DJ, Ferris CD, *et al.* (2000). D-serine is an endogenous ligand for the glycine site of the N-methyl-D-aspartate receptor. Proc Natl Acad Sci U S A 97**:** 4926-4931.

Narita M, Yoshida T, Nakajima M, Narita M, Miyatake M, Takagi T, *et al.* (2006). Direct evidence for spinal cord microglia in the development of a neuropathic pain-like state in mice. J Neurochem 97**:** 1337-1348.

Nieto FR, Cendan CM, Sanchez-Fernandez C, Cobos EJ, Entrena JM, Tejada MA, *et al.* (2012). Role of sigma-1 receptors in paclitaxel-induced neuropathic pain in mice. J Pain 13**:** 1107-1121.

Nishimura T, Ishima T, Iyo M, Hashimoto K (2008). Potentiation of nerve growth factor-induced neurite outgrowth by fluvoxamine: role of sigma-1 receptors, IP_3 receptors and cellular signaling pathways. PLoS One 3**:** e2558.

Obata K, Noguchi K (2004). MAPK activation in nociceptive neurons and pain hypersensitivity. Life Sci 74**:** 2643-2653.

Ossipov MH, Bian D, Malan TP, Jr., Lai J, Porreca F (1999). Lack of involvement of capsaicin-sensitive primary afferents in nerve-ligation injury induced tactile allodynia in rats. Pain 79**:** 127-133.

Osuka K, Watanabe Y, Usuda N, Atsuzawa K, Aoshima C, Yamauchi K, *et al.* (2007). Phosphorylation of neuronal nitric oxide synthase at Ser847 in the nucleus intermediolateralis after spinal cord injury in mice. Neuroscience 145**:** 241-247.

Palacios G, Muro A, Vela JM, Molina-Holgado E, Guitart X, Ovalle S, *et al.* (2003). Immunohistochemical localization of the sigma1-receptor in oligodendrocytes in the rat central nervous system. Brain Res 961**:** 92-99.

Panatier A, Theodosis DT, Mothet JP, Touquet B, Pollegioni L, Poulain DA, *et al.* (2006). Glia-derived D-serine controls NMDA receptor activity and synaptic memory. Cell 125**:** 775-784.

Parpura V, Zorec R (2010). Gliotransmission: Exocytotic release from astrocytes. Brain Res Rev 63**:** 83-92.

Petrenko AB, Yamakura T, Baba H, Shimoji K (2003). The role of N-methyl-D-aspartate (NMDA) receptors in pain: a review. Anesth Analg 97**:** 1108-1116.

Piao ZG, Cho IH, Park CK, Hong JP, Choi SY, Lee SJ, *et al.* (2006). Activation of glia and microglial p38 MAPK in medullary dorsal horn contributes to tactile hypersensitivity following trigeminal sensory nerve injury. Pain 121**:** 219-231.

Qin M, Wang JJ, Cao R, Zhang H, Duan L, Gao B, *et al.* (2006). The lumbar spinal cord glial cells actively modulate subcutaneous formalin induced hyperalgesia in the rat. Neurosci Res 55**:** 442-450.

Raghavendra V, Tanga FY, DeLeo JA (2004). Complete Freunds adjuvant-induced peripheral inflammation evokes glial activation and proinflammatory cytokine expression in the CNS. Eur J Neurosci 20**:** 467-473.

Roh DH, Kim HW, Yoon SY, Seo HS, Kwon YB, Han HJ, *et al.* (2008a). Depletion of capsaicin-sensitive afferents prevents lamina-dependent increases in spinal N-methyl-D-aspartate receptor subunit 1 expression and phosphorylation associated with thermal hyperalgesia in neuropathic rats. Eur J Pain 12**:** 552-563.

Roh DH, Yoon SY, Seo HS, Kang SY, Moon JY, Song S, *et al.* (2010). Sigma-1 receptor-induced increase in murine spinal NR1 phosphorylation is mediated by the PKC α and ε, but not the PKC ζ, isoforms. Neurosci Lett 477**:** 95-99.

Roh DH, Kim HW, Yoon SY, Seo HS, Kwon YB, Kim KW, *et al.* (2008b). Intrathecal administration of sigma-1 receptor agonists facilitates nociception: involvement of a protein kinase C-dependent pathway. J Neurosci Res 86**:** 3644-3654.

Roh DH, Choi SR, Yoon SY, Kang SY, Moon JY, Kwon SG, *et al.* (2011). Spinal neuronal NOS activation mediates sigma-1 receptor-induced mechanical and thermal hypersensitivity in mice: involvement of PKC-dependent GluN1 phosphorylation. Br J Pharmacol 163**:** 1707-1720.

Roh DH, Kim HW, Yoon SY, Seo HS, Kwon YB, Kim KW, *et al.* (2008c). Intrathecal injection of the sigma-1 receptor antagonist BD1047 blocks both mechanical allodynia and increases in spinal NR1 expression during the induction phase of rodent neuropathic pain. Anesthesiology 109**:** 879-889.

Romero L, Zamanillo D, Nadal X, Sanchez-Arroyos R, Rivera-Arconada I, Dordal A, *et al.* (2012). Pharmacological properties of S1RA, a new sigma-1 receptor antagonist that inhibits neuropathic pain and activity-induced spinal sensitization. Br J Pharmacol 166**:** 2289-2306.

Ruscher K, Shamloo M, Rickhag M, Ladunga I, Soriano L, Gisselsson L, *et al.* (2011). The sigma-1 receptor enhances brain plasticity and functional recovery after experimental stroke. Brain 134**:** 732-746.

Sandkuhler J (2009). Models and mechanisms of hyperalgesia and allodynia. Physiol Rev 89**:** 707-758.

Sasabe J, Chiba T, Yamada M, Okamoto K, Nishimoto I, Matsuoka M, *et al.* (2007). D-serine is a key determinant of glutamate toxicity in amyotrophic lateral sclerosis. EMBO J 26**:** 4149-4159.

Scemes E, Giaume C (2006). Astrocyte calcium waves: what they are and what they do. Glia 54**:** 716-725.

Schipke CG, Ohlemeyer C, Matyash M, Nolte C, Kettenmann H, Kirchhoff F (2001). Astrocytes of the mouse neocortex express functional N-methyl-D-aspartate receptors. FASEB J 15**:** 1270-1272.

Sorkin L, Svensson CI, Jones-Cordero TL, Hefferan MP, Campana WM (2009). Spinal p38 mitogen-activated protein kinase mediates allodynia induced by first-degree burn in the rat. J Neurosci Res 87**:** 948-955.

Su TP, Hayashi T, Vaupel DB (2009). When the endogenous hallucinogenic trace amine N,N-dimethyltryptamine meets the sigma-1 receptor. Sci Signal 2**:** pe12.

Su TP, Hayashi T, Maurice T, Buch S, Ruoho AE (2010). The sigma-1 receptor chaperone as an inter-organelle signaling modulator. Trends Pharmacol Sci 31**:** 557-566.

Svensson CI, Fitzsimmons B, Azizi S, Powell HC, Hua XY, Yaksh TL (2005). Spinal p38β isoform mediates tissue injury-induced hyperalgesia and spinal sensitization. J Neurochem 92**:** 1508-1520.

Swanson RA, Graham SH (1994). Fluorocitrate and fluoroacetate effects on astrocyte metabolism in vitro. Brain Res 664**:** 94-100.

Terayama R, Omura S, Fujisawa N, Yamaai T, Ichikawa H, Sugimoto T (2008). Activation of microglia and p38 mitogen-activated protein kinase in the dorsal column nucleus contributes to tactile allodynia following peripheral nerve injury. Neuroscience 153**:** 1245-1255.

Trang T, Beggs S, Wan X, Salter MW (2009). P2X4-receptor-mediated synthesis and release of brain-

derived neurotrophic factor in microglia is dependent on calcium and p38-mitogen-activated protein kinase activation. J Neurosci 29**:** 3518-3528.

Tsuda M, Mizokoshi A, Shigemoto-Mogami Y, Koizumi S, Inoue K (2004). Activation of p38 mitogen-activated protein kinase in spinal hyperactive microglia contributes to pain hypersensitivity following peripheral nerve injury. Glia 45**:** 89-95.

Tsuda M, Shigemoto-Mogami Y, Koizumi S, Mizokoshi A, Kohsaka S, Salter MW, *et al.* (2003). P2X4 receptors induced in spinal microglia gate tactile allodynia after nerve injury. Nature 424**:** 778-783.

Ueda H (2006). Molecular mechanisms of neuropathic pain-phenotypic switch and initiation mechanisms. Pharmacol Ther 109**:** 57-77.

Verge GM, Milligan ED, Maier SF, Watkins LR, Naeve GS, Foster AC (2004). Fractalkine (CX3CL1) and fractalkine receptor (CX3CR1) distribution in spinal cord and dorsal root ganglia under basal and neuropathic pain conditions. Eur J Neurosci 20**:** 1150-1160.

von Hehn CA, Baron R, Woolf CJ (2012). Deconstructing the neuropathic pain phenotype to reveal neural mechanisms. Neuron 73**:** 638-652.

Wake K, Yamazaki H, Hanzawa S, Konno R, Sakio H, Niwa A, *et al.* (2001). Exaggerated responses to chronic nociceptive stimuli and enhancement of N-methyl-D-aspartate receptor-mediated synaptic transmission in mutant mice lacking D-amino-acid oxidase. Neurosci Lett 297**:** 25-28.

Wang S, Song L, Tan Y, Ma Y, Tian Y, Jin X, *et al.* (2012). A functional relationship between trigeminal astroglial activation and NR1 expression in a rat model of temporomandibular joint inflammation. Pain Med 13**:** 1590-1600.

Wen YR, Suter MR, Ji RR, Yeh GC, Wu YS, Wang KC, *et al.* (2009). Activation of p38 mitogen-activated protein kinase in spinal microglia contributes to incision-induced mechanical allodynia.

Anesthesiology 110: 155-165.

Weyerbacher AR, Xu Q, Tamasdan C, Shin SJ, Inturrisi CE (2010). N-Methyl-D-aspartate receptor (NMDAR) independent maintenance of inflammatory pain. Pain 148: 237-246.

Wu HE, Sun HS, Cheng CW, Tseng LF (2006). p38 mitogen-activated protein kinase inhibitor SB203580 reverses the antianalgesia induced by dextro-morphine or morphine in the mouse spinal cord. Eur J Pharmacol 550: 91-94.

Wu S, Barger SW (2004a). Induction of serine racemase by inflammatory stimuli is dependent on AP-1. Ann N Y Acad Sci 1035: 133-146.

Wu SZ, Bodles AM, Porter MM, Griffin WS, Basile AS, Barger SW (2004b). Induction of serine racemase expression and D-serine release from microglia by amyloid β-peptide. J Neuroinflammation 1: 2.

Xu L, Huang Y, Yu X, Yue J, Yang N, Zuo P (2007a). The influence of p38 mitogen-activated protein kinase inhibitor on synthesis of inflammatory cytokine tumor necrosis factor α in spinal cord of rats with chronic constriction injury. Anesth Analg 105: 1838-1844.

Xu M, Bruchas MR, Ippolito DL, Gendron L, Chavkin C (2007b). Sciatic nerve ligation-induced proliferation of spinal cord astrocytes is mediated by κ opioid activation of p38 mitogen-activated protein kinase. J Neurosci 27: 2570-2581.

Ying B, Lu N, Zhang YQ, Zhao ZQ (2006). Involvement of spinal glia in tetanically sciatic stimulation-induced bilateral mechanical allodynia in rats. Biochem Biophys Res Commun 340: 1264-1272.

Zhang H, Nei H, Dougherty PM (2010). A p38 mitogen-activated protein kinase-dependent mechanism of disinhibition in spinal synaptic transmission induced by tumor necrosis factor-α. J Neurosci 30: 12844-12855.

Zhang H, Yoon SY, Zhang H, Dougherty PM (2012). Evidence that spinal astrocytes but not microglia

contribute to the pathogenesis of Paclitaxel-induced painful neuropathy. J Pain 13**:** 293-303.

Zhang X, Wang J, Zhou Q, Xu Y, Pu S, Wu J, *et al.* (2011). Brain-derived neurotrophic factor-activated astrocytes produce mechanical allodynia in neuropathic pain. Neuroscience 199**:** 452-460.

Zhao J, Ha Y, Liou GI, Gonsalvez GB, Smith SB, Bollinger KE (2014). Sigma receptor ligand, (+)-pentazocine, suppresses inflammatory responses of retinal microglia. Invest Ophthalmol Vis Sci 55**:** 3375-3384.

Zhuang ZY, Gerner P, Woolf CJ, Ji RR (2005). ERK is sequentially activated in neurons, microglia, and astrocytes by spinal nerve ligation and contributes to mechanical allodynia in this neuropathic pain model. Pain 114**:** 149-159.

Zhuang ZY, Wen YR, Zhang DR, Borsello T, Bonny C, Strichartz GR, *et al.* (2006). A peptide c-Jun N-terminal kinase (JNK) inhibitor blocks mechanical allodynia after spinal nerve ligation: respective roles of JNK activation in primary sensory neurons and spinal astrocytes for neuropathic pain development and maintenance. J Neurosci 26**:** 3551-3560.

국 문 초 록

신경 손상에 의한 물리적 이질통 형성에 있어 척수 내 별아교세포 sigma-1 수용체의 역할

지도교수: 이 장 헌

서울대학교 대학원
수의학과 수의생리학 전공
문 지 영

실험배경 및 연구목적

말초 신경의 손상에 의해 유도되는 신경병증성 통증과 같은 만성 통증은 물리적 이질통 (통증을 일으키지 않는 가벼운 자극에도 통증을 느끼는 것)과 열성 통각과민증 (약간의 통증을 일으킬만한 열적 자극에 더욱 아파하는 것) 등의 증상이 나타나는 것으로 알려져 있다. 하지만 이러한 물리적 이질통과 열성 통각과민증이 어떻게 형성되는지 자세한 기전은 알려져 있지 않다. 최근 좌골신경의 만성압박 손상 모델을 이용한 말초 신경병증성 통증에서 sigma-1 수용체가 척수 내 중추성 감작 현상을 통한 물리적 이질통의 형성에 중요한 역할을 담당하고 있다고 보고되었다. 하지만, 이러한 sigma-1 수용체와 관련된 척수 내 특정 조절

기전은 명확히 밝혀진 바가 없다.

따라서 본 연구는 (1) sigma-1 수용체의 척수 내 세부적인 분포를 확인하고 mitogen-activated protein (MAP) kinase 신호 전달 기전으로 알려져 있는 extracellular signal-regulated kinase (ERK), p38 및 c-Jun amino-terminal kinase (JNK)가 sigma-1 수용체에 의해 활성화 되는지, sigma-1 수용체에 의한 물리적 이질통에 관여하는지를 조사하였다. (2) 좌골신경 만성 압박 손상 모델에서 수술 유발 후 3일째에 sigma-1 수용체, p38 인산화, 별아교세포 (astrocyte) 및 미세아교세포 (microglia) 의 활성을 확인하였다. sigma-1 수용체 및 p38 인산화의 억제가 좌골신경 만성 압박에 의해 증가한 별아교세포의 활성에 미치는 영향을 조사하고, 이러한 sigma-1 수용체에 의한 별아교세포의 활성이 척수 내 D-serine의 증가와 관련이 있는지를 검증하였다. (3) 마지막으로, 이러한 sigma-1 수용체에 의한 p38 활성화 및 D-serine의 증가가 좌골신경 만성 압박 손상에 의한 물리적 이질통의 형성에 기여함을 검증하고자 하였다.

실험방법

생후 1-2일 된 C57BL/6 마우스 뇌에서 별아교세포를 일차 배양하여 실험에 사용하였다. 그 외에 다른 실험에는 20-25g의 수컷 ICR 마우스를 사용하였으며, 신경병증성 통증은 Bennett과 Xie에 의해 고안된 좌골신경의 만성압박 손상에 의해 유도되었다. 각각의 약물은 척수 지주막하강 내로 직접 주입하였다. 무해한 물리적 자극에 대한 반응은 0.16g von Frey filaments를 이용하여 반응빈도로 측정하였다. 열자극에 대한 회피반응 시간이 단축되는 열성 통각과민증은 hot plate 검사와 Hargreaves 검사를 시행하여 측정하였다. 약물은 각각의 실험목적에 따라 처치되었다. sigma-1 수용체 효능제인 PRE-084 (3 nmol)와 길항제인 BD-1047 (100

nmol), ERK 억제제인 PD98059 (3, 10, 30 nmol), p38 억제제인 SB203580 (0.1, 0.3, 1, 3, 10 nmol), 별아교세포 대사억제제인 fluorocitrate (0.003, 0.001, 0.03 nmol), 그리고 serine racemase (Srr) 억제제인 LSOS (1, 3, 10 nmol)가 사용되었다. 면역조직화학법 및 Western blot assay를 실시하였으며, 컴퓨터와 연계된 image analysis program인 Metamorph를 이용하여 단백질의 발현 정도를 분석하였다.

실험결과

1. 신경손상 유발 후 3일째에 척수 내 sigma-1 수용체의 발현이 별아교세포에서 현저히 증가하였다. 일차 배양된 별아교세포에서도 sigma-1 수용체가 발현되었고, sigma-1 수용체의 선택적 효능제인 PRE-084 처치 시 ERK와 p38의 활성화된 형태인 인산화가 증가하였다. PRE-084를 척수 내로 주입 시 물리적 이질통과 열성 통각과민증이 유도되는데, ERK 억제제인 PD98059를 전처치시 물리적 이질통 및 열성 통각과민증이 모두 억제되는 반면, p38 억제제인 SB203580을 전처치시 물리적 이질통은 억제되지만, 열성 통각과민증에는 영향이 없었다. 정상적인 동물에서 PRE-084를 척수 내로 주입 시 p38의 인산화가 시간 별로 증가하고, 이러한 증가는 sigma-1 수용체 길항제인 BD-1047에 의해 억제되었다.

2. 좌골신경 만성 압박 손상 후 3일째에 척수 내 신경교세포 및 미세아교세포의 활성이 증가됨을 각각의 표시인자인 GFAP 및 Iba-1의 증가를 통하여 확인하였다. BD-1047을 만성통증이 유발되는 초기 (수술 후 0일에서 3일째)에 처치 시 신경손상에 의한 별아교세포의 척수 내 발현 증가를 억제 시킨 반면, 미세아교세포의 활성에는 영향이 없었다. p38 인산화는 별아교세포와 신경세포에서 발현이 증가하였으며, 미세아교세포에서는 발견되지 않았다. 흥미롭게도, BD-1047의 척수 내 처치는 별아교세포내의 p38의 인산화만 억제하였다. 더욱이, p38 억제제

의 척수 내 처치는 별아교세포의 발현 증가를 억제시켰다. 척수 내 D-serine 및 D-serine을 형성하는 효소인 Srr의 발현 역시 신경손상 유발 초기에 증가하였다. D-serine은 별아교세포와 신경세포 주변에 위치하고 있었으며, Srr은 주로 별아교세포에서 발견되었다. 신경손상에 의한 D-serine의 증가는 BD-1047 처치에 의해 억제되었고, Srr의 발현 역시 BD-1047처치에 의해 억제되며, Srr은 sigma-1 수용체와 같은 세포에 존재하였다.

3. 신경손상 유발 초기에 지속적인 BD-1047의 척수 내 처치는 물리적 이질통의 형성만 억제하였고, BD-1047과 fluorocitrate를 함께 처치 시 이러한 억제 효과가 더욱 증가하지만, 열성통각과민증에는 영향이 없었다. 더욱이, p38 억제제와 fluorocitrate를 함께 처치 시에도 물리적 이질통의 형성을 더욱 강력하게 억제할 수 있었다. 또한, Srr 억제제의 지속적인 척수 내 처치 역시 물리적 이질통의 형성만 억제하였고, BD-1047에 의한 물리적 이질통의 억제는 외인성 D-serine을 척수 내 투여 시 반전됨을 보여주어, 신경병증성 통증 유발 시 sigma-1 수용체가 별아교세포에서 p38 인산화 및 D-serine을 증가를 통해 물리적 이질통의 형성에 기여함을 제시하였다.

결론

본 연구는 척수 내 sigma-1 수용체는 p38의 인산화 증가를 통해 신경병증 성 통증의 물리적 이질통의 형성에 기여하고 있으며, sigma-1 수용체는 별아교세포에 존재하고, sigma-1 수용체의 활성억제는 p38 인산화의 감소를 통해 별아교세포의 활성을 저해하여 물리적 이질통의 형성을 억제할 수 있음을 검증하였다. 또한 sigma-1 수용체에 의한 물리적 이질통의 형성은 별아교세포에서 Srr 발현 증가에 따른 D-serine의 증가로 인해 나타남을 증명하였다. 이러한 연구 결과들은 척수

내 sigma-1 수용체의 활성화가 신경 병증 성 통증 중 물리적 이질통의 형성에 기여하고 있는 세부 기전을 보다 명확히 제시해주고 있다.

주요어: 신경병증성 통증, sigma-1 수용체, 물리적 이질통, p38, 별아교세포, D-serine

학번: 2008-21738